Department of Precision and Microsystems Engineering

Design of a setup to measure and adjust the height and tilt of an element of a microscope on the micron scale

Koen Hennissen

Report no	: 2022.050
Coaches	: Dr. ir. J.F.C. van Gurp (ASML) & Ir. F. Walvoort (ASML)
Professor	: Prof. dr. ir. J.L. Herder
Specialisation	: Mechatronic System Design
Type of report	: Thesis
Date	: 18-08-2022

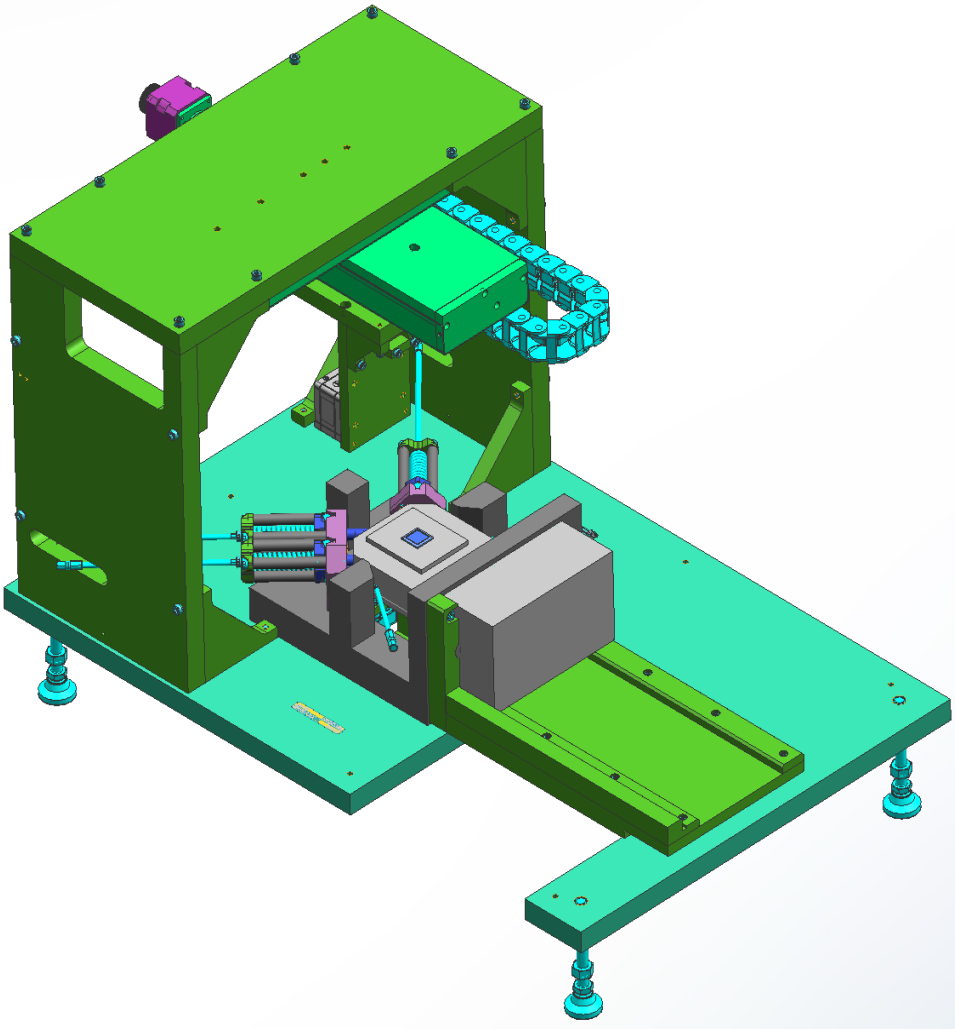

TU Delft Delft University of Technology

ASML

Abstract

This report will describe the design, build and verification of a setup to measure and adjust the Rx, Ry, and Z coordinates of an element within a microscope at ASML to improve the precision of a microscope. The required tolerance budget for the measurement and adjustment of these coordinates are ± 1 *mrad* in Rx and Ry and 0.1 *mm* in Z. The design is done by first finding different solutions for the sensor, the calibration approach and the adjustment. These different solutions are then combined to create different concepts for the setup. Subsequently, these concepts are traded off against each other using different selection criteria. The selected concept uses a lasertriangulator on an X and a Y directed stage that measures the height of a selection of preselected locations on a coplanar reference, which has the desired Rx, Ry, and Z coordinates. This set of data points is then used to make a plane fit from which the Rx, Ry, and Z coordinates of the reference can be retrieved. Subsequently, the same process is used to determine the Rx, Ry and Z coordinates of the element. The required adjustment of the element can then be calculated from the difference between the two sets of coordinates. After a 3D design is made for the setup, the different subsystems of the setup are elaborated and their tolerances are budgeted. To verify the setup, the setup is build in the cleanroom and the different subsystems are tested for their functionality and their performance. These results are then compared with the calculated tolerances. Since most of the tolerances are approximately the same as budgeted and the setup works as expected, it can be concluded that the selected design is suitable. This is however with the exception the tolerance due the stage wobble, which could not be measured as accurately as desired, and with the exception of the tolerance due to the heat generated by the stages, which was unexpected. In the end, recommendations are given on how to improve the setup. From these recommendations, changing the lasertriangulator for a sensor which preforms better on a reflective surface and implementing a solution for the tolerance due to the heat generated by the stages are the most important to alter the setup and make it a production ready design. If a sensor would be implemented that can measure reflective surfaces, the stage wobble, which is the last unknown tolerance contributor, could also be measured after which it can be fully concluded whether the setup works.

Contents

Chapter 1 Introduction

As the worldwide demand for computer chips continues to expand, ASML rises to the challenge by designing increasingly complex machines that produce increasingly smaller computer chips. Since these increasingly complex machines become more expensive, there is a drive to increase the overall yield of the chip production process per machine. One way to increase the yield is to check chips for production errors so that alterations can be made to correct these errors, which thus increases the successful output of the chip-producing machines. This thesis focusses on a microscope at ASML, to deliver a massive leap forward in high-resolution wafer inspection. This microscope houses an element that regulates the resolution of the microscope. To reach the desired resolution of the microscope, it is important to align this element with the optical axis. The subject of this thesis is to design and build a setup that can measure the orientation of the element with respect to the optical axis, as well as adjust the position of the element to match the optical axis.

In this chapter first, some background information will be given about the module in which the element is housed. Then, the project description will be given. After this, the layout of the thesis will be presented, highlighting the content of each chapter.

1.1 Background information

To clarify the subject of this thesis first some more background information needs to be given about the module in which the element is housed. This module will from now on be called the "element module".

The element and element module shown in the report are a dummy of a module which is being considered for development. Only the geometrics and specifications that are important for this thesis will be shown. The setup however will be shown in full detail since it is the subject of this report.

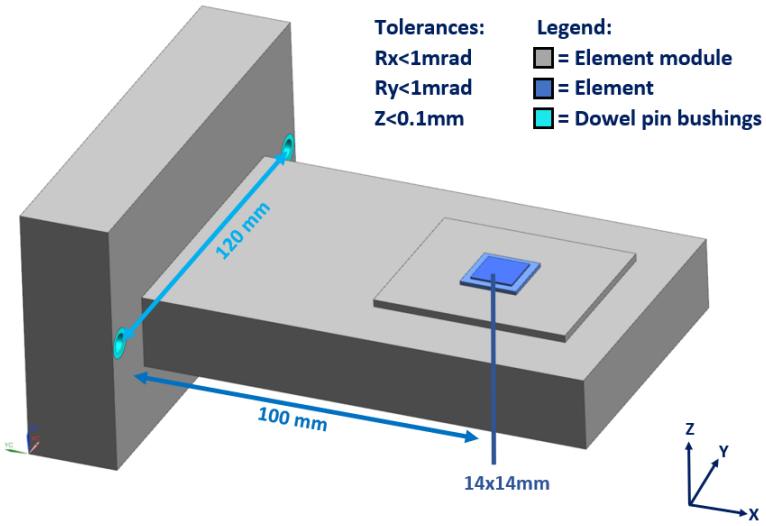

Figure 1.1: Element module dimensions

The element used in the microscope exists out of a $14x14$ mm part on the top and a $19x19$ mm part on the bottom which is made from gold coated silicon. The top $14x14$ mm part of the element is the part that needs to be calibrated with the optical axis of the microscope. To enable handling of the element in the microscope, it is housed in a metal frame, called the element module. Part of the element module will act as a flange to assemble the module within the microscope. The element is located at $100mm$ from the flange of the module, indicated with the blue square in figure 1.1. The grey square on which the element is placed is from now on called "the element mount" and can be adjusted independently from the rest of the module. To align the element module in the microscope a dowel pin connection is used for which two dowel pin bushings are located in the flange 120 mm apart from each other. These dimensions are important as they will be used several times later in the document.

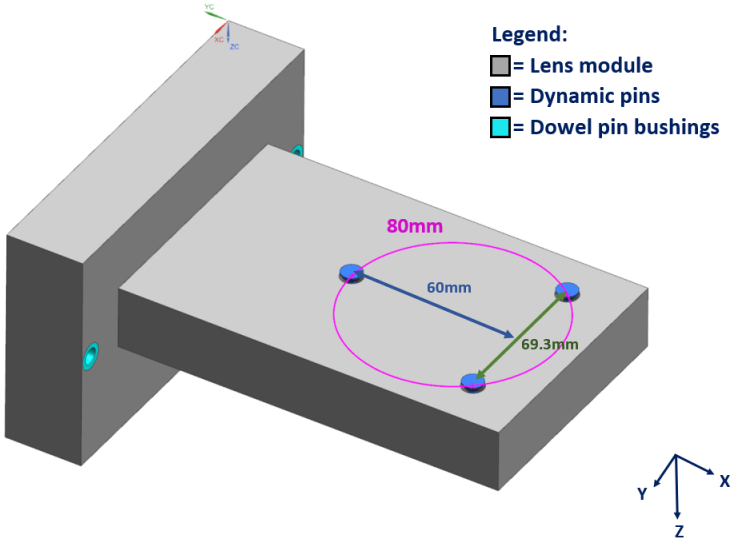

Figure 1.2: The bottom side of the element module

The bottom side of the element module has 3 pins, from now on called dynamic pins, which are located for the adjustment in the Z, Rx, and Ry directions of the element mount and thus the element with respect to the rest of the element module. This can be seen in figure 1.2. The dynamic pins are located evenly spaced on a circle with a diameter of 80 mm of which the center is underneath the nominal position of the center of the element. The maximum distance along the X-axis between the dynamic pins is equal to 60 mm and the maximum distance along the Y-axis is equal to 69.3 mm. Each of the pins can travel approximately 0.5 mm up and $1.2mm$ down from its nominal position.

1.2 Project description

During the project description, first, the goal of this thesis will be given. Then, all requirements the setup must fulfil and the boundary conditions it has to take into consideration will be discussed. After that, there will be discussed what is covered by this thesis in the section about the scope of the thesis.

1.2.1 Goal of the thesis

The element needs to be precisely configured in all 6 Degrees of freedom (DOF) within the element module so that the element is aligned with the optical axis once the element module is assembled in its designated place in the SEM. If this is done correctly within tolerances, the parallel electron beams would pass through the element in such a way that the desired resolution of the microscope will be reached.

The choice has been made to split these 6 DOF up into two different setups, which each account for 3 different degrees of freedom. The X, Y, and Rz coordinates of the element are already measured with an existing setup and are adjusted inside the SEM to their desired location. The goal of this thesis is therefore to design and build a setup that can measure and adjust the remaining Rx, Ry and Z coordinates of the element with respect to the flange and dowel pin bushings of the element module.

1.2.2 Requirements and boundary conditions

As previously said, for the microscope to reach its desired resolution, the element should be aligned with the optical axis of the microscope within specific tolerances. When the module is placed inside the microscope its Rx and Z configuration is determined by the two dowelpin bushings. Therefore the Rx and Z configuration of the element must also be calibrated with respect to the line on which the two dowelpin bushings lie. The calibration of the Ry configuration should be done with respect to the flange of the module. This is because the Ry configuration of the module is determined by the contact of the flange with the housing of the microscope when it is assembled into it. To reach the desired resolution, the element should be configured within $Rx = 1\ mrad$, $Ry = 1\ mrad$ and $Z = 0.1\ mm$ of its nominal position.

Next to these requirements, there are some other boundary conditions:

- The element should not be touched since this could cause damage or particles.
- The surface of the element is reflective.
- The lateral dimensions of the element are 14x14 mm, which is a relatively small measurement surface.
- The to-be-designed setup will be placed in a cleanroom, thus no particle-generating parts can be chosen for the design.
- The to-be-designed setup needs to fit on a tabletop.
- The setup should be intuitive to use by an operator such that operational errors will be minimized.
- The total range of the dynamic pins is approximately between $-1.2\ mm$ and $0.5\ mm$ of its nominal location.
- the design of the element and the element module should not be altered.

This set of requirements with the novel element and its application requires a specially designed calibration setup. There does not exist a previously used applicable solution that can be used for the calibration of the element and thus a novel design is needed for this specific use. The different aspects of the setup call for three different questions that need to be answered before a design can be made that will incorporate these solutions.

These questions are:

- How to measure the Rx, Ry, and Z coordinates of the element? The different options for this question will be discussed in section 2.3.1, the most suitable options for this project will be selected in section 3.2.2, and a decision will be made in section 3.4.
- How to measure the configuration of the element in respect to the flange and dowel pin bushings? The different options for this question will be discussed in section 2.3.2, the most suitable options for this project will be selected in section 3.1, and a decision will be made in section 3.4.
- How to adjust the configuration of the element? The answer to this question will be first discussed in section 2.3.3, and a decision will then be made in section 3.3.2.

1.2.3 Scope of the thesis

The scope of this thesis was originally to build a production-ready prototype that could be directly implemented by ASML. However, due to the long delivery times of the required tightly toleranced parts needed to get the setup within the required tolerance budget, it was later decided to only build a feasibility demonstrator of the selected design for the setup. This decision has been made so that it still would be possible to build and verify the selected design within the given time span of the thesis. Although the initially required tolerances may not be met because of this, in this way it is still possible to test which aspects of the conceived design work as expected and in which areas there are unforeseen complications that require further thought before a production-ready design can be made. Recommendations on how to improve the design to make it a production-ready design will be given at the end of the thesis.

1.3 Layout of the thesis

In order to design, build and validate a measurement and adjustment setup that satisfies the requirements, first, a literature study is done to gather necessary information on various topics that are relevant to the design. The literature study can be found in the second chapter. In the third chapter, the information found during the literature study is used to generate a concept design for the setup. In the fourth chapter, the concept design is elaborated into a fully-fledged 3D design and all different aspects of the design will be discussed. In this chapter, all tolerance budget will be made for all of the subsystems of the setup. In the chapter after that, chapter five, all sub-systems of the design will be validated through a series of tests. In chapter six, the results of the tests will be discussed and the tolerances obtained from the tests will be compared with the budgeted tolerances found in the fourth chapter. Furthermore, recommendations will be given on how to improve the design. In the last chapter a conclusion will be given.

Chapter 2 Literature study

In this chapter, a combination of different sources is consulted to explore the different topics that have to do with this project. These sources include scientific papers, educational books, information from manufacturers of high precision equipment, and information gained via discussions with the specialists at ASML. The information found will be used in the next chapter for the development of a concept design. First, the key design considerations will be discussed to explain which topics need to be researched to gain useful information for this project. After that, relevant information found about tolerances, measurement and adjustment will be elaborated. In the end, some general design considerations will be discussed.

2.1 Key design considerations

As stated in subsection 1.2.2, the main requirement is to design a setup that is able to position the element with respect to the optical axis within the given tolerances. This has to be done by combining a suitable calibration approach with a fitting sensor and a way to adjust the element. The difficulty of this project is finding a suitable combination while still satisfying the requirements and boundary conditions. To find a suitable solution information is needed on all the different key design considerations. These will first be specified after which information is gathered in the coming sections.

For being able to design a setup within the given tolerance budget, it is important to understand the different sources of uncertainty that lead to tolerances. By consulting different literature, a list can be made of the different sources of deviation that lead to tolerance. This list can later be used for the different concept designs to check their tolerance. After these different sources of deviation are found a suitable method to calculate the total tolerance budget will be discussed such that the tolerance requirement can be validated.

For each of the different questions stated in section 1.2.2 an answer should be found which can be incorporated into the design during the design process. To find applicable solutions for these questions it is important to check for existing solutions to similar problems. First, different types of sensors will be discussed that are being used in the field of metrology on the micro and nano scale. This will be done by discussing how they work and what kind of specifications belong to each kind of sensor. Then different calibration approaches will be discussed and put into different categories to find a way to measure the configuration of the element within the element module in regard to the dowel pin bushings and the flange. After that, a solution will be discussed for the adjustment of the element.

When the answers to the three questions of section 1.2.2 are found, a setup has to be designed that can interoperate these solutions. A few considerations for incorporating these solutions together to form a design have to be investigated such that the findings can be used in the design generation.

2.2 Tolerances

First, the different sources of deviations and uncertainties that result in tolerances will be researched and discussed. Then a calculation method, about how to add up the different tolerances, will be discussed.

2.2.1 Sources of deviation

From page 252 of the book "Geometrical dimensioning and tolerancing for design, manufacturing, and inspection" [1] the following sources of deviation in a measurement setup are given. The different sources will be elaborated and for each source will be discussed what it will mean for the to-be-designed calibration setup. The list is based on the deviation sources prescribed in the book with a few alterations such that it includes all the important sources of deviation needed.

1. Deviation of the calibration standard;

When measuring certain values it is always measured relative to a certain calibration standard. To keep the tolerances strict, a calibration standard could only be used within a certain temperature range or within a maximum workload to exclude certain deviations. The calibration should be done from time to time since the measurement done by the measurement setup could slightly change over time due to plastic deformation and aging of the parts.

2. Deviation of the measuring equipment;

A sensor also has a certain tolerance to account for. A distinction could be made between tolerance added due to precision uncertainty and tolerance added due to accuracy uncertainty[2], as can be seen in figure 2.1a:
- Precision, often also referred to as repeatability, is the value of how close several readings of a measurement are to one another if the same spot is measured repeatability under the same conditions. A possible contributor to the precision of a sensor is its resolution or the presence of noise in the signal [3].
- Accuracy is the value of how close the readings are to the actual value. A possible contributor to an accuracy uncertainty could add a certain offset or a linear error, as can be seen in figure 2.1b to the output of the sensor in reference to the actual value.

The difference between the two uncertainties is that the accuracy uncertainty occurs during an absolute measurement (a measurement without a reference value) or if a measurement is done with a reference value on another location. However, if a measurement is done with a certain reference value that is on the same point at the range of the sensor, the accuracy uncertainty can be neglected. For example, if the input is the same in figure2.1b, the output is also the same despite the possible presence of accuracy uncertainty. The precision uncertainty does have to be accounted for, however. This will be used in the next chapter for creating concept designs for the setup.

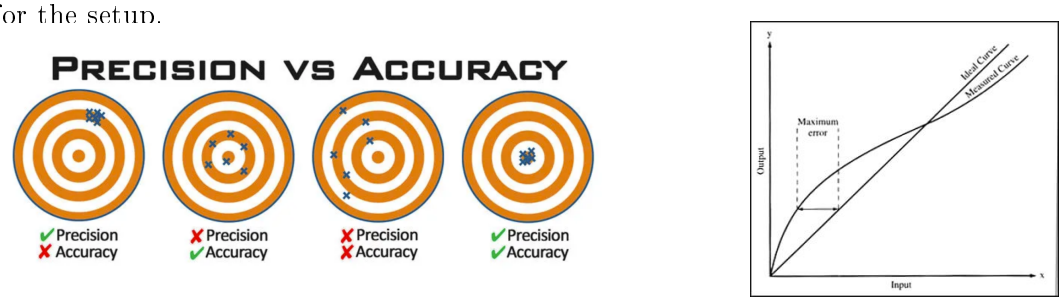

(a) Precision vs accuracy (from[4])

(b) Linear error (from[5])

Figure 2.1: Deviation sources of a sensor

3. Deviation caused by geometric uncertainties;

Each part is made within specific tolerances and these geometric tolerances have to be taken into account while designing a setup with high precision. The source of this deviation is the manufacturing process. For a part that is milled for example, the precision of the milling machine used, the change in temperature during manufacturing, and certain vibrations present during the manufacturing process, all contribute to a certain deviation of the part after the manufacturing process.

4. Deviation caused by support and alignment of the workpiece;

The alignment of two body's with respect to each other creates a certain amount of tolerance due to an unintentional shift or rotation in respect to each other. Also, the possibility of burrs or debris in between parts has to be taken into account for the total tolerance. This tolerance is especially big if the two bodies are not specifically designed for alignment purposes. The deviation can be minimized by taking precautions while designing the setup. For example, dowel pins can be to align certain parts with high precision. However, Dowel pins still account for some tolerance. This is because the dowel pins have a geometrical tolerance, the holes belonging to the dowel pins have a tolerance, and the intended slack that makes both parts slide into each other also accounts for a certain tolerance.

5. Deviation caused by temperature influences;

A change in temperature causes material to shrink or expand. The maximum temperature fluctuation in the cleanroom is 1 $^{\circ}C$. This means the total added tolerance due to temperature will be almost negligible. Aluminium 6082-T6, the material that will be most likely used for most parts of the setup, has a thermal expansion coefficient which is equal to $24 \cdot 10^{-6} K^{-1}$. This means, that if a certain part is 400 mm long, which is a suitable dimension for a tabletop design, and the temperature rises with 1 $^{\circ}C$, the part becomes $24 \cdot 10^{-6} \cdot 400 \cdot 1 = 1$ μm longer.

6. Deviation caused by measuring force (deformations);

If the measurement device would exceed a certain force on the measuring sample, it could influence the measurement. However, although the book [1] mostly covers deformation due to a force, deviation on a micro or nano scale could also be caused by the heat, vibrations, and magnetic and electronic fields caused by the measuring device. This has to be taken into account when doing the tolerance analysis for the design of the setup.

7. Deviation caused by gravity influences on the workpiece (deformations);

The force of gravity on the setup could cause certain parts to bend. However, most parts can be made stiff enough to prevent bending by the weight if the setup. Therefore, the influence of gravity on the total tolerance will be almost be negligible. To be certain, still a calculation has to be made for the final design to check for possible bending. The same is true as explained during the previous deviation source, even though the book [1] only mentions gravity as an external force, other external forces, like vibrations, radiation, or electro, should also be considered.

8. Deviation caused by the metrologist;

The metrologist, operator of the setup, could be a source of uncertainty since there are certain limitations on how precise he could operate the setup. Furthermore, the heat of the metrologist could cause deformation of the setup due to temperature differences. To minimize the deviation caused by the metrologist, the process could be automated by a computer. This reduces the deviation since a computer can do the tasks with high repeatability and the metrologist, and thus its body heat, does not have to touch the setup. Another example would be standardizing the tasks of the operator as this could reduce the deviation between measurement cycles.

2.2.2 Tolerance Calculations

Now that the different sources of deviation and uncertainties are known, a way to calculate the different tolerances will be discussed. There are different methods to add up different tolerances in a tolerance chain.

The first method is to use a convolution integral as explained in the book "The Fourier integral and certain of its applications"[7]. The convolution integral expresses the amount of overlap of a function g as it is shifted over another function f. The resulting equation can be seen below with function f and g having a finite range $[0, t]$.

$$[f * g](t) \equiv \int_0^{\tau} f(\tau) g(t - \tau) d\tau \tag{2.1}$$

If for example two tolerances would be uniformly distributed between ± 0.5 of the nominal value, using the formula above the sum when using both tolerances can be calculated. This would result in the graphical representation in figure 2.2.

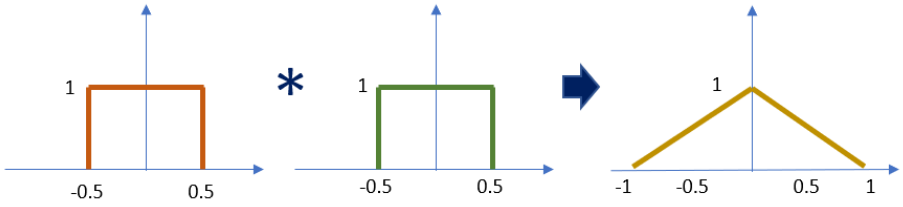

Figure 2.2: Example convolution for uniform distributed tolerance

However, the problem is that the distribution of the tolerance is unknown. Therefore the addition of tolerances must be approximated. This can be done with two different methods.

The first of these methods is the worst-case analysis, which is just a sum of all tolerances. The formula for the worst-case method can be seen below. The weakness of this method is that for example for multiple parts with ± 0.5 tolerances, all deviations would be taken as if they would be $+0.5$, while in reality, the deviation of a part could also be negative. If a bigger number of parts would be taken the chance that all of their deviations would account for a positive amount would be negligible. The worst-case method would thus account for an over-approximation of the real value.

$$\Delta Y = \sum_{i=1}^{n} \delta_i \tag{2.2}$$

With:
ΔY = Total Tolerance
n = Number of instances of tolerance
δ_i = Amount of tolerance for each instance

On the other hand, there is a more statistical tolerance addition approach. This approach does assume that all tolerances are only positive or only negative but that if a big number of tolerance contributors are taken, it is a combination of both. for a statistical approach the Root Sum Square method can be used, for which the formula can be seen below. Both the worst-case method and the statistical tolerance can be found on both pages 6-8 of "Geometrical Tolerance Stack Up Techniques" [8] and pages 3 and 4 of "Design Issues in Mechanical Tolerance Analysis." [9].

$$\Delta Y = \sqrt{\sum_{i=1}^{n} \delta_i^2} \tag{2.3}$$

To make the difference clear between the two different calculation methods, they are visually represented in figure 2.3. The different colored boxes represent different rectangle shapes with tolerances. The middle square represents a stack of deviation origins if there would have been no tolerances, the left stack represents how the stack would be perceived with tolerances using the worst-case approach and the right stack represents how the stack would be perceived with tolerances using the Root Sum Square method. Just adding the maximum of the tolerances together would result in an over-exaggeration of the total tolerance like on the left. On the right can be seen a more realistic view, with both positive and negative tilted geometric deviations added up together.

Figure 2.3: Tolerance stacking example.

To be on the safe side of the statistical method both the worst-case scenario and the statistical method are combined to get the formula that will be used for this project. Combining equation 2.3 and equation 2.2 gives:

$$\Delta Y = \frac{\sum_{i=1}^{n} \delta i}{2} + \frac{\sqrt{\sum_{i=1}^{n} \delta_i^2}}{2} \tag{2.4}$$

2.3 Measurement and Adjustment

In this section, more information is gathered about the different options how to measure the element and how to align it with the optical axis of the microscope. In the first section, literature about how to measure Rx, Ry, and Z coordinates of a sample is discussed. After that, different calibration approaches will be discussed and categorized. In the last section, the adjustment of the element will be discussed.

2.3.1 Measuring the Rx, Ry and Z position of the element

Each of the dynamic pins on the bottom side of the element module, that was discussed in section 1.1 can go approximately 1.2 mm up and down from its nominal position. This means that the total range for the Z of the element is also equal to 2.4 mm. Using the maximum distance between the dynamic pins, shown in figure 1.2, The total range for Rx is equal to $2.4/69.3 = 34.6$ $mrad$ and the total range for Ry is equal to $2.4/69.3 = 30$ $mrad$. This is important since this means that a suitable sensor should be able to measure over these ranges. Furthermore, for the sensor to not be too big of a factor in the tolerance chain, the added tolerance of the sensor should be somewhere around 1% of the maximum allowed tolerance. So 1 μm in z and 0.01 $mrad$ in Rx and Ry. This is only used as a guideline such that sensors can be found with roughly this specification. At a later stage, the added tolerance of the sensor will be validated if it still meets the requirements.

There are a couple of different options to measure the Rx, Ry and, Z positions of the element. One would be to measure at least 3 Z coordinates across the element such that the Rx,Ry and Z position could then be retrieved via a plane fit through these points. Another way would be to measure the Rx, Ry, and Z positions separately via a combination of a tilt and distance sensor.

To find what kind of sensor would be suitable for this project, different types of sensors that are used for similar measurements, found across different literature and sensor manufacturers will be discussed. In this chapter, mainly information will be presented about the different sensors and their specifications. In the next chapter a choice will be made between these sensors on which sensor is the most suitable for the project.

Probe measurement

The first sensor that will be discussed is a measurement probe. This probe extends until it makes contact with the surface of the sample. By measuring its own extension, the distance to the sample can be known. Although the element should not be damaged and touching the element with a probe could cause damage, if only a few points would be gently touched such that no damage would be done, a probe may still be an interesting consideration to measure the surface. If a probe would be preferable a test should be done to exclude the possibility of damage. An example of a probe would be the Heidenhain sensor as displayed in the figure 2.4. The precision, accuracy, and range of a probe would be fit for the measurement that needs to be done.

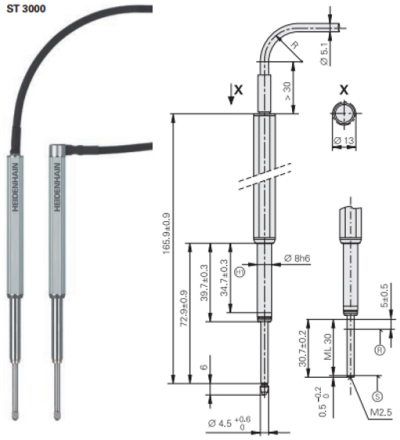

System accuracy	±1 µm	
Position error per signal period	≤ ±0.2 µm	
Short-range accuracy typically	0.3 µm	
Reference mark	≈ 5 mm below upper stop	
Measuring range	12 mm	30 mm

Figure 2.4: Heidenhain sensor with mechanical data (from [11])

Interferometry

Another possibility to measure the different coordinates of the element would be to use interferometry. Interferometry uses the interference of superimposed waves to extract information [12]. It typically uses electromagnetic waves to measure distance or tilt to generate a formation of fringes that differ depending on the tilt and or distance of the measured sample in regard to the configuration of a reference mirror, as can be seen in figure 2.5. The disadvantage is that an interferometer only gives a reference measurement as it measures the difference between two distances[13]. It only gives the phase difference of the returning waves. Since the total amount of difference between the distances stays unknown, the interferometer is probably not a suitable sensor to use.

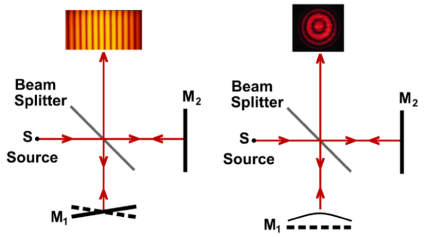

Figure 2.5: interferometry (from [14])

Lasertriangulation

A lasertriangulation sensor is composed of a collimated light source, light-guiding optics and a photosensitive detector [15]. These components are packed inside a portable lasertriangulator. The transmitted laser light interacts with the surface and, due to diffuse reflection, a portion of the resulting scattered light is observed by the photodetector. Depending on the distance of the measured surfaces in regard to the detector, the reflected beam hits a different portion of the light-sensitive detector and thus a different signal is conceived. The working principle of a lasertriangulator can be seen in the figure 2.6a. A typical lasertriangulator and its properties are shown in figure 2.6b. The properties of the lasertriangulator align with the required properties specified at the beginning of this subsection, thus the lasertriangulator would be a suitable choice. The smallest lasertriangulator (NCDT1420 from [16]), which still has a sufficient repeatability, has a 8 mm distance between the laser and the side of the sensor. This is important for possible design options that will be discussed in the next chapter.

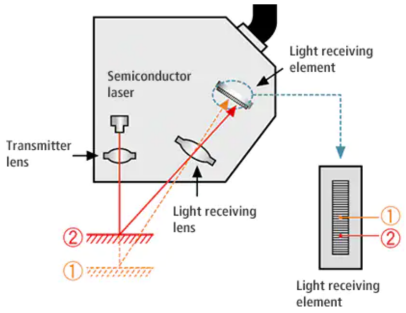

(a) Lasertriangulation (from [15])

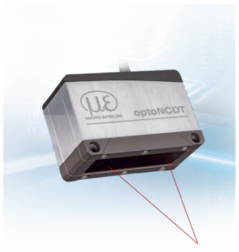

Model	ILD1900-2	ILD1900-10
Measuring range	2 mm	10 mm
Start of measuring range	15 mm	20 mm
Mid of measuring range	16 mm	25 mm
End of measuring range	17 mm	30 mm
Measuring rate [1]		7 adjustabl
Linearity [2]	< ±1µm < ±0.05 % FSO	< ±2 µm
Repeatability [3]	< 0.1 µm	< 0.4 µm

(b) Lasertriangulator properties (from [16])

Figure 2.6: Lasertriangulator

Chromatic Confocal microscopy

Chromatic Confocal microscopy works a bit like the lasertriangulor but uses the different wavelengths of the different colours inside white light to increase its precision. Due to this difference in wavelength, the different colors all have a different focus distance when transmitted out of the element. When the chromatic confocal sensor measures an object, a spectrometer senses which color is in focus, and thus the distance between the sensor and the object is known[17]. A schematic representation of a chromatic confocal sensor can seen in figure 2.7a.

In figure 2.7b, an example of an existing chromatic confocal sensor is given with its specifications[18]. It can be seen that the resolution is even better than that of the lasertriangulator. Another advantage of a chromatic confocal sensor is the fact that it can measure each type of surface, Reflective, diffusive or transparent. A chromatic confocal sensor is thus a suitable option.

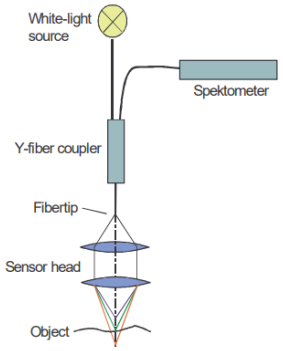

(a) Schematic representation (from[17])

IFS2403-4 - Confocal chromatic hybrid sensor ø8 mm

Ideal for precise distance measurement on smooth & shiny surfaces

Measuring range:	4 mm
Resolution:	100 nm
Light spot diameter:	28 µm
Max. tilt angle:	± 6°
Numerical aperture:	0,15
Sensor diameter:	ø 8 mm

(b) Example sensor properties (from[18])

Figure 2.7: Chromatic confocal sensor

Autocollimation

Another way to measure the desired coordinates would be to measure the tilt separate from the distance of the sample. This could be done with an autocollimator. An autocollimator measures small angular differences, changes, or deflections of a specific sample. The sensor emits parallel beams of light and, due to the angular difference of the sample with respect to the optical axis, the reflected rays converge to another point on the focal plane. Depending on the location of this point, the tilt in both Rx and Ry can be determined [19] as can be seen in figure 2.8a. In figure 2.8b, an example of an existing autocollimator can be seen. Since 8170 and 6840 *arcsec* correspond with 40 and 33 *mrad* respectively, and since 3 *arcsec* corresponds with 0.014 *mrad*, the specifications of the sensor satisfy the range and accuracy requirements. The diameter of the element is 40 mm.

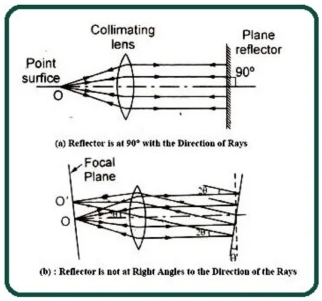

(a) Schematic representation(from [20])

Accuracy (arcsec)*	± 3
corresponds in µ/m	± 15
Number of measuring axes	2
Number of measuring modes	2 (short distance, long distance)
Measuring mode (short) large measuring range, short measuring distance (X) x (Y) (arcsec)	8170 x 6840 up to 0.2 m 7090 x 6830 at 0.4 m 5700 x 5700 at 0.6 m 1540 x 1490 at 0.8 m 1320 x 1320 at 1 m

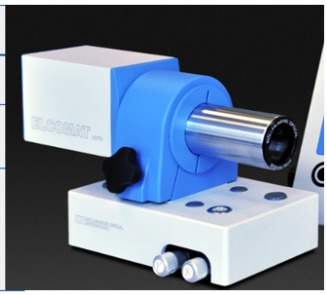

(b) Example sensor properties(from [21])

Figure 2.8: Autocollimator

2.3.2 Calibration approaches

Now that multiple options for a suitable sensor are found, the next question that needs to be answered is how to calibrate the element with respect to the flange and the dowel pin bushings as specified in section 1.2.1. To get a distinction between different calibration approaches, certain splits between different calibration approaches can be made as can be seen in figure 2.9. In this way, the different calibration approaches can be categorized. The knowledge is gained by looking at different measurement examples and by having multiple discussions with experts in the field.

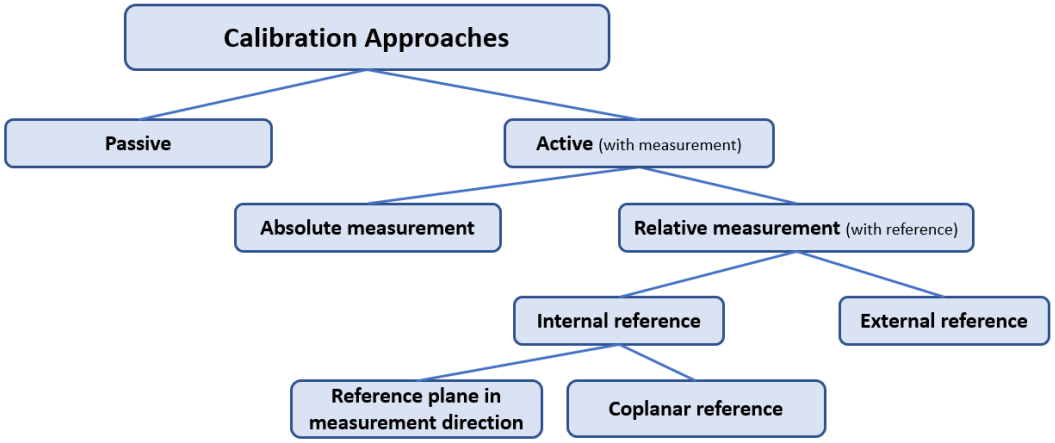

Figure 2.9: Measuring techniques overview

Passive vs active calibration

First, a split can be made between a passive and active calibration. A passive calibration system would not use a sensor and would use a specific made unit which has the desired specifications. An example would be using a certain amount of tablespoons while measuring the amount of sugar needed for a dish while following a specific recipe. An active measurement would use a sensor to actively measure a sample. So in this case use a scale to measure the amount of sugar.

Absolute vs relative measurement

Furthermore, for an active measurement, a split can be made between an absolute and relative measurement. The difference is that an absolute measurement system would measure a certain sample and would use the raw measurement as a definite value, while a relative measurement would first compare the raw measurement value to a reference value, which is obtained by measuring a certain reference object.

An absolute measurement is often used in measurements with a bigger tolerance allowance. This is because, since the sensor is only calibrated before it is put into the setup, the path to the sensor is included in the tolerance chain which is often more difficult to design within tight tolerances. Often relative measurements are used to replace a part of the tolerance chain with a part that could be made with tighter tolerances. Especially with precise measurements, this plays a big role.

Internal vs external reference

Relative measurement can be further split into an internal and an external reference, meaning if the reference is included in the setup or if it is a separate part. While using an external reference it can be placed in and out of the measuring setup at the same position as where the to-be-measured sample would be placed. The disadvantage of having an external reference is that it needs to be positioned within strict tolerances when used for calibration. This can be difficult to do. This difference between an internal and external reference can be better seen in figure 2.10.

In the article [22], a way of using an external reference to calibrate the measuring system is proposed. It is proposed to make a reference with a certain pattern on it that is made with tight tolerances. By measuring the pattern with the sensor and knowing what the output of the sensor should be, the sensor can be calibrated. A similar way to calibrate a lasertriangulator with an external reference is also proposed in article [23], in this a reference existing out of an object with planes on two different known heights is used to calibrate the lasertriangulator. using a predefined reference, either with different heights or with a certain pattern on it, that is designed within tight tolerances, could be a useful way to calibrate the setup. However, a way to link the external reference to the coordinates of the dowelpins and the flange should be added when using an external reference since this is what the sample should be calibrated to.

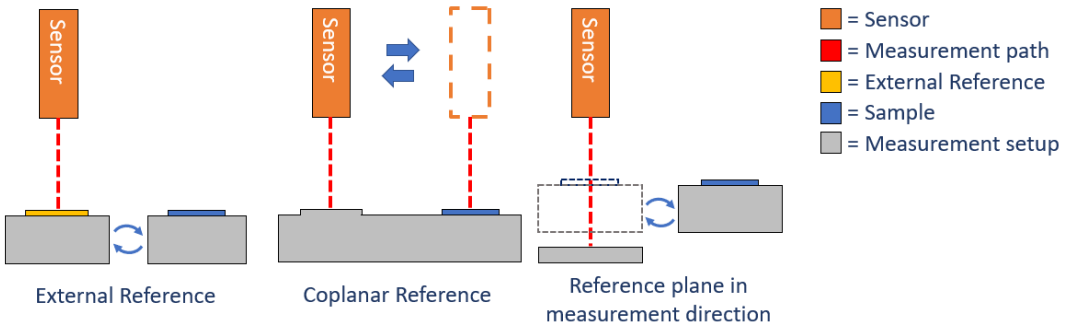

Figure 2.10: Different reference possibilities overview

Coplanar reference vs Reference plane in measurement direction

Since it is not possible while having an internal reference to have it positioned at the same place as the to-be-measured sample, a choice has to be made for the reference to be located in the same plane as the sample, thus coplanar, or for the reference to be in the measurement direction, thus directly above or below the sample.

If the reference would be coplanar to the sample, the sensor would need to travel across a big plane. Using moving stages to gain a certain range in the planar (X and Y) directions could solve this issue but these would also add a specific tolerance. If the reference would be located above or below the sample the sensor would need to measure points at different heights. To do this, a sensor with a fairly long range would be required. A third option would be having the reference at a different X, Y, and Z coordinates, but this would be less interesting as it would only combine both disadvantages of the alternatives.

2.3.3 Adjustment

After the position of the element is measured and the distance to its nominal position is known, the element can be adjusted. Since the element may not be touched as specified in section 1.2.2, the best option to alter the configuration of the element would be to use the designated dynamic pins as explained in section 1.1.

Different kinds of actuators could be used to adjust the dynamic pins. The requirements for a suitable actuator are the dimensions, the actuating range, the stepsize and, the force that the actuator can provide.

For the dimension requirement it is important that three actuators can fit next to each other underneath the dynamic pins. The dimensions of the actuator should therefore all be smaller than roughly 50 mm when looking at the dimensions of the dynamic pins in figure 1.2.

The requirement of the minimal range of the actuators is equal to the total possible motion range of the dynamic pins. As discussed in section 1.1, the element can be moved approximately 1.2 mm down and 0.5 mm up from its nominal position. The minimum range of the actuator thus becomes 1.7 mm.

The next requirement is the stepsize requirement, this is because the stepsize of the actuator is part of the total tolerance budget. A factor of 100 underneath the total tolerance budget assures that there are 100 steps within the tolerance range and reduces the added tolerance of the actuator to almost 1% of the total tolerance.

The last requirement is the amount of force that the actuator can produce. The part of the element module that rests on the actuators when the dynamic pins are unlocked is roughly 1 kg. Next to this weight, each pin is preloaded with 3 N. The load on each pin becomes $\frac{1 \cdot 9.81 + 3}{3} = 6.3$ N. Since there is also a certain amount of friction present while moving the pin, an assumption can be made that the actuator would need a force of at least 10 N to work properly.

The requirements for the actuator are not as strict as for the sensor and are not critical to the type of design of the setup. Therefore it is less of a tradeoff and just has to be selected such that it satisfies the requirements. A suitable actuator will be presented in the next chapter during the concept generation.

2.4 General design considerations

In this section, two different design considerations will be discussed that will be important during the generation of different concepts of possible setups in the next chapter. These considerations were made after certain discussions with the specialists at ASML. First, the possibility to measure the setup after manufacturing to find out certain tolerances will be discussed. After that, the consideration of using monoparts or breaking parts up into an assembly of multiple parts will be discussed. Then, the usage of the flange for the setup will be discussed. After that, multiple deviation sources that result in tolerance that have to be taken into account for the setup will be discussed.

2.4.1 Measurement after manufacturing

An option would be to measure an unknown deviation after manufacturing. In this way, the deviation could be compensated for, for example by implementing it in the software of the setup. The big disadvantage however would be that this data would be specific for each different instance of the setup and thus needs to be implemented in the software of the measurement system. Although unknown deviations would be reduced, this would be highly user-unfriendly. It would add big risks in using the right values for the specific instance since these values need to be documented and implemented the right way. The setup will be built by a different company when the definite design is determined and be used by another different company to align the element. It is very disadvantageous if multiple specific values would have to be communicated between these different companies and be implemented in the right way since this often goes wrong and a small error would result in the measurement and adjustment being flawed without a way of knowing. Therefore it is decided to use the tolerances of the manufactured parts without measuring them afterwards as this would be desired for the setup.

2.4.2 Monopart setup vs Assembly

Another choice that is important is whether the manufactured parts should be made from one part or be made from different parts and assembled afterwards. The advantage of making the setup out of one part, or monopart, is that if there are fewer tolerances to deal with than when adding multiple parts together. This is because each part has a geometric tolerance of its own but also has an alignment tolerance when multiple parts are added together, as explained in sections 2.2.1.3 and 2.2.1.4. The advantage of making multiple parts however is that these would be easier to manufacture and therefore could also lead to better geometric tolerances. This trade-off has to be taken into account when designing the different measurement and adjustment setups. When the best concept is chosen and expanded upon a decision will be made on which parts of the setup would be better as separate parts or as monopart.

2.4.3 Using the flange for the setup

To define the Rx, Ry, and Z coordinates of the element with respect to those of the flange and dowel pin bushings, a setup can be made with the same interface as the microscope, Thus with the same flange and set of dowel pins. In this way, if the configuration of a certain part of the setup with respect to the connection with the element module is known, it could be used instead to align the element to. Although this does add a certain tolerance chain from this location to the connection of the element module, it creates a solution for the hard-to-measure locations of the flange and the dowel pin bushings.

2.4.4 Dowel pin tolerances

As will be mentioned in the next chapter during the various tolerance chain analysis of the calibration approaches, one of the tolerances that have to be taken into account is the dowel pin tolerances. This is due to the geometric tolerance of the dowelpins and the alignment tolerance when these dowelpins are used. The calculations for these tolerances can be found in Appendix A.

2.4.5 Locking tolerance

After the element is aligned to the optical axis by the dynamic pins, shown in section 1.1, the pins have to be locked in their new position. This is done by a locking mechanism. The locking mechanism pushes the dynamic pins against their housing in the module to lock them in their place which can be seen in figure 2.11. since the dynamic pins could move during the locking process, it could slightly alter the position of the element. This disposition should be taken into account as a tolerance in the tolerance chain. The figure below represents an intersection of the element module when viewed from the side. In the figure below, the dynamic pins can be seen in their locked position. An approximation of this tolerance can be seen in Appendix B.

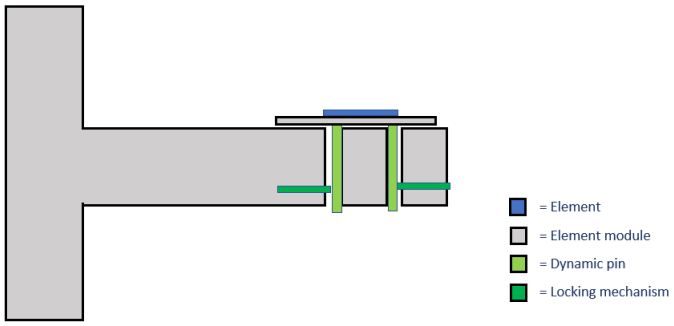

Figure 2.11: Locking mechanism

2.4.6 Geometric tolerance with CNC milling

Computer numerical control milling, or CNC milling, is often used to manufacture precise parts[24]. The maximum precision that could be reached with CNC milling is around 0.001 mm [25]. However, this is difficult to achieve and requires a long and costly process. A maximum precision around 0.02 mm is often better to achieve with conventional precision CNC milling machines. This will be used in the next chapter as the geometrical toleranceof the different aluminium parts that are used for the setup.

Chapter 3 Concept Design

By combining the information retrieved in the previous chapter, different concepts can be made for the design of the setup. In section 3.1 , The different types of calibration approaches that were found can be elaborated into different designs for the setup. By looking at the designs, the most relevant measuring techniques can be selected for this project. Thereafter, in section 3.2 suitable measurable locations will be inspected. In this section also suitable sensors will be selected by discussing the sensors presented in the previous chapter. In section 3.3, a test for stick-slip will be done and a suitable actuator for the adjustment of the dymanic pins will be selected. Finally, in section 3.4, all found subsolutions will be put together to form design concepts. From these concepts, a most suitable design for the setup will be chosen.

3.1 Calibration approaches

The differences between different calibration approaches have been made clear in the last chapter, section 2.3.2. In this section, measurement concepts will be elaborated on for each of the different calibration approach categories to see which calibration approach is the best suitable to measure the element with respect to the flange and the dowelpin bushings within the required tolerance. In the figure 3.1, an overview of all the different concepts can be seen, linked to their respective calibration approach category.

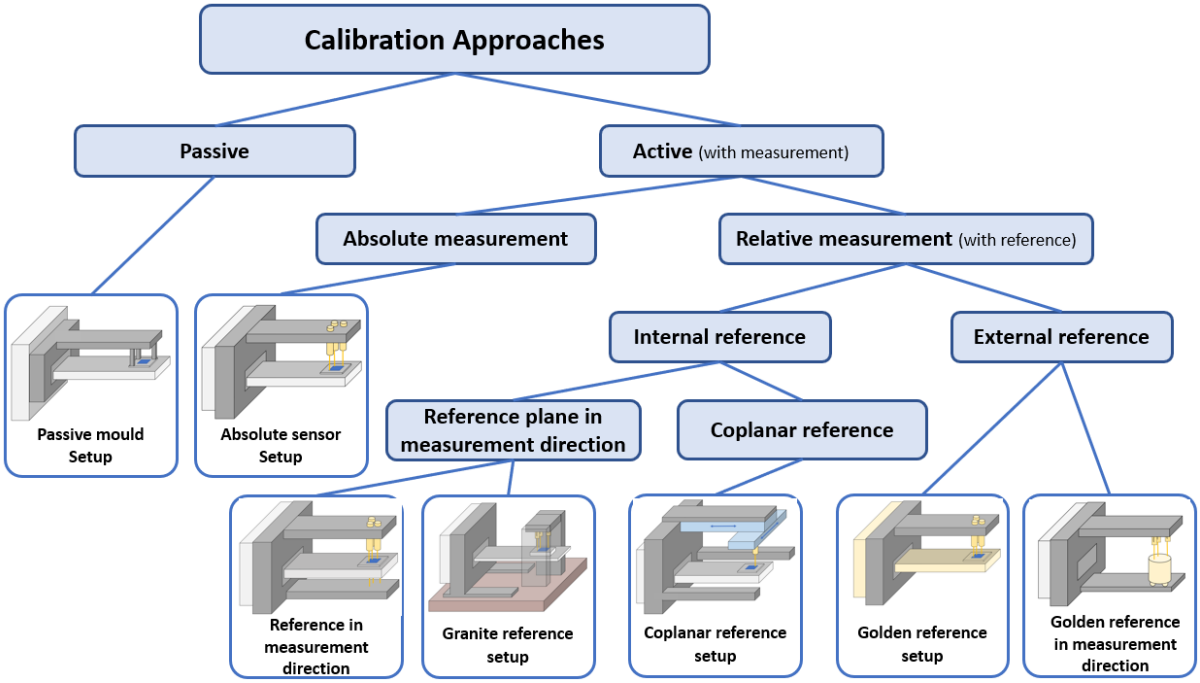

Figure 3.1: Overview of different measurement concepts

Each of the different calibration approach concepts will be discussed individually. For each calibration approach will be discussed how they work and if they would be suitable for the specific use case of this project. Then, if the concept is suitable, the specific tolerance chain will be elaborated, using the deviation sources discussed in section 2.2.1. The concepts will be elaborated on the next pages as shown in the figure from left to right.

3.1.1 Passive mould calibration

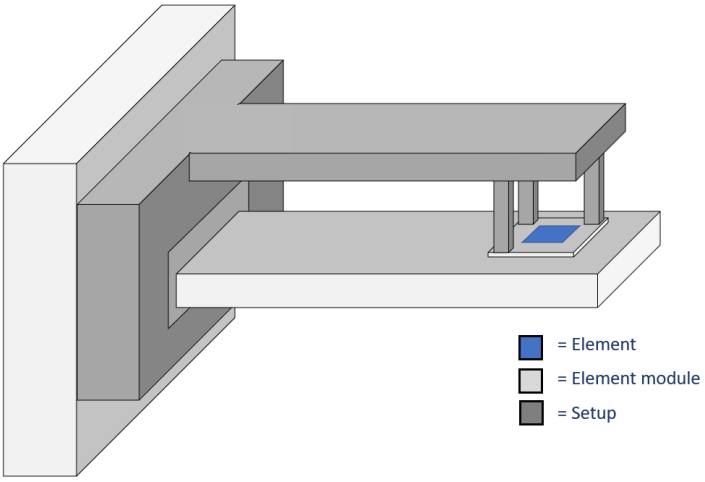

Figure 3.2: Absolute mold setup

The idea of a passive mould calibration, of which an example can be seen in figure 3.2, is to make the setup touch the mount holding the element when the element mount is actuated till the position that the element is in the exact position. This is an example of a passive calibration approach since a sensor that measures the stack is not needed. If it is viable it would be a fairly simple solution to adjust the element to the right position since no electronics, which often bring their complications, would be needed. Since the element must not be damaged, the setup could use the element mount for its calibration.

The first problem however is the fact that the element mount has a too big tolerance with respect to the element. This means that if the element mount would be adjusted to the right position, the element could still be out of tolerance of its desired position. This will be further discussed while looking at the locations suitable to use for the calibration in section 3.2.1.
Another problem that, since the element module can only be implented into the setup with its dowel pins and flange interface, it could only be implemented horizontally into the setup. Therefore, the "fingers" of the calibration setup would need to lift off the element mount while implementing the element module to prevent contact damage. This requires something like a joint that would even further increase the total tolerance.

Given these two problems and given the requirement that the element module can not be altered, The passive calibration approach is thus not viable for this project.

3.1.2 Absolute sensor measurement

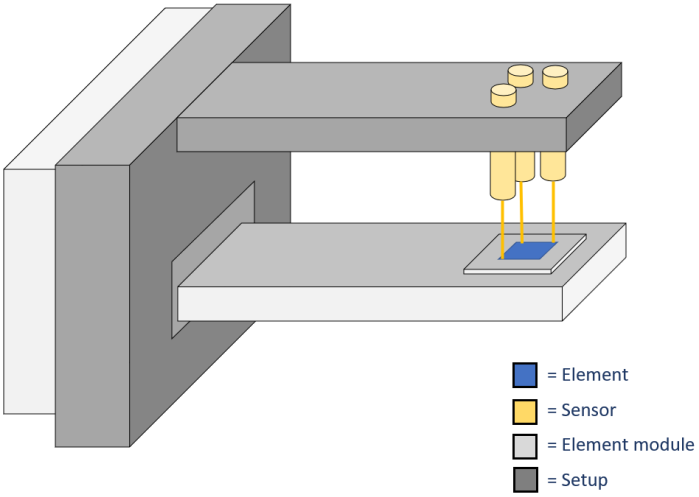

Figure 3.3: Absolute measurement sensor setup

With an absolute measurement, of which an example can be seen in figure 3.3, the element will be actuated until the sensor reaches the value that corresponds to the nominal position of the element. This is possible by calculating the value that the sensor should give when the element is positioned at its desired location. The tolerance chain for this calibration approach will start at the location where the element module is docked into the setup and goes through the top of the setup, through the sensor to the element. A schematic overview of each component of the resulting tolerance chain can be seen in figure 3.4.

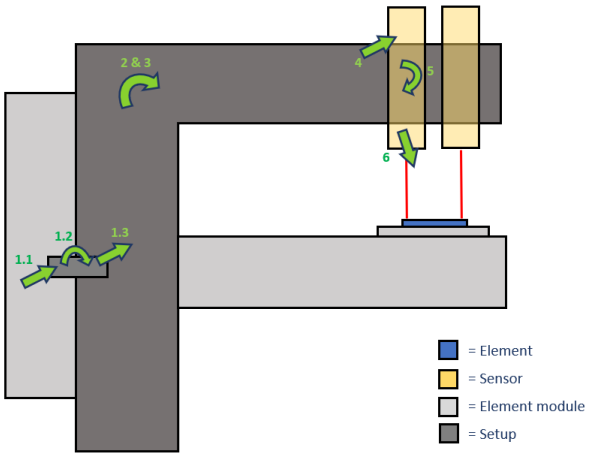

Figure 3.4: Tolerance chain absolute measurement

The tolerances that would make up the different components of the tolerance chain while using this measuring technique are:
1.1. The reproducibility tolerance of the dowelpin due to misalignment when the module is docked (as explained in section 2.2.1.4).
1.2. Geometric tolerance of the dowelpin itself (as explained in section 2.2.1.3).
1.3. misalignment tolerance of the connection from the dowelpin to the setup(as explained in section 2.2.1.4).
2. Geometric tolerance of the setup (as explained in section 2.2.1.3).
3. Temperature tolerance of the setup (as explained in section 2.2.1.5).
4. Misalignment tolerance of sensor (as explained in section 2.2.1.4).
5. Geometric tolerance of the sensors (as explained in section 2.2.1.3).
6. Tolerance due to Accuracy and precision of the sensors (as explained in section 2.2.1.2).

Looking at the different components of the tolerance chain, there are a couple of problems with using an absolute calibration approach for this case.

The first one, which corresponds to the 4th and 5th tolerance, is that the tolerance chain passes through the sensor. This would cause a problem with distance sensors since you would have to know the exact location (within tight tolerances) where the origin of the sensor is. This is often not specified by the manufacturers since this specification is not needed most of the time. You would also have to position the sensors within tight tolerances within your setup which could be also difficult since not all sensors have a built in way for precise alignment.

The last problem corresponds to the 6th tolerance. Since you do not use a reference both the accuracy and the precision add up to the total tolerance of the measurement. Which is less favourable then only needing the precision tolerance.

An absolute calibration approach would thus be undesirable for the most precise measurements. The other option would be to measure the element relative to a reference. The next couple of measurement concepts focus on relative measurements.

3.1.3 Reference plane in measurement direction

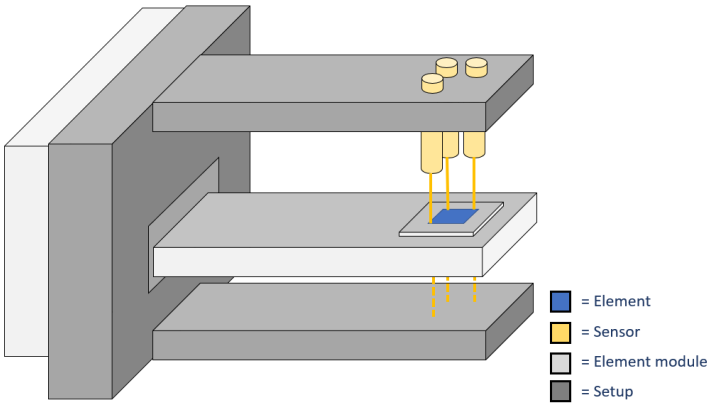

Figure 3.5: Reference plane in measurement direction setup

The next setup is the reference plane in measurement direction setup, of which an example can be seen in figure 3.5. This setup uses an active measurement system to measure the element relative to an internal reference which is located below the element. The setup is made out of the docking part with two extensions out of wich the bottom functions as a reference for the measurement and is part of the same body as the interface for the module.

Since the bottom part serves as a reference for the element, the tolerance chain does not go through the sensor but through the bottom part instead. Therefore, the alignment and geometric tolerances of the sensor are not part of the tolerance chain. This is because the coordinates of the stack are measured in comparison to the coordinates of the reference. The position of the sensor and its tolerance is not relevant for the tolerance chain since it is the same in both measurements. However, since the sensor still has tolerances for its measurement, the measuring tolerances of the sensor have to be taken into account twice for both measurement of the element as for the measurement of the reference.

This gives the tolerance chain that can be seen in the figure 3.6.

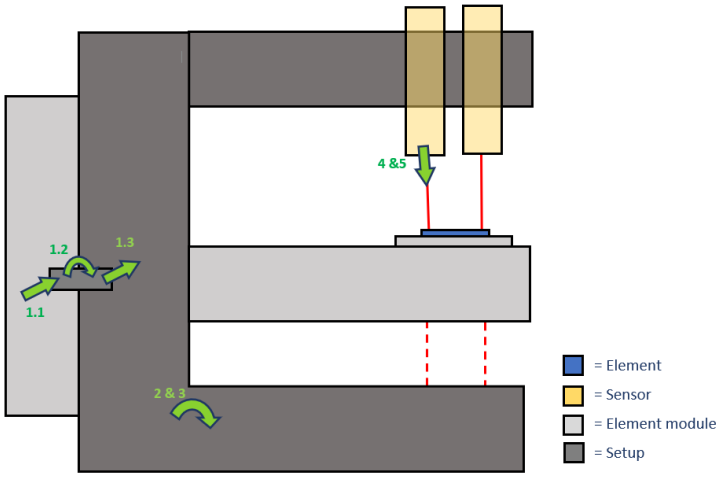

Figure 3.6: reference plane in measurement direction setup

The tolerances that would make up the different components of the tolerance chain while using this measuring technique are:
1. The tolerances of the dowelpin connection, this would be the same as with the absolute measuring technique
2. Geometric tolerance of the setup(as explained in section 2.2.1.3) . This would also be roughly the same as with the previous measurement concept since both parts would be roughly the same size and would have the same features.
3. Temperature tolerance of the setup (as explained in section 2.2.1.5).
4. & 5. Tolerance due to the accuracy and precision of the sensors while measuring the element(as explained in section 2.2.1.2). Since the sensor would have to measure two different instances along its range, both the accuracy, due to a possible linearity error, and the precision of the sensor have to be taken into account.

Note that the undesirable components of the tolerance chain that were present with the absolute measuring method, components 4, 5, and 6, are not part of this tolerance chain due to using a reference for the measurement. This makes the relative measurement method a better option than the absolute measurement method. Using a relative calibration approach does add the tolerance component of the sensor a second time since two different measurements have to be done. However, this is a much smaller component for the tolerance chain since sensors are designed for their precision and not for their geometric tolerance.

Since this reference is located below the element, a suitable sensor should have an appropriate amount of measuring range such that it can both measure the element as the reference from where it is housed in the setup. Due to measuring along a range, not only precision but also the linearity error from the sensor play a role in its tolerance, as explained in section 2.2.1.2.

Due to the mentioned advantages of the tolerance chain of this calibration approach, it could be suitable for the design of the setup. The reference plane in measurement direction setup will therefore be taken into account while deciding for the design later in this chapter.

3.1.4 Granite reference setup

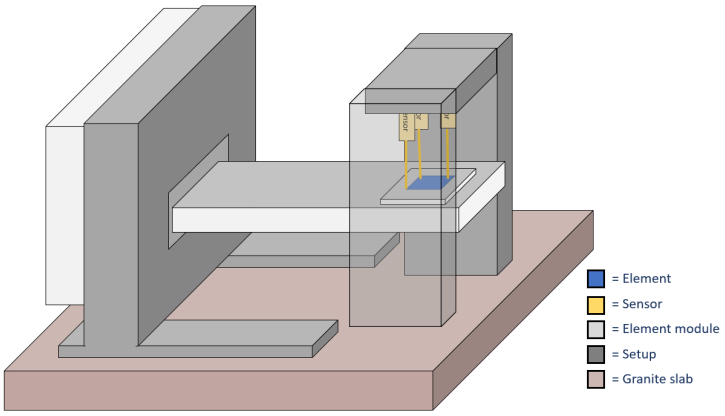

Figure 3.7: Granite reference setup

Since there are some limitations in making metal with high precision, it is interesting to take a different material into account. A material that is often used in high precision measurement setups is granite. This is because that a granite slab can be made very flat (<2 µm flatness tolerance [27]). Due to these tight tolerances, it could therefore be used to act as a reference for the sensors, an example of such a setup can be seen in figure 3.7.

Since the flange can not be made out of granite, due to the limitations in manufacturability of granite, the problem is that the setup would have to be split up into two different parts. A granite part and a metal part for the flange, can be seen in the figure below. As discussed in section 2.4.2, making the setup out of different parts would not only add the geometric tolerance of both parts, it also adds an extra alignment tolerance to the tolerance chain. This is disadvantageous since this combination of tolerances would be bigger than making it purely out of one part of metal.

3.1.5 Coplanar reference setup

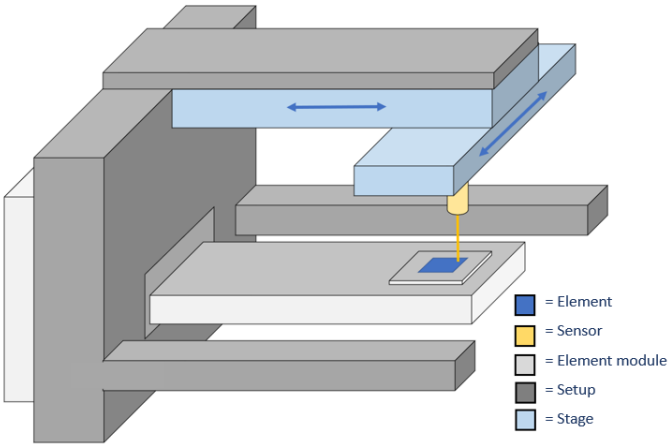

Figure 3.8: Coplanar reference setup

Other than having the reference under the element, the reference could also be placed next to the element, of which an example can be seen in figure 3.8. This brings its own set of advantages and disadvantages. Since the sensor has to travel across a big XY plane to reach the reference, stages are needed. A stage is a platform that can move along a linear axis to specified coordinates. These stages bring their own z tolerance, as the axes where the sensor would travel along, have a certain wobble (deviation perpendicular to the axis, due to geometric geometric uncertainties or gravity influence) in the z-direction. This is included for both stages for both measurements in the tolerance chain below. Like the previous two setups, the alignment uncertainty and geometric uncertainty of the stages and the sensor are not part of the tolerance chain by using a reference.

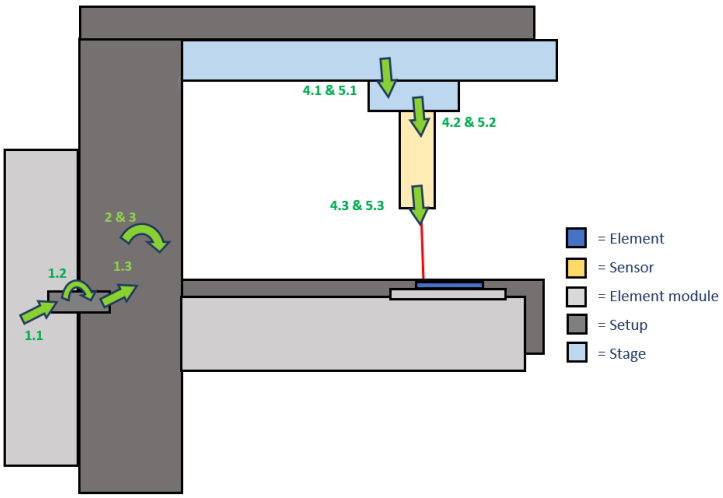

Figure 3.9: Coplanar reference setup tolerance chain

The different tolerances, which can be seen in figure 3.9, that would make up the different components of the tolerance chain while using this measuring technique are:
1. The tolerances of the dowelpin connection, would be the same as with the absolute measuring technique

2. Geometric tolerance of the setup, this would also be roughly the same as with the previous measurement concept. (as explained in section 2.2.1.3).
3. Temperature tolerance of the setup (as explained in section 2.2.1.5).
4.1 Tolerance due to wobble in the X stage during the reference measurement
4.2 Tolerance due to wobble in the Y stage during the reference measurement
4.3 Tolerance due to the accuracy and precision of the sensors while measuring the reference (as explained in section 2.2.1.2)
5.1 Tolerance due to wobble in the X stage during the element measurement
5.2 Tolerance due to wobble in the Y stage during the element measurement
5.3 Tolerance due to the accuracy and precision of the sensors while measuring the element(as explained in section 2.2.1.2)

For the assessment of the different calibration approaches it can be assumed that the wobble of the stage is relatively small. This assumption can be made since these types of stages are often used for similar purposes within the precision mechanics. However, since the wobble of the stage is often not specified by the manufacturer, it should be verified at a later stage.
A big advantage of this calibration approach is that a bigger reference plane can be used. This is advantageous for the calculation of tilt. Tilt can be calculated by the difference in height(δh) between two points divided by the distance between the two points (r), thus $\frac{\delta h}{r}$. Thus, when the distance between the measured points is made bigger, the tolerance for the tilt due to the tolerance of the height measurement becomes smaller.

An advantage of having the reference on the same height as the element surface is that the tolerance due to the accuracy of the sensor does not add tolerance to the tolerance chain any more. This is because, as explained in section 2.2.1, two points at the same distance from the sensor would have the same value if a sensor would only have an accuracy error (and no precision error).

Another advantage of this calibration approach is that by using stages, multiple points can be measured. By measuring more points the tolerance due to the precision error of the sensor goes down. This is due to the formula that can be seen below, in which the tolerance due to precision gets smaller the more samples that are used for the measurement.

$$SE = \frac{\sigma}{\sqrt{N}} \tag{3.1}$$

The standard error, in this case, tolerance, is represented by SE.
The standard deviation, in this case, the precision error, is represented by σ
The amount of samples is represented by N

A disadvantage for using stages and measuring multiple measurement points is that it adds complexity to the system. Instead of only using 3 measurement points on the element that have to be synchronised with 3 measurement points on a reference, a computation needs to be done that makes a fit using multiple data points. This requires dedicated software that needs to be verified to prevent unintentional errors in the calibration process due to the added complexity.

Due to the advantages mentioned above, this calibration approach could be suitable for the design of the setup. It therefore will be taken into account while deciding for the design later in this chapter.

3.1.6 Golden reference setup

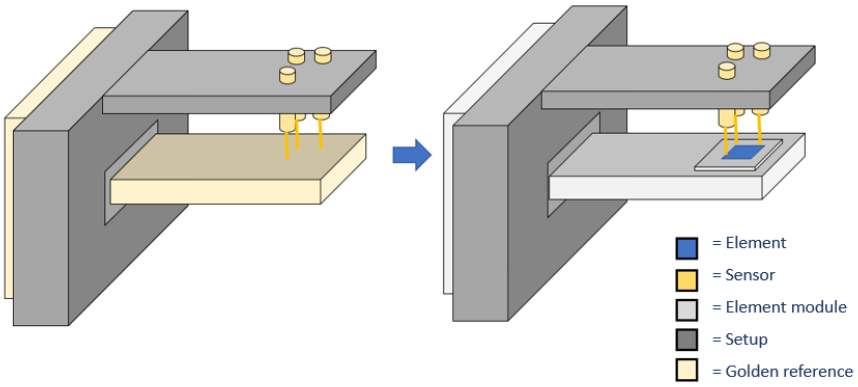

Figure 3.10: Golden reference setup

Next to having the reference below or beside the element, there is also an option to have the reference at the same location as the element, of which an example can be seen in figure 3.10. However, this is only possible if the reference would be a separate part from the rest of the setup and is swappable with the element module.

This can be done by designing the reference, from now on called "golden reference", like the element module which is designed to have its measurable surface at the desired location of the element, within the geometric tolerances that are possible for making such a reference. It could be integrated with the same integration method as the element module, using the tight tolerances of the dowelpin connection.

In contrast to the absolute measurement technique, this causes all geometric and alignment tolerances of the setup itself to disappear from the tolerance chain. The geometric tolerances of the golden reference and the alignment tolerances of the dowelpin connections, of the setup and of the golden reference, remain.

The tolerance train would look as can been seen in figure 3.11:

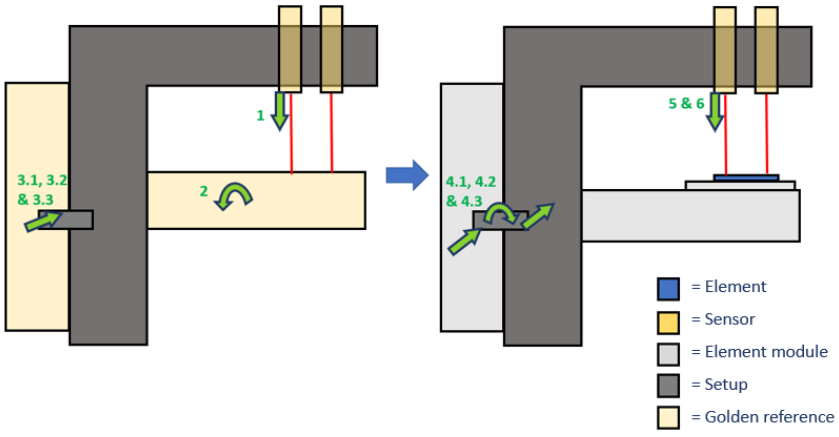

Figure 3.11: Golden reference tolerance chain

The tolerances that would make up the different components of the tolerance chain while using this measuring technique are:
1. The tolerance due to the accuracy and precision of the sensors while measuring the golden reference(as explained in section 2.2.1.2)2. Geometric tolerance of the golden reference (as explained in section 2.2.1.3).
3.1 Misalignment tolerance of the dowelpin bus connection(as explained in section 2.2.1.4). 3.2 Geometric tolerances of the bus of the dowelpin bus2.2.1.3). 3.3 The reproducibility tolerance of the dowelpin due to misalignment when the module is docked (as explained in section 2.2.1.4).
4 The remaining tolerances of the dowelpin connection are the same as with the previous measurement concepts.
5.Temperature tolerance of the setup (as explained in section 2.2.1.5).
6. Tolerance due to the accuracy and precision of the sensors while measuring the element (as explained in section 2.2.1.2)

As can be seen in the tolerance chain, the golden reference needs to have the bushings for the dowelpin connection to be assembled into them such that the flange interface can be used for precise docking. This is why next to the dowel pin tolerances of the element module, also 3 dowel pin tolerances for the golden reference are included in the tolerance chain.

Just like with the reference plane measuring technique, because that the reference is at the same distance from the sensor as the element, the accuracy error of the sensor is negligible. This is advantageous for the total tolerance of the setup.

Since this setup has some great advantages and no undesirable components in the tolerance chain. It will be taken into account for the design of the setup later in this chapter.

3.1.7 Golden reference in measurement direction

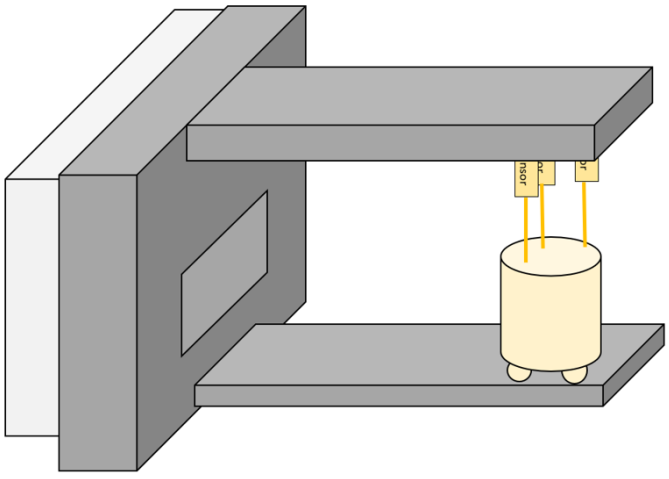

Figure 3.12: Golden reference in measurement direction setup

A combination would be possible between the golden reference setup and the reference plane in measurement setup, of which an example can be seen in figure 3.12. As a way to reduce the required range needed for the sensor of the reference plane in measurement direction setup, a smaller external golden reference could be made to be placed on the lower part of the setup. However in comparison with the last setup, next to the geometric tolerances of the golden ref-

erence, the geometric tolerances of the setup would also have to be taken into account. This would be disadvantageous for the total tolerance in respect to the previous setup. This is because having two geometric tolerances and two sets of alignment tolerances (for the module to the setup and from the setup to the golden reference) would add up to a higher tolerance then having only one geometric tolerance and two sets of alignment tolerances as with the last setup.

3.1.8 Suitable calibration approaches

after discussing all 7 different calibration approaches from figure 3.1, 3 calibration approaches have emerged that are the most suitable for this project. These are the reference plane in measurement direction approach, the coplanar reference approach, and the golden reference approach. These calibration approaches can be seen in figure 3.13 and will be taken into account when forming design concepts by combining the calibration approach with the selected sensors and the actuator for the adjustment of the element.

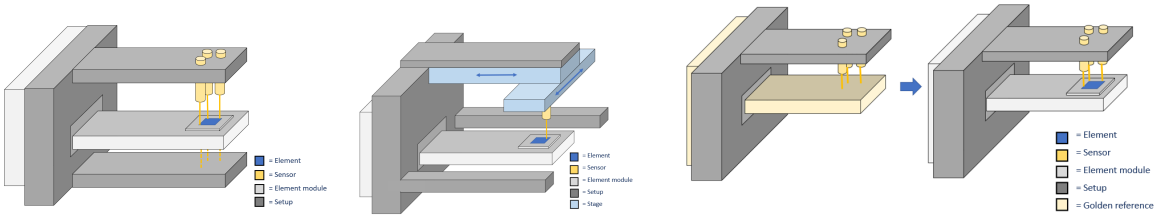

(a) Reference at the measurement direction

(b) Coplanar reference setup

(c) Golden reference setup

Figure 3.13: Selected calibration approaches

3.2 Sensors

Now that the suitable calibration approaches have been determined, a selection for suitable sensors has to be made. To make a selection it is important to determine which parts of the element module are within tight tolerance of the element such that they can be used for the measurement of the element.

3.2.1 measurable location

To know which sensors could be usable for the setup, it is important to know which parts of the element module are within the tolerance budget to the 14x14mm part of the element, which needs to be calibrated. The element mount, the 19x19mm part of the element and the 14x14 mm part of the element will be discussed as they will be adjusted by the dynamic pins and therefore make for a measurable location.

In appendix C, both the geometric tolerances of the 19x19mm part of the element, and the element mount can be seen as well as their respective alignment tolerances to the 14x14mm part of the element. It can be concluded that the 19x19mm part of the element is within the tolerance budget to the 14x14mm part of the element and could be used for the measurement. however, the alignment tolerance between both parts of the element and the geometric tolerance of the 19x19mm part of the element should be taken into account of the tolerance train when using this part for the measurement. Futhermore, for the element mount only the z coordinate with respect to the 14x14mm part of the element is inside the tolerance budget and could be used for the measurement. Thus, it is not possible to measure the Rx and Ry coordinates of the 14x14mm part of the element within the given tolerance budget.

3.2.2 Sensor selection

Now that the measurable locations are known, looking back on section 2.3.1, the different sensors will be discussed to determine a selection of suitable sensor options.

Probe measurement

This would be a valid measurement method. Especially when a large range is needed. The drawback of this sensor is the fact that it touches the element and therefore could do damage to the element. If this sensor would be chosen, a test should be done to determine if it could do damage to the gold coated silicon top layer of the element.

Since the diameter of the probe is 13 mm, as can be seen in figure 2.4 of section 2.3.1, it would not be possible to fit 3 probes above the 14x14mm part of the element, due to some extra space required for the clamping of the sensors, but it will be possible to fit 3 sensors above the 19x19 mm part of the element. However, measuring the 19x19mm part of the element would add some extra tolerance, as described in the last section (section 3.2.1)

Interferometry

As explained in section 2.3.1, an interferometer only measures the difference in phase of the wavelength between the sample and its internal reference [13]. This becomes a problem when a difference in phase is measured but it is unknown how many wavelengths difference in distance there is between the measured sample and its desired position. This makes interferometry not a suitable option.

Lasertriangulation

A lasertriangulator would be a valid option for the setup. This is because it has good specifications and contrary to the probe, it does not touch the element physically. The measurement range of the lasertriangulator is somewhat limited in comparison with the probe, but this is not a problem for some of the measurement concepts. Since the minimal distance between the laser and the side of the sensor is 8 mm, as was presented in 2.3.1, using multiple sensors, only the 19x19 mm part of the element could be used as a measurement surface. This would add the alignment tolerance between the 19x19mm and the 14x14mm part of the element to the tolerance chain.

Confocal microscopy

(Chromatic) Confocal microscopy can be used in the same type of setups as lasertriangualtors. The advantage of confocal microscopy is that they usually have higher accuracy and precision and that they are more suitable for reflective surfaces. However, since the price of a confocal sensor is almost 5 to 10 times higher than that of a lasertriangulator, a lasertriangulator is more suitable for the feasability demonstrator setup. If after verification, the tolerance of the sensor would add too big of a tolerance to the tolerance chain, a recommendation could be made to use a chromatic confocal sensor for the production-ready design.

Autocollimator

The autocollimator is an interesting option as it can measure the tilt with high precision. Something that might be a problem is that the element surface might not be big enough for the autocollimator to work properly, since the element of the autocollimator, discussed in section 2.3.1, is 40 mm wide. However, the autocollimator option should still be investigated as a solution could be found for this problem.

The autocollimator should be paired with a distance sensor since the autocollimator can not measure distance. The best option would be to have the autocollimator measure the 14x14mm element and the distance sensor to measure the element mount directly since it would not fit to have them both above the 14x14mm or 19x19mm part of the element. Both the lasertriangulator and probe would be a good option for the distance sensor. A lasertriangulator would be preferable to measure this surface. The autocollimator will therefore be paired with the latertriangulator to be able to measure all 3 degrees of freedom.

Movable Sensor

Due to the advantages the moving a sensor with one or multiple stages brings, as discussed in section 3.1.5, it would be a suitable solution for measuring multiple points across an XY plane. Also since only one sensor would be needed, the 14x14 mm part of the element could be used for the measurement. The alignment tolerance between the 14x14 and 19x19 part of the element does therefore not need to be included in the tolerance chain. Since a probe has the probability to do damage and since more time would be needed to measure multiple coordinates due to the probe needing to be retracted and slowly expanded after each measurement, a lasertriangulator would again be a better option to combine with a stage. The autocollimator could also not be paired with a stage since it is highly sensitive to any small tilt deviation that is generated by the motion of the stage.

Another option would be to use a stage in the direction of the z-axis to make up for the limited range of certain sensors. However, if the reference is in the measuring direction, this is not needed and would only add an extra component to the tolerance chain.

3.3 Adjustment

to adjust the stack the dynamic pins must be guided towards their desired position. This will be done by an actuator. As discussed in section2.3.3, it will be selected in this subsection. However, to be able to adjust the stack with high precision, not only does the actuator need to have a small step size, but the pin must also be able to move smoothly. If the dynamic pins would have stick-slip, the pins would not follow the actuator during a downwards movement of the actuators. This causes the element mount, and thus the element itself, to be non-adjustable by moving the dynamic pins by a normal pushing actuator. Therefore first a test needs to be done to check for stick-slip.

3.3.1 Stick-slip test

To test for stick-slip a test setup has been made as shown in figure 3.14. The test features the element module with 3 adjustable screws underneath the dynamic pins to act as actuators for the pins. By unlocking the dynamic pins and adjusting the screws an observation can be made if the dynamic pins indeed follow the adjustable screws during a upwards and downwards motion.

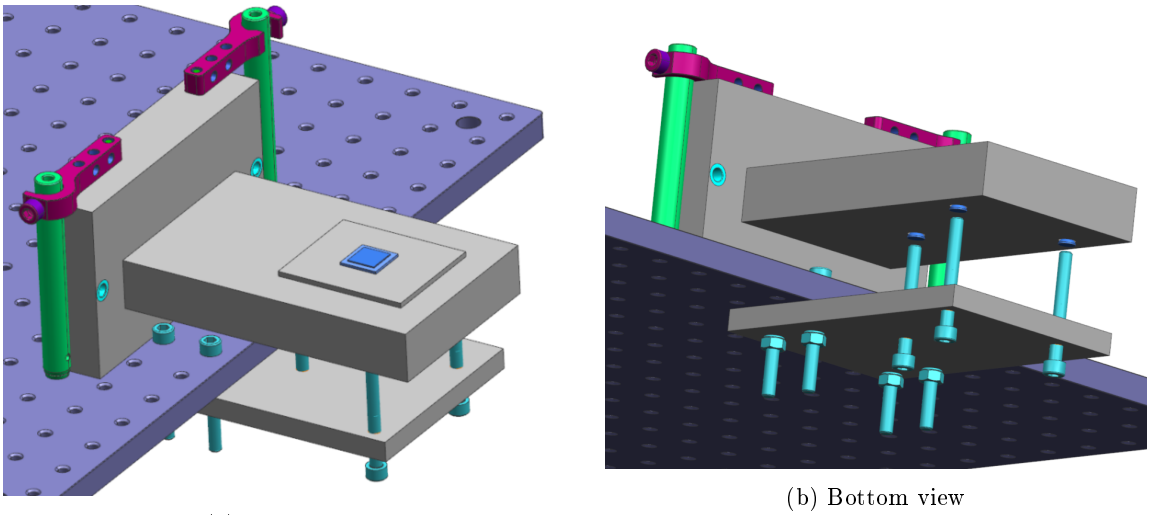

(a) Top view

(b) Bottom view

Figure 3.14: Stick-slip test

From the test, it could be concluded that the dynamic pins can follow the three screws when they where adjusted both upwards as downwards. However, this was only possible while the element mount positioned in its nominal X, Y, Rz position. This is because, as mentioned in section 1.1, the X, Y, Rz adjustment is done with 3 actuators inside the microscope, that push against the element mount. When these actuators are not pushing against the mount, it will be pushed against endstops due to internal springs inside the module. When pushed against the endstops, due to the friction between the endstops and the element mount, the element mount is locked and can not move smoothly in the Rx Ry and Z direction.

To fix this problem, 3 actuators are needed for this setup to that can provide a force equal to the internal springs to the element mount in the X, Y, and Rz direction. This causes the element mount to be released from its endstops such that a frictionless mobility is possible again. However, This is only possible if the there is low friction between the actuator and the element mount such that the element mount can move vertically. A solution for these X, Y, and Rz positioners will be presented in the next chapter as it will not influence the design decision that needs to be made in this chapter.

3.3.2 Actuator selection

A possible solution would be to use a piezo actuator. These are compact, have a small step size, and can have a substantial load capacity. In figure 3.15 an example of a piezo actuator, called "picomotor"[28], is given. Its specifications satisfy the requirements presented in section2.3.3.

(a) Picomotor

Models	8301NF
Travel Range	12.7 mm
Maximum Speed	1.2 mm/min
Axial Load Capacity	22 N
Minimum Incremental Motion	<30 nm
Drive Torque	0.018 Nm
Frequency	2 kHz
Mounting	9.5 mm Shank

(b) Picomotor specifications

Figure 3.15: Selected piezoactuator (from [28])

As explained in section 2.3.3, the design of the setup is a lot less reliant on the choice of the actuator than it is on the combination of calibration approach and the sensor. Since the actuator presented above satisfies the requirements, and since this actuator is more commonly used within ASML, it will also be used for this application.

3.4 Concept selection

Now that all suitable solutions for the sub-problems have been found, the different solutions will be combined to form different concept designs for the whole setup. These different concepts will be discussed and by using various selection criteria the most suitable concept will be selected by using a trade-off with selection criteria.

3.4.1 Selection criteria

Before the concepts are generated and discussed, the different selection criteria will be elaborated that will be used for the trade-off in section 3.4.3 to select the most suitable concept. These selection criteria are based on the requirements and boundary conditions discussed in section 1.2.2. For each criterion, a score will be given. An overview of the different scores of each criterion can be seen in table 3.1, with a "Low" score being preferable. The selection criteria are ordered from most important to least important criterion.

	Low	Medium	High
Total tolerance	Tolerance<100%	100%<Tolerance<150%	Tolerance>150%
Risk of failure	Adjustable	Partly adjustable	Not adjustable
Operator actions	2 operator actions	3 operator actions	4 or more operator actions
Complexity	5 subsystems	6 subsystems	7 or more subsystems

Table 3.1: Different selection criteria

Total tolerance

The in section 1.2.2 stated requirements for the total tolerance build up of the setup is ± 1 *mrad* in Rx and Ry and 0.1 *mm* in Z. All concepts that have a calculated tolerance within the requirements therefore score a "Low" on this criterion. If a concept would score within 150% of the requirements it would score a "Medium". This is because although the requirements are not met, a discussion could be held if a slight deviation from the requirements would still be acceptable, since it would require other tolerance budgets of the module to be more strict than was originally planned for. A total tolerance of above 150% of the requirements would be unacceptable and would, therefore, score a "High".

Risk of failure

As discussed in section 3.2.2, most of the sensors have a specific risk of not meeting the requirements and boundary conditions when used to measure the element. These risks include, doing damage to the element, having to little margin for error, and doing a wrong measurement. If a certain failure would occur but could be still be fixed with some slight adjustments it would score a "Low". If some big adjustments need to be made or it could only be partial adjustable, it would score a "Medium". If a concept would fail if a certain risk occurs without a way to adjust it, it would score a "High".

Required operator actions

One of the boundary conditions is that the setup should require as less operator actions as possible. This is because manual actions could lead to deviations as discussed in section 2.2.1.8. Since the locking of the dynamic pins and the integration of the module is necessary for each possible concept, the need of 2 mechanical actions preformed by the operator for a concept is scored as "Low", 3 required manual mechanical actions is scored as "Medium", and 4 or more required manual mechanical actions is scored as "High".

Complexity

Since a setup with more interacting electrical and mechanical systems would require more testing and calibration, this is also one of the selection criteria. Calibration needed imposes a risk of a wrong calibration that would result in the setup malfunctioning. The minimum amount of required subsystems would be 5, consisting out of the sensor, the docking with the flange (as discussed in section 2.4.3), the locking mechanism(as discussed in section 2.4.5), The X, Y, Rz positioners (as discussed in section 5.6.3), and the actuators (as discussed in section 3.3.2). 6 subsystems would resulst in a "Medium" score for complexity, and 7 or more would result in a "high" complexity score.

3.4.2 Concept generation

As discussed in section 3.1, the most suitable calibration approaches are: having a reference in the measurement direction, using a golden reference, and using a coplanar reference. As discussed in section 3.2.2, the most suitable sensors are: the probe, the lasertriangulator, using a autocollimator in combination with a lasertriangulator, and using a stage with a lastertriangulator. These can be seen in figure 3.16.

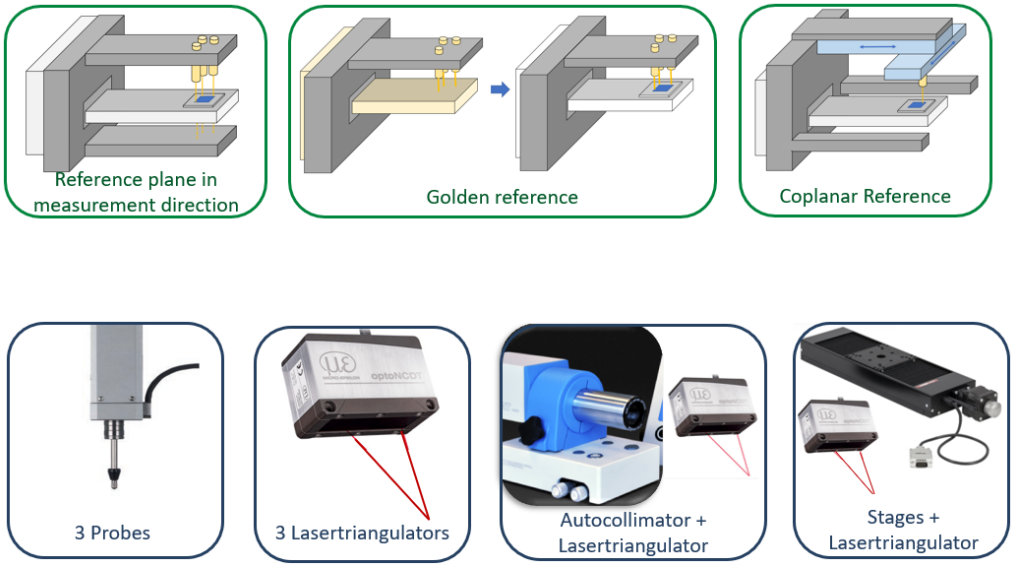

Figure 3.16: Most suitable options for the subsystems

These options will be combined to form concepts for the design of the setup. Not all combinations are equally viable however. Therefore, for each of the calibration methods will be explained what viable sensors options are.

For the reference in measurement direction calibration method, a sensor which can measure over a long range is desired. This can be done by either having a sensor with a long range itself or by having a sensor on a stage in the Z direction. The addition of a stage in the Z direction will not be explored since it would add a considerable tolerance component to the tolerance chain, which is not necessary since there are other options. Since the probe is the only sensor with a large range, the reference in measurement direction calibration method will be paired with the probe to form the first concept.

The golden reference can be paired up with all four sensor options. However, it does not require a sensor with a long measuring range. Therefore, the other three sensor options are more beneficial than the probe sensor, since they do not have the risk of damaging the element. The golden reference will thus be paired with the lasertriangulator, the autocollimator and lasertriangulator combination, and the stages and lasertriangulator combination.

The coplanar reference setup requires a sensor on a stage. As explained in section 3.2.2, an autocollimator or a probe on a stage are less desirable options then the lasertriangulator. Therefore, the coplanar reference setup is paired with the lasertriangulator to form the fifth concept.

These combinations can be seen in figure 3.17.

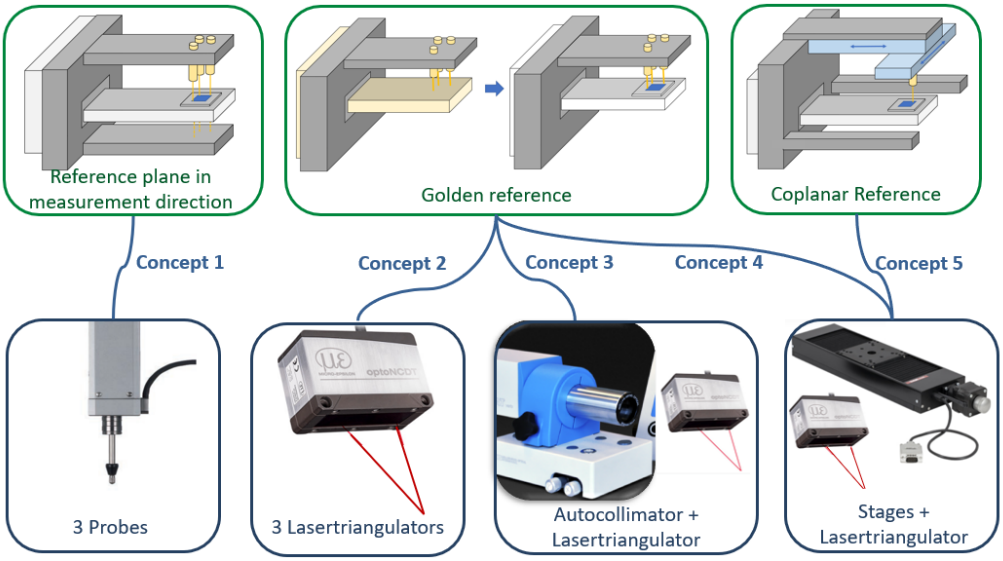

Figure 3.17: concept creation

The different concepts will now be discussed separately and the most suitable concept will be chosen for the design. The respective tolerance chains can be found in appendix D. The tolerance chains are based on the tolerance chains of section 3.1 and have the tolerances of the actuator, the chosen sensor, and the tolerances of the locking mechanism added. They are calculated via the calculation method discussed in section 2.2.2.

Concept 1: Probe with reference below element

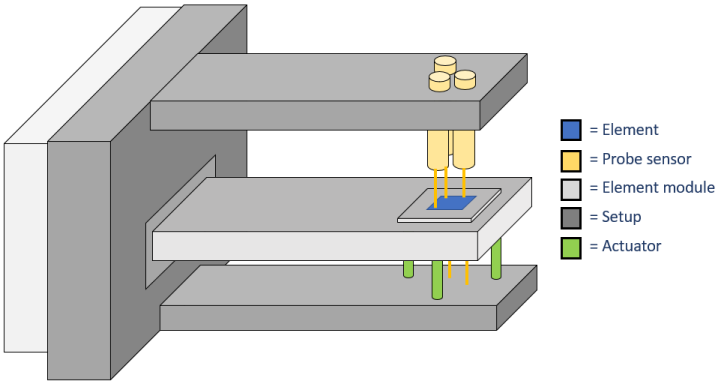

Figure 3.18: Concept 1

The first concept, which can be seen in figure 3.18, is a combination of the probe sensor and calibration method with the reference below the element. First the sensors would measure the reference plane, which is positioned at the bottom of the setup. Then the operator would integrate the element module so that the element can be measured. The actuators would then, after the dynamic pins are unlocked, adjust the element to equal the same Rx and Ry of the reference plane and the predefined Z with respect to the reference plane. The dynamic pins can then be locked again and the element module can then be disintegrated from the setup with its element positioned in its desired position within the required tolerance.

The advantage of the first concept is that it has a rather simplistic design; it requires only two operator actions and exists only out of the minimal 5 subsystems. This gives it a "Low"

score for both required operator actions and Complexity of the selection criteria. The total tolerance of the concept, which can be seen in Appendix D, is within the requirements. The disadvantages are however that there is a possibility of damage due to the probe sensors touching the element. Another disadvantage is that, since the sensors could only measure three predefined locations on the element, the risk of particle on one of the designated measurement locations makes for a wrong measurement. Although there are solutions to this issue, if the probe would do damage to the element this would not be easy fixable. This concept therefore scores a "High" the risk of failure selection criterion.

Concept 2: lasertriangulation golden reference

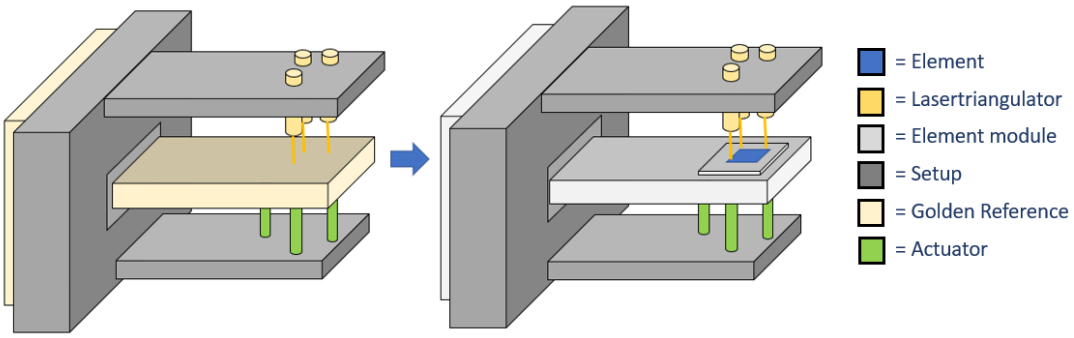

Figure 3.19: Concept 2

The second concept, which can be seen in figure 3.19, is a combination of three lasertriangulators and a golden reference. First the operator would integrate the golden reference into the setup to measure the golden reference with the sensors and get the reference values for Rx, Ry and Z. Next, the operator would extract the golden reference from the setup and integrate the element module. The sensors will then measure the Rx, Ry and Z coordinates of the element after which the required adjustment of the element will be calculated. Next, the actuators will adjust the element, after the dynamic pins are unlocked, so that coordinates of the element matches the Rx, Ry, and Z coordinates of the golden reference. Lastly, the dynamic pins can be locked again and the module can be disintegrated from the setup.

As can be seen in Appendix D, the tolerance of this setup is well within the required tolerance budget. It thus scores a "Low" for total tolerance. Furthermore, the setup is not that complex it only has the basic subsystems described in section 3.4.1 and therefore scores also scores a "Low" for complexity. However, one of the downsides of this concept is that due to the golden reference, it requires an additional operator handling, and therefore scores a "Medium" for operator actions. Another downside is the risk of failure. Since the three sensors need to be placed close to eachother it is rather limiting for the design and the choice of sensors. Especially if the sensors would not comply with the required tolerance or can not measure the reflective element and other more expensive sensors would need to be chosen. Since this concept poses strict geometric constraints next to the performance requirements on the sensor, it scores a "Medium" in risk of failure.

Concept 3: Autocollimator golden reference

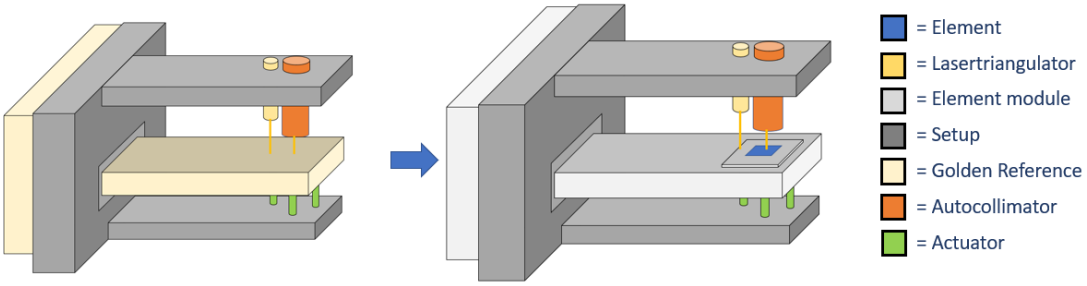

Figure 3.20: Concept 3

The third concept, which can be seen in figure 3.20, is a combination of the golden reference with an autocollimator and a lasertriangulator. First the golden reference will be implemented into the setup to obtain the desired coordinates of the element for the sensor. Then the element module will be implemented and the element will be measured. After the dynamic pins will be unlocked, the element will be adjusted by the actuators until it reaches the desired coordinates. The dynamic pins can then be locked and the element module can be disintegrated from the setup.

The advantage of this setup is that it, just as the previous two concepts, does not feature extra subsystems and it therefore scores a "Low" on complexity. However, there are a couple of disadvantages. The first disadvantage, as can be seen in appendix D, is that its total tolerance not satisfy the tolerance requirements due to the height measurement done by the lasertriangulator, that, due to a lack of space next to the autocollimator, is required to be done on the element mount and thus adds the tolerance chain in Z from the element mount to the element. Since the Z tolerance is still within 150% of the requirements, it scores a "Medium" for total tolerance. The other disadvantage is that it is not sure if the autocollimator could properly measure the element due to its small surface. If this would not be the case, the whole concept would fail without room for adjustment to still make it work. Therefore, it scores a "High" on risk of failure. Furthermore, just like the previous concept, the setup would require an extra operator action, which lets it score a "Medium" on operator actions.

Concept 4: lasertriangulator on a stage with golden reference

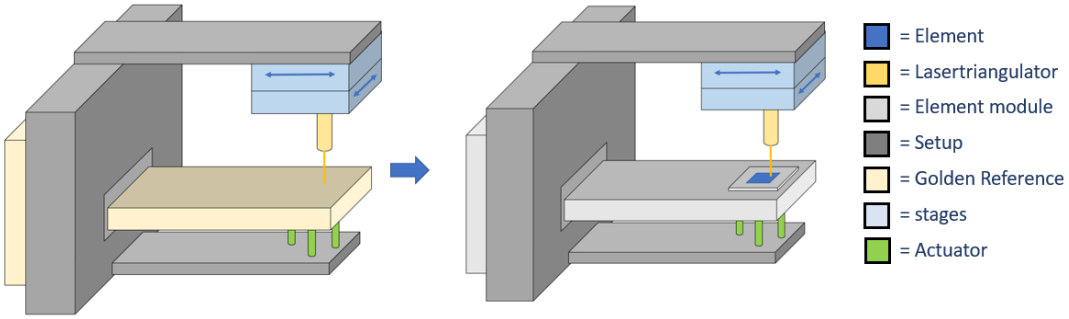

Figure 3.21: Concept 4

The fourth concept, which can be seen in figure 3.21, is a combination of a golden reference and a sensor on a X and Y stage. First the golden reference will be integrated into the setup, then multiple coordinates points will be measured with the sensor using the stages to measure the Rx, Ry, and Z coordinates of the golden reference. Next, the element module will be integrated into the setup so that the element can measure these same coordinates on the element. The required adjustment will then be calculated and, after the dynamic pins are unlocked, the actuators will adjust the element to till it reaches the same Rx, Ry, and Z coordinates as the previously measured golden reference. The dynamic pins will then be locked again and the module will be disintegrated from the setup.

The total tolerance of this setup is within the requirements as can be seen in appendix D, thus, it scores a "Low" on total tolerance. Another advantage is that the risk of failure is "low". This is because if the lasertriangulaor does not work due to a too high reflectiveness of the element, it can be simply swapped by a lasertriangulator or chromatic confocal sensor that is better in measuring reflective surfaces, this is because there are little geometric constraints for the sensor in contrast to the previously discussed concepts. Furthermore, if the repeatability of the sensor needs to be improved, more coordinates can be measured on the element to reduce the repeatability error, as described in section 3.1.5. The disadvantages of this concept are that because of the golden reference it requires an extra operator action and because of the stages it would require another component that needs to be tested and calibrated, thus scoring a 'Medium" for these criteria.

Concept 5: lasertriangulator on X and Y stages with a coplanar reference

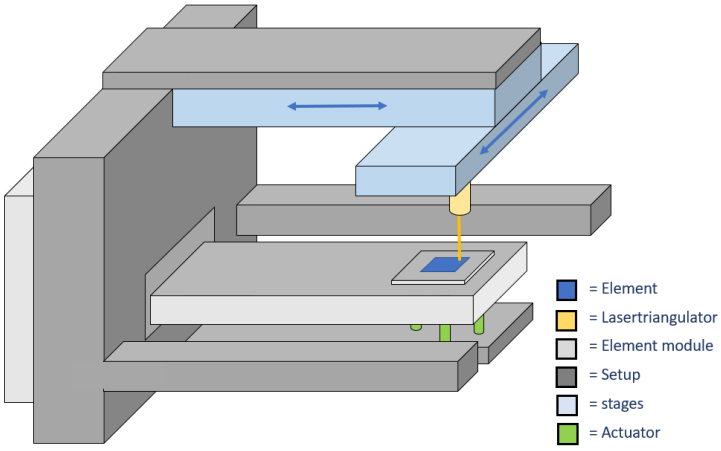

Figure 3.22: Concept 5

The fifth and last concept, which can be seen in figure 3.22, is a combination of a lasertriangulator on a X and Y stage with a coplanar reference. After the element module is integrated into the setup, the lasertriangulator first measures multiple coordinates on the coplanar reference, determining its Rx, Ry, and Z coordinates. Then multiple coordinates on the element are measured so that required displacement in Rx, Ry and Z can be calculated needed to adjust the element to the same Rx, Ry and Z coordinates as the reference. After the dynamic pins are unlocked and the element is adjusted, the dynamic pins can be locked again an the element module can be disintegrated from the setup.

Next to having the same advantages on total tolerance and risk of failure as the previous concept (and thus scoring "Low" on these categories). It also does not require the implementation of a golden reference and thus has a better score ("Low") for required operator actions. However,

just like the previous concept, the downside is that the stages would require some testing and calibration of their own and it thus scores a "Medium" for complexity.

3.4.3 Concept trade-off

Concepts	Total tolerance	Risk of failure	Operator actions	Complexity
1 Probe sensors reference below element	Low	High	Low	Low
2 Three lasertriangulators golden reference	Low	Medium	Medium	Low
3 Autocollimator golden reference	Medium	High	Medium	Low
4 Sensor on XY stage golden reference	Low	Low	Medium	Medium
5 Sensor on XY stage coplanar reference	Low	Low	Low	Medium

Figure 3.23: Trade-off concepts

An overview of the scoring of each of the different concepts can be seen in table 3.23. Since the importance of the selection criteria are ordered from left to right, it can be seen that the fifth concept scores the best overall. As discussed it only has a downside of having a bit of a higher complexity but with some extra tests, this should not be too big of a problem. Therefore, the lasertriangulator on X and Y stages with a coplanar reference, as can be seen in figure 3.24 is chosen to be designed for this project. In the next chapter it will a 3D design will be made of the concept which will be verified in chapter 5.

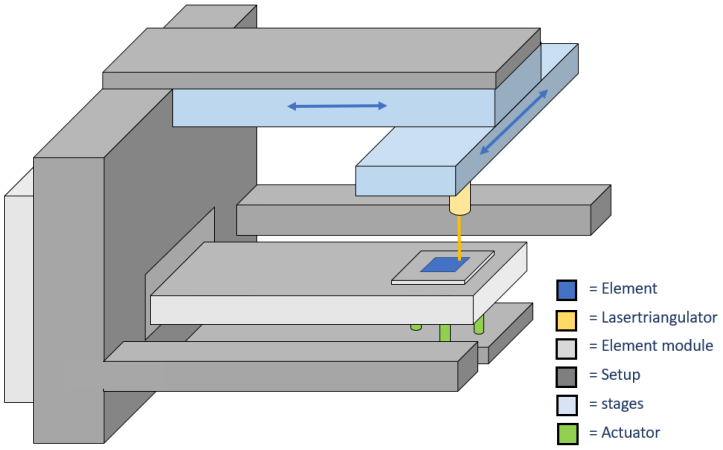

Figure 3.24: Selected concept

Chapter 4 Design

In this chapter, the 3D design of the setup will be elaborated. First, a general explanation of the setup will be given. After that, the different sub-systems within the design will be discussed more extensively.

4.1 Design overview

The setup with all its sub-features can be seen in the figure 4.1. It functions by measuring the orientation of the element with respect to a reference plane consisting of the top surface of three pillars, which are coplanar (have the same Z, Rx, and Ry positions) with the desired orientation of the element.

To gather information about the orientation of the stack with respect to the reference pillars, the height (Z) of multiple points (in X and Y) is measured such that two planes can be fitted through these points. One plane for the element and one plane for the reference pillars.

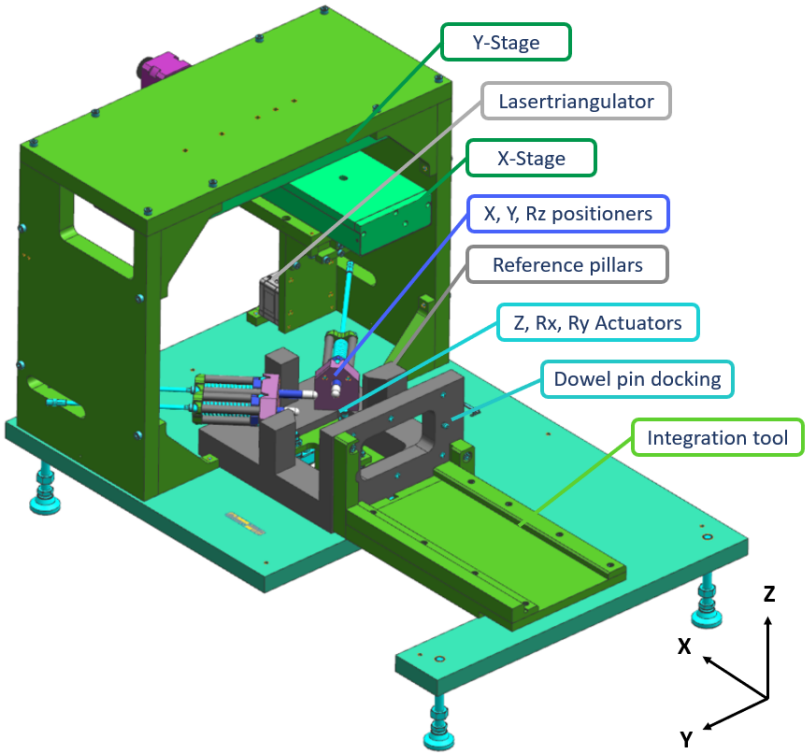

Figure 4.1: Design overview without the element module

To measure the height of these points a lasertriangulator is used that is positioned by an X and a Y stage to the different locations. After the points for the two planes are measured and the planes are fitted the adjustment is calculated and is carried out by three actuators located under the three dynamic pins, as you can see on the next page in figure 4.2a.

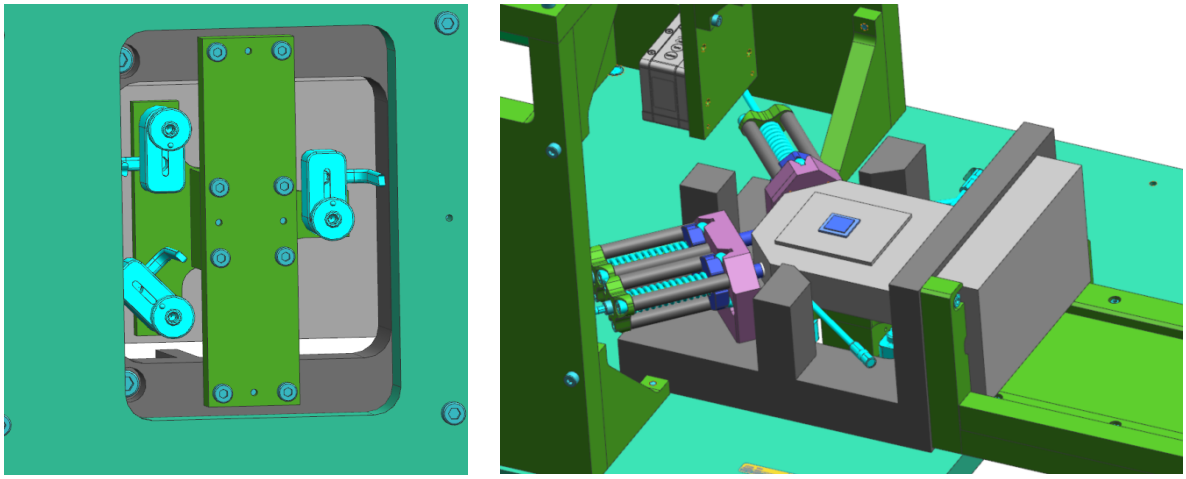

(a) Adjustment actuators (b) X, Y, Rz positioners

Figure 4.2: Two sets of actuators in the setup

The last part of the setup is the three positioners that can be seen in figure 4.2b. They are used to postition the element mount in its nominal X, Y, and Rz position such that the dynamic pins can move stick-slip-free, as has been discussed in section 2.3.3. These positioners will be called "X, Y, Rz positioners" henceforth. The other three actuators located at the bottom of the setup will be called "adjustment actuators".

In the next sections, the different parts of the setup will be discussed more extensively.

4.2 Integration of the element module

To insert the element module into the setup, the same integration tool will be used as is previously used for another element module calibration tool. This integration tool can be seen in figure 4.3. Furthermore, the same interface for the connection of the element module is used as is present on the microscope. This interface exists out of two dowel pins (of which one diamond-shaped dowel pin) to align the element module with the setup and out of 6 bolts to fix the module into the setup. Since the reference setup is made from aluminium, to prevent galling and secure longevity of the connection after multiple uses, helicoil inserts[33] are used.

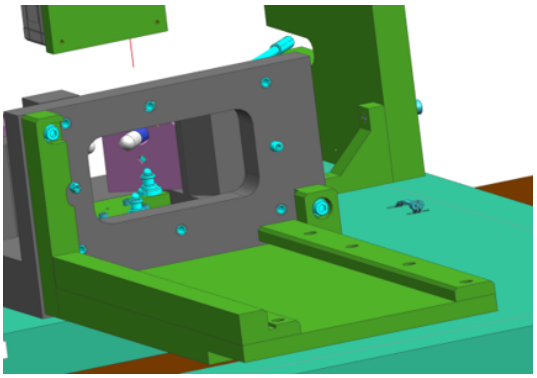

Figure 4.3: Integrating the element module

The operator can insert the element module by sliding it along the integration tool until it reaches the flange of the setup. The integration tool ensures that the module is aligned with the dowel pins such that the operator can just secure the module in place with bolt connections. To ensure a good reproducibility the prescribed integration procedure for this connection interface is used.

The setup is supported by a support plate, which has a cut-out such that the integration tool can be adjusted to its desired position during the assembling of the whole setup. The integration tool needs a one time adjustment so that the the dowel pin bushings of the mounted element module line up perfectly with the dowel pins.

4.3 Measurement

In this section, the measurement process will be futher explained. First, the selected sensor will be presented, then the chosen stages will be presented. After that, the reference pillars that act as the coplanar reference for the element will be further explained.

4.3.1 Sensor

To measure the height of the different points on the element and the calibration pillars, the ILD1900-10 lasertriangulator from Micro-Epsilon is chosen. The sensor and its specifications can be seen in figure 4.4.

Model		ILD1900-2	ILD1900-10
Measuring range		2 mm	10 mm
Start of measuring range		15 mm	20 mm
Mid of measuring range		16 mm	25 mm
End of measuring range		17 mm	30 mm
Measuring rate [1]			7 adjustabl
Linearity [2]		< ±1 µm	< ±2 µm
		< ±0.05 % FSO	
Repeatability [3]		< 0.1 µm	< 0.4 µm
Temperature stability [4]			
Light spot diameter (±10 %) [5]	SMR	60 x 75 µm	115 x 150 µm
	MMR	55 x 65 µm	60 x 65 µm
	EMR	65 x 75 µm	120 x 140 µm
	smallest diameter	55 x 65 µm with 16 mm	60 x 65 µm with 25 mm

Figure 4.4: ILD1900-10 lasertriangulator (from [16])

The possible z displacement of the element spans over a range of approximately 1.7 mm, as specified in section 1.1. This means, that both a sensor with a range of 2 mm and a sensor with a range of 10 mm would be suitable options. However, since the repeatability of the 10 mm range sensor is sufficient for the tolerance budget, as will be discussed on the next page, and since this leaves more space for the height tolerances in z of the alignment from the sensor to the element, the sensor with the 10 mm range is chosen.

As discussed in section 3.1.5 only the precision of the sensor accounts for the tolerance of the sensor. This is represented with the repeatability error in figure 4.4 and is equal to 0.4 μm. To calculate the Rx, Ry and, Z orientation of the element multiple points are measured on its surface and a plane is fitted through these points to calculate its angles and height.

From different tests in the past, it is known that the repeatability of the X and Y location of the element within the element module is approximately 0.4 mm in-between different. Next to this repeatability, the laser of the sensor also needs to be positioned fully on the element. Since the element would be measured around the middle of the range of the sensor, from figure 4.4 it could be concluded that the spot size would be between 60 and 100μm. Half of this diameter (50μm) will be added to the buffer zone. Lastly the X, Y, Rz positioners, which will be more thoroughly discussed in section 4.4.1, have a specific tolerance in X, Y, Rz and would therefore also add a small portion to this buffer zone. Since they are designed specifically to

have a small X, Y, Rz tolerance, it is estimated that this would be around $50\mu m$, even after the adjustments made to the original design. This will be tested in section 5.5.4. This means that the sensor can measure up to 0.5 mm from each side of the element. Since the element is $14x14$ mm, a measurable surface of $13x13$ mm remains.

If two points would be measured with an uncertainty of $0.4\mu m$ at 6.5 mm from the center to calculate Rx or Ry, this would result in a tolerance of $0.062mrad$. As can be seen in figure 4.5.

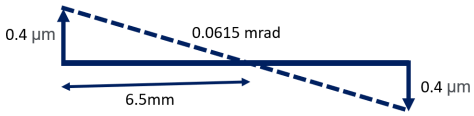

Figure 4.5: Geometrical representation measurement tolerance

However, since the sensor can measure multiple points to determine the orientation of the element the added tolerance due to the sensor can be reduced. Using the formula presented in section 3.1.5 ($SE = \frac{\sigma}{\sqrt{N}}$) and taking into account that the tilt tolerance can be calculated by $\sigma_{tilt} = \frac{\sigma}{r}$ the following formula can be derived to describe the measurement tolerance for tilt.

$$SE_{tilt} = \frac{\sigma}{r_{avg} \cdot \sqrt{N}} \tag{4.1}$$

SE_{tilt} is the measurement tolerance for tilt
σ is the precision tolerance of the sensor
r_{avg} is the average arm (distance) between a point and the middle of the measured sample.
N is the amount of data point measured.

To reduce the Rx and Ry measurement tolerance 36 points for measurement are chosen at 6.5, 6 and, $5.5mm$ from the center of the element, as can be seen in figure 4.6, thus having an average of 6 mm. This results in a remaining measurement tolerance of 0.0011 $mrad$ for the tilt and a 0.0067 μm measurement tolerance for the height. Note that the reduction of the tolerance of the sensor is important since the sensor tolerance will probably be higher than specified in figure 4.4 since these are the properties of the sensor in ideal circumstances.

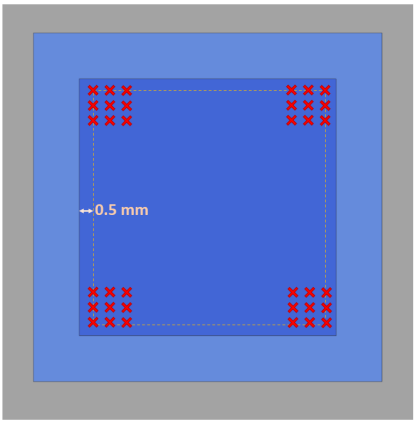

Figure 4.6: measurement locations

4.3.2 Stages

To bring the sensor to the different points two identical stages are used with a travel range of 150 mm. They are mounted orthogonal to each other such that one is responsible for the translation in X and the other in Y. The selected stages can be seen below. The wobble of the stages (deviation in Z while moving in X or Y) is not specified but will be tested during the verification process. It is expected that it will add a tolerance of around ± 0.05 $mrad$ in Rx and Ry and ± 5 μm in Z.

Key Specifications[a]	
Travel Range	150 mm (5.9")
Velocity (Max)[b]	30 mm/s
Minimum Achievable Incremental Movement	0.1 µm
On-Axis Accuracy[c]	2.0 µm (Typical) 5.0 µm (Max)
Bidirectional Repeatability[d]	1 µm
Backlash[e]	<3 µm
Horizontal Load Capacity (Max)	20 kg (44 lbs)
Vertical Load Capacity (Max)	5 kg (11 lbs)
Actuator Type	Stepper Motor
Cable Length	3.0 m (9.8 ft)
Recommended Controller	Benchtop Stepper Motor Controllers

Figure 4.7: Selected stages (from [29])

The surfaces of the pillars span a plane of 184 mm in X and 120 mm in Y. When the lasertriangulator is mounted on the stages, it can cover a square of 150 by 150 mm. Although this square covers the element and most of the surface of the pillars, as can be seen in figure 4.8a, the outer 17 mm of the left and right pillars can't be reached. However, since 150 mm in Y and 120 mm is sufficient, as will be discussed in section 4.3.3, this is not a problem.

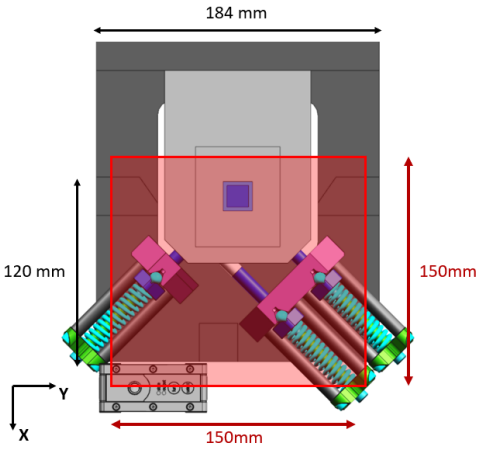

(a) Range of the sensor due to the stages

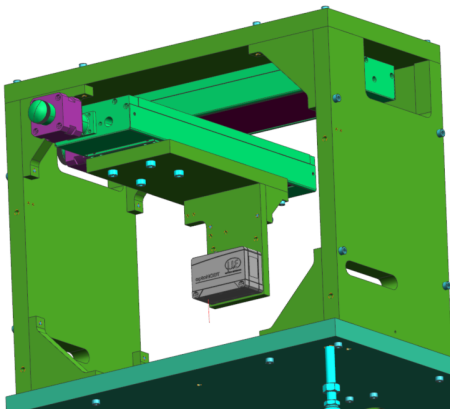

(b) Stages inside setup

Figure 4.8: The stages and their range

The connection part between the lasertriangulator and the stages, which can be seen in figure 4.8b, has a Z offset such that the pillars (thus the surface of the element) are positioned in the middle of the sensor range. This is because the sensor has the best precision while measuring in the middle of its range[16].

Although the stages are not tested if they are fully cleanroom compatible due to the possibility of particle generation from the moving parts, a bellow covers the moving parts in the stage such that any particles created can hardly leave the stage. To even further reduce the probability of contamination of the element, the connection part has an X offset to capture any falling particles and to keep the moving parts of the stages 30 mm away from the element and thus prevent particle contamination of the element.

4.3.3 Reference pillars

The geometric tolerances of the reference pillars have to be very small such that when the element is calibrated to the same orientation it is within the desired tolerances; these tolerances add up to the total tolerance train. As discussed in section 4.3.2, the total range that can be measured for these pillars is 120 mm in X and 150 mm in Y.

The top surfaces of the three pillars are defined as a common zone (denoted as "CZ") for their geometric tolerances. This means that the constraints act on the zone instead of on all of the surfaces individually, which is beneficial to the strictness of the constraints. This zone is represented with the blue plane in figure 4.9. If the axes of the dowel pin connections are denoted with A and B, the plane that connects these two axes is denoted with A-B (the red plane in figure 4.9), and the plane of the flange on which the element module is docked , denoted as C, the three geometric properties of the common zone can be defined.

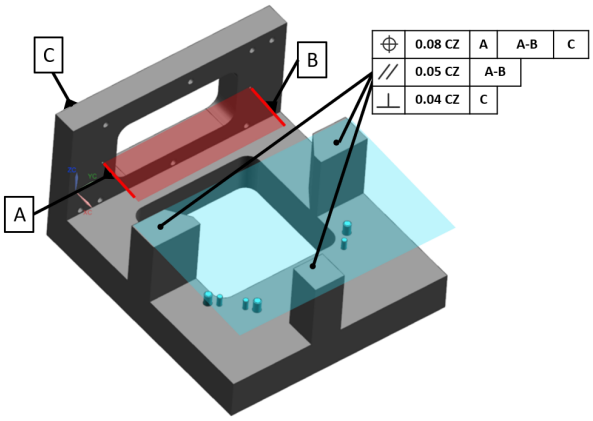

Figure 4.9: Geometric specifications reference pillars

Since for small angles the tangent goes to 1, the added tolerance due to the geometric specifications can be calculated as follows:

- The 0.08 mm position deviation corresponds to the Z tolerance of the pillars. Since the geometric specifications are equal to the total tolerance range, dividing them by 2 gives the tolerance for Z, thus $\frac{0.08}{2} = 0.04\ mm$.
- The 0.05 mm parallel deviation with a line that goes through both A and B of figure 4.3.3 corresponds to the Rx tolerance. This means that the plane could have a tilt to the point that, at the same X value, The two outer Y values of the pillars could either have a plus 0.05 mm height difference or a minus 0.05 mm height difference. Since for small angles, the tangent goes to 1, and since the range in Y of the common zone is equal to 184 mm, the added Rx tolerance is equal to $\frac{0.05}{184} = 0.27\ mrad$.
- The 0.04mm perpendicular deviation corresponds to the Ry tolerance. Using the same approach as with the Rx tolerance and a 120 mm range in X, the Ry tolerance due to the geomteric specifications is equal to $\frac{0.040}{120} = 0.33\ mrad$.

Next to the geometric tolerances, just like when measuring the element, also the measurement tolerances apply. Using the same calculation as described in section 4.3.1, This gives a 0.23μm tolerance in Z, a 0.0027 $mrad$ tolerance in Rx, and a 0.0034 $mrad$ tolerance in Ry using an arm of 116 mm and 146 mm respectively. Just like with the element, these tolerances can be reduced by using multiple measurement points if the tolerance of the sensor is higher than expected.

4.4 Adjustment

In this chapter, the adjustment of the element will be discussed. For the element to be adjusted, X, Y, Rz positioners are needed, these will be discussed in the first section. Then, the positioning of the actuators will be elaborated. In the last section, a calculation will be given that connects the sensor output to the required adjustment of the actuators.

4.4.1 X, Y, Rz positioners

As explained in section 3.3.1, the element mount needs to be pushed away from its end-stops for it to be able to move freely. To push the element mount off of its end-stops, the same actuators are used as has been previously used in the X, Y, Rz measuring setup mentioned in section 1.1. The documentation for these positioners can be found in the critical design report of ASML for that design [30].

There has been made two changes however. Firstly, the original positioners had tree ceramic balls per positioner that pressed against two ceramic plates each to fully restrict the positioners in all 6 DOF without overconstraining them. However, since the precision and repeatability for the actuators are less important for this setup, to reduce the long lead time on the specific needed ceramic parts, the balls where replaced with steel balls and the the ceramic plates where left out of the design so that the balls press against the aluminium of the setup (against the purple part in 4.10). Secondly, the original actuators were equipped with wheels on the tips to push against the element mount. This creates a line contact on the element mount that would have created too much friction on the element mount to let it move in the Z-direction. Since this is necessary for this setup, however, the wheels that were positioned on the tips of the actuators have been replaced by spherical tips made out of POM (Polyoxymethylene). Since it is spherical it only makes point contact with the moving body and since POM is a very hard plastic, the X, Y, Rz positioners apply force in the direction they face and apply way less friction when the element mount is moved upwards by the adjustment actuators. A closeup of the resulting actuators can be seen in the figure below.A calculation for the forces that act on the positioners can be seen in appendix E.

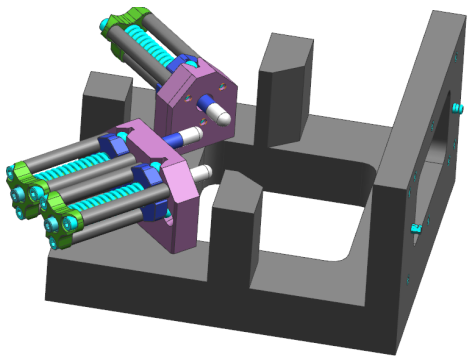

Figure 4.10: Modified X, Y, Rz positioners

4.4.2 Actuators

Underneath the dynamic pins, the actuators, that were chosen in section 3.3.2 are positioned. They are connected with the reference part via three different bodies depicted in green in the figure to the right. This is because it would be a too complex part to be made out of one body and the desired function can sill be met when splitting it in three separate bodies. The bodies are connected via dowel pins to each other and to the reference part to position the actuators accurately underneath the centres of the dynamic pins. The actuators and the bodies that connect it to the reference part can be seen in figure 4.11. Note that a dummy version of the element module is depicted as specified in section 1.1.

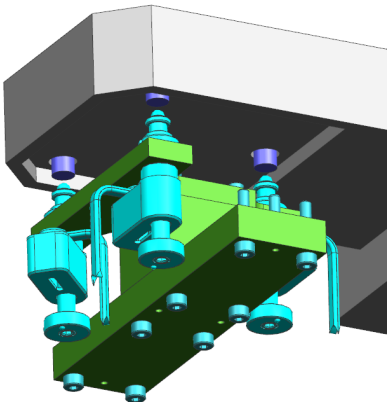

Figure 4.11: Actuators underneath the dynamic pins

The tips of the actuators are positioned roughly 6 mm below the nominal position of the dynamic pins when the actuators are in their retracted position. Before the dynamic pins are unlocked, the actuators need to extend such that they can keep the dynamic pins from moving below the lowest point of their range, which is 1.2mm underneath the nominal position of the pins (as described in section 1.1).

However, the problem is that the actuators are not positioned in the Z direction within tight tolerances (± 0.1 mm) with respect to the dynamic pins. This is due to the alignment and geometric tolerances of a numerous amount of bodies that connect the dynamic pins to the actuators. Another part of this problem is that the dynamic pins are located at an unknown Z coordinate along their range. Since this is the case, the actuators need to be calibrated so that their position and their required extension before the pins can be unlocked is known. A way to calibrate these actuators will be presented in the next chapter in section 5.6.2

4.4.3 Coordinate systems

There is a difference between the coordinate system of the stages and the coordinate system of the element. For the input of the stages, it is important to use the stage coordinates, which are represented in red in the figure on the right. To avoid confusion, the coordinate system used for the stages will denoted as K, L, M. For the fit it is important to use the element coordinates, this coordinate system is represented in blue in the figure on the right. For Y there is a 75 mm offset plus a calibration offset. For X there is both a 122.5 mm offset plus a calibration offset and the direction of the axis is reversed. Note that the angle between both coordinate systems does not have to be taken into account. The is setup makes that the stages have a small enough angle difference with respect to the element that it does not have an influence on the calculations. The element coordinates with respect to the stages can thus be calculated with:

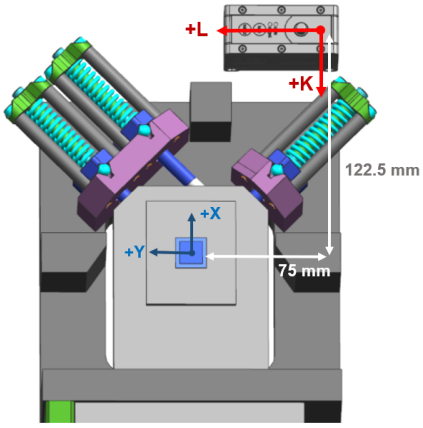

Figure 4.12: Coordinates systems

$$X_{element} = -(K_{stage} - 122.5 + K_{calibration}) \tag{4.2}$$

$$Y_{element} = L_{stage} - 75 + L_{calibration} \tag{4.3}$$

Calibration of these offsets will be done after assembling the setup by measuring the location of the pillars relative to the (0;0) point of the stages. This calibration process will be elaborated in the next chapter.

From the figure of the bottom of the element module presented in section 1.1 the coordinates of the dynamic pins with respect to the coordinate system of the element can be obtained. This can be seen in figure 4.13. After the points are measured and the plane fit of the element stack and the plane fit of the pillars is done. The displacement of the actuators can be calculated with:

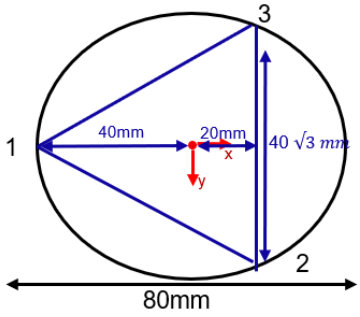

Figure 4.13: coordinates actuators

$$(dZ, dRx, dRy) = (Z_{pillars}, Rx_{pillars}, Ry_{pillars}) - (Z_{element}, Rx_{element}, Ry_{element}) \tag{4.4}$$

Using the geometrics of figure 4.13, the desired displacement of the actuators (dZ1, dZ2, and, dZ3) in regard to a certain change in plane fit between the pillars and the element can be calculated with:

$$dZ1 = y1 \cdot dRx - x1 \cdot dRy + dZ = 0 + 40dRy + dZ \tag{4.5}$$

$$dZ2 = y2 \cdot dRx - x2 \cdot dRy + dZ = 20\sqrt{3}dRx - 20dRy + dZ \tag{4.6}$$

$$dZ3 = y3 \cdot dRx - x3 \cdot dRy + dZ = -20\sqrt{3}dRx - 20dRy + dZ \tag{4.7}$$

4.5 Controllers and cables

To get all the different electrical components working, controllers and cables to these controllers are needed. First, the different controllers will be discussed. After that, the cable layout will be elaborated.

4.5.1 Controllers

To control the different electrical components, controllers are used. These are connected to a PC via USB and Ethernet connection. This can be seen in the figure 4.14.

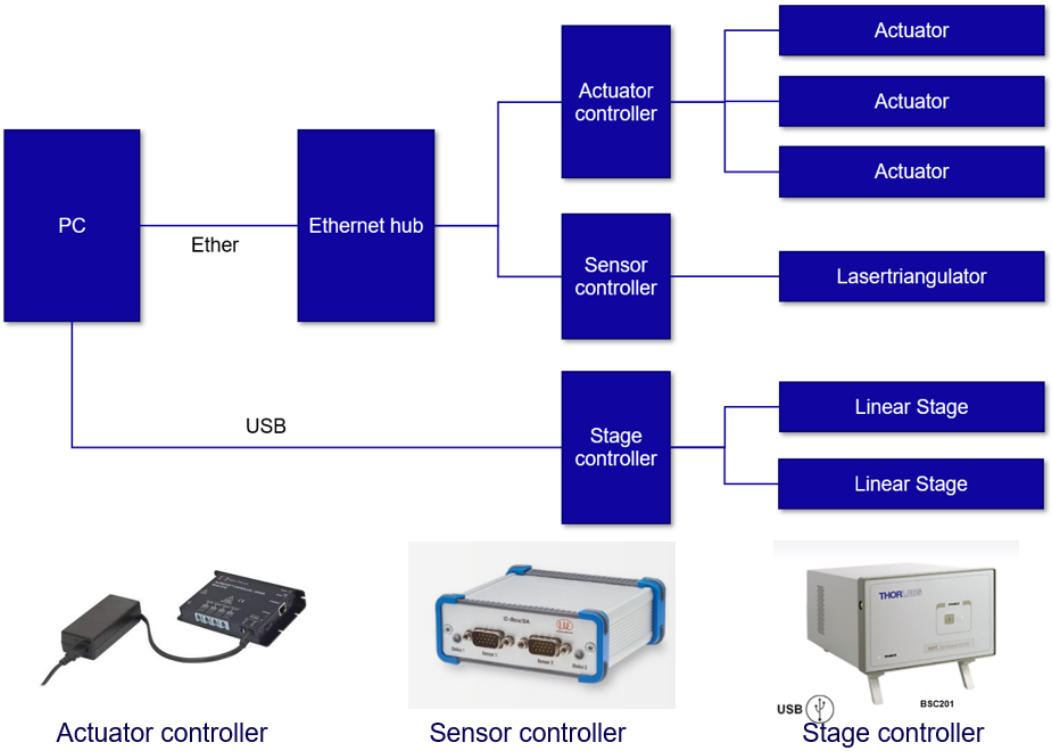

Figure 4.14: control schematics

4.5.2 Cable routing

The cable routing can be seen in figure 4.15, where the setup is placed on a 1x1 meter table with its controllers. The cables of the stages don't go across the setup and thus can be easily connected to the controller of the stages. For the cables of the actuators, a cable channel with tywraps is made that guides the cable from the actuators, under the baseplate, to the controller for the actuators.

The cable of the sensor does go over the element module and thus needs to be guided to prevent it from touching the element module, where it otherwise could do damage or generate particles. To guide the cable of the sensor, a drag chain is used which can guide the cable from the sensor to the controller along the range in which the sensor can move. The orientation of the dragchain constraints the cable of the sensor in an XY plane and thus prevents it from bending in the Z direction. Note that the drag chain will be connected during the build of the setup.

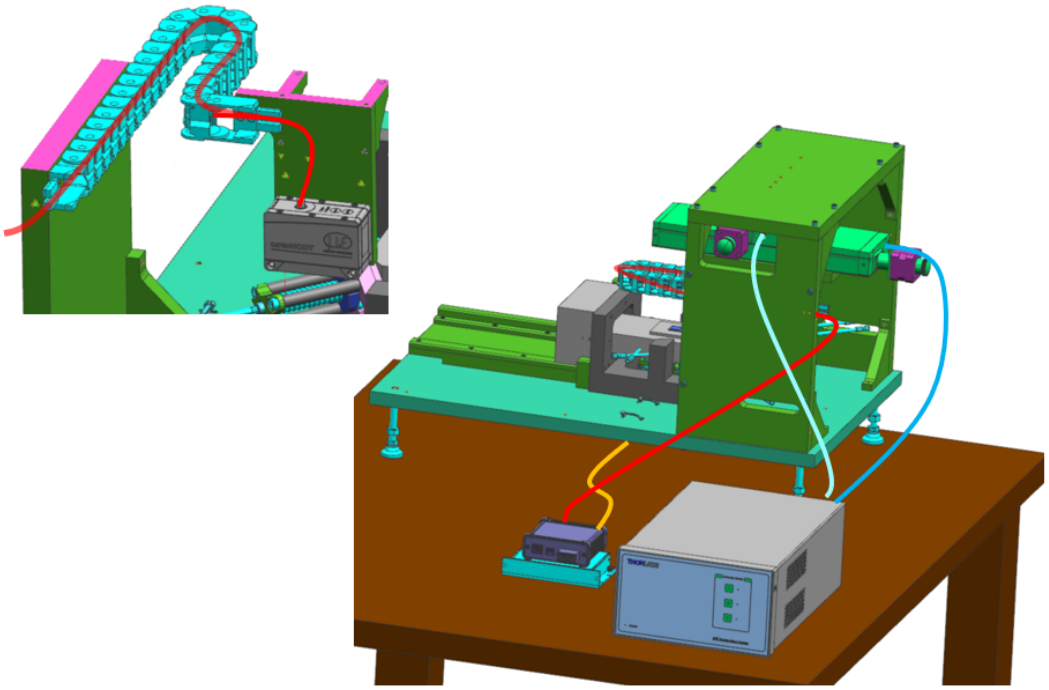

Figure 4.15: Cable routing

4.6 Process overview

Now that all the different aspects of the setup have been discussed, the process of the measurement will be elaborated. First, a flowchart of the process will be discussed. Then, all the required variables will be elaborated. Finally, the software will be presented.

4.6.1 Flowchart

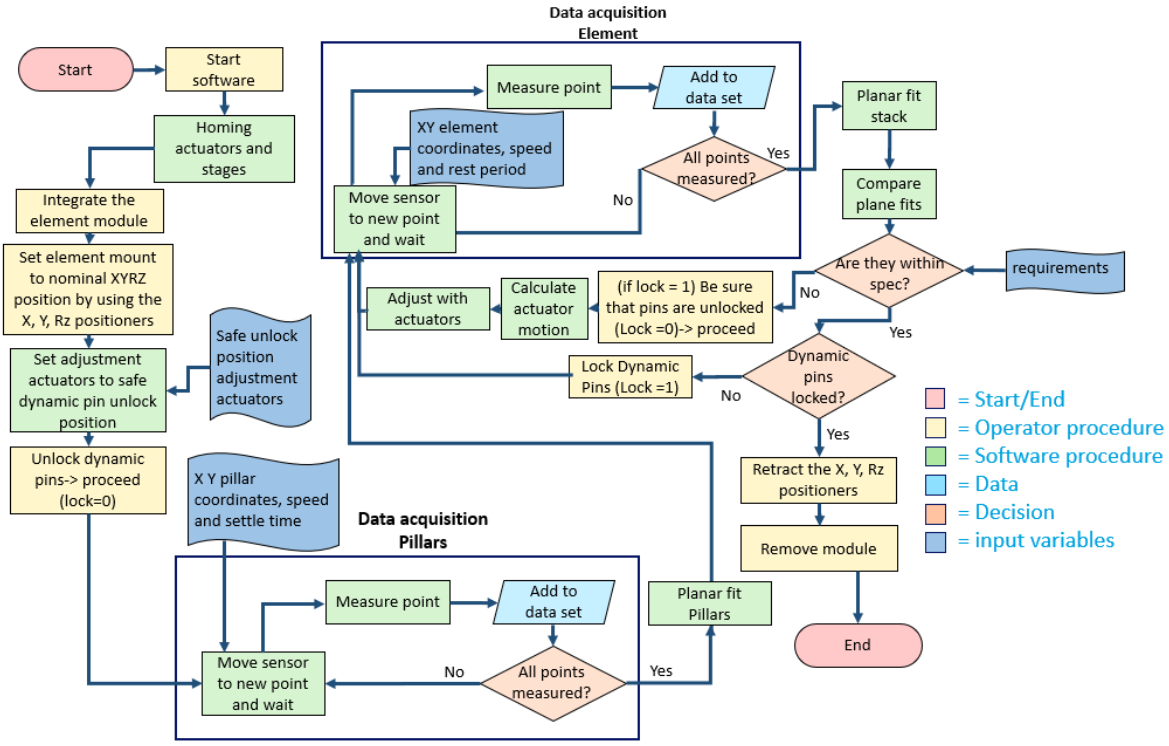

Figure 4.16: Flowchart calibration process

In figure 4.16 a flowchart of the calibration process can be seen. The calibration process is a combination of operator and software procedures. The decisions that are depicted by the orange diamond-shaped boxes are made by the software. To run the procedure successfully, a certain amount of variables are needed. These are listed below:

- Safe unlock position adjustment actuators: this is the extension of the actuators needed to prevent the dynamic pins from falling below their range once they are unlocked. The procedure to determine this variable is discussed in section 4.4.2.
- XY pillar coordinates: These are the calibration values needed to describe the location of the pillars more accurately to account for any alignment deviations that are made during the assembling of the setup. This is described in section 4.4.3.
- XY element coordinates: Just like for the pillars a similar calibration needs to be done for the element after it is put in its nominal position by the X, Y, Rz positioners.
- Stage speed and settling time: the optimal speed and required settling time for the stages such that they do not interfere with the measurement of the sensor will be tested in the next chapter.

- Requirements: these are the tolerance requirements specified in section 1.2.2 ($Z < 0.1\ mm, Rx < 0.1\ mrad, Ry < 0.1\ mrad$)) minus the geometric tolerances of the pillars and the added tolerance of the sensor since these are not taken into account while subtracting both plane fits from each other.
- Lock dynamic pins: This is a boolean of which the software asks the operator to give a status update. This is to prevent the automatic system to try to adjust the pins while they are in the locked position since this could cause damage to the module.

4.6.2 Adjusted flowchart

To decrease the amount of required software for the feasibility demonstrator, the flowchart is a bit adjusted. The adjusted flowchart can be seen in figure 4.17 The firmware of the actuators is used instead of having to write specially designed software. Furthermore, the purple decisions are decisions that will not be made with the software but need to be made by the operator. While these alterations do decrease the amount of required software, it only slightly increases the amount of operator work. This is because these operations does not have to be done simultaneously with the data acquisition, which involves short steps that have to be done after each other, and instead can be done after the data acquisition is done.

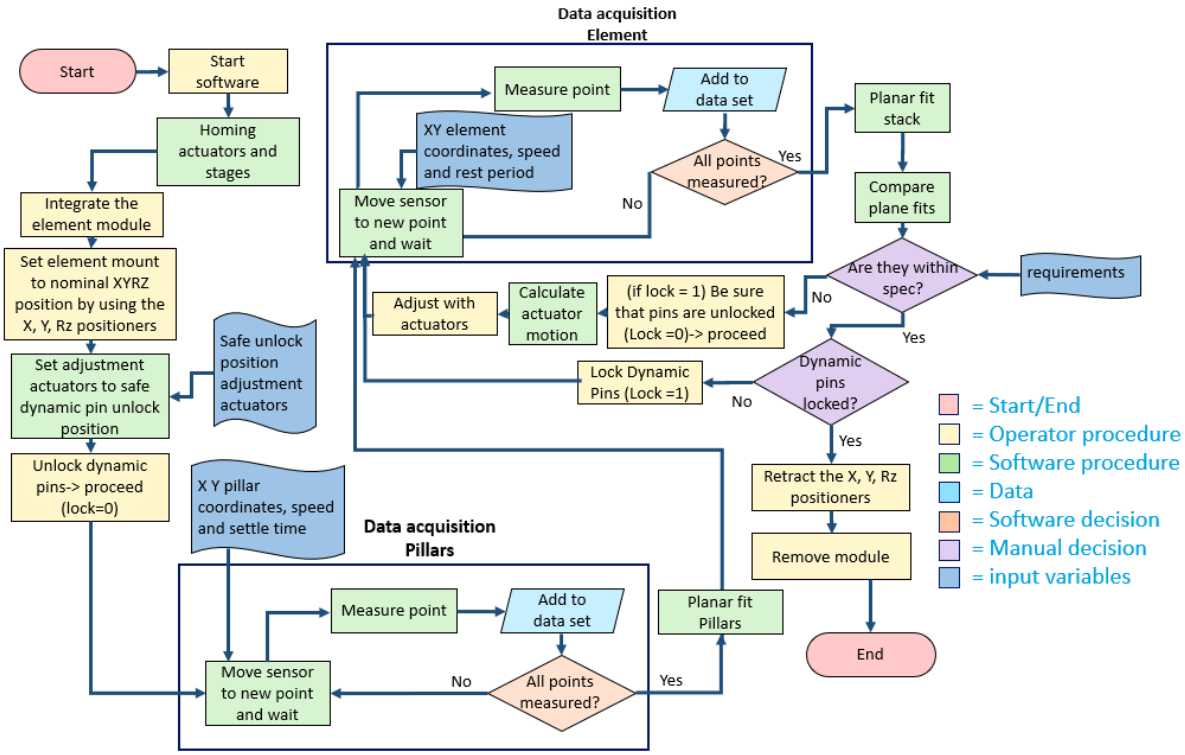

Figure 4.17: adjusted flowchart

To communicate with the different controllers of the electrical components and to run the flowchart, software was made by a software engineer within ASML.

4.7 Tolerances designed setup

In this section first, the remaining unknown tolerances will be calculated such as the tolerances due to bending and due to frequencies.

4.7.1 Bending

There are two bodies in the setup that could pose a risk to add a deviation due to bending. The first one is the top plate of the stage portal. In Theory the moving stage could bend the baseplate and thus add a deviation to the measurement. However, since the top plate is 20 mm thick and is supported by the Y stage across its length, it is safe to say that bending will cause any deviations that have to be taken into account. A simple calculation of possible bending due to the stages and sensor mount acting as a point mass on the middle of the top plate, is given in appendix E. Since the bending of the top plate is approximately 1 nm, it can be concluded that bending of the top plate can be neglected and does not have to be taken into account in the tolerance chain.

The other body that could add a certain tolerance to the tolerance chain due to bending is the support plate. This is because in theory, the 15 kg that rests on the middle of the support plate could cause the support plate and the part of the pillars to bend. This could alter the orientation of the surfaces of the reference pillars which would add a certain amount of tolerance to the tolerance chain. As can be seen in the simplified calculation in appendix E, the bending of the support plate is also around 1 nm, it can therefore be concluded that the bending of the support plate can be neglected and does not have to be taken into account in the tolerance chain.

4.7.2 Vibrations

The vibrations that act on the setup add to the precision in which the sensor can measure. The tolerance due to possible vibrations add up to the total tolerance of the sensor. Since the moving elements inside the setup move in the X and Y direction and the sensor measures in the Z direction. No big deviations due to internal vibrations are expected that will not subside after a short settling time. This will be tested in the next chapter in section 5.4.2.

Next to the internal vibrations there could also be external vibrations that influence the measurement accuracy. However, since all connections within the setup are stiff, since they are bolted together, it is not expected that this will have a big influence on the measurement accuracy. The influence of frequencies due to external vibrations will be tested in the next chapter in section 5.5.6.

4.7.3 Tolerance chain

The different tolerance contributors can be seen in figure 4.18. Their values can be found in table 4.1 on the next page.

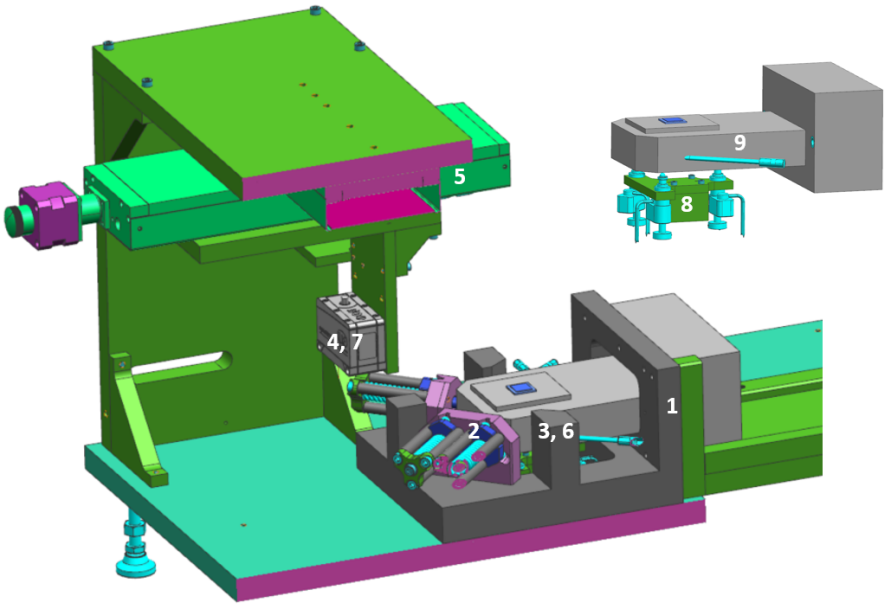

Figure 4.18: Tolerance contributors

1. When the element module is inserted into the setup, the first tolerance contributors are the docking tolerances. These are the tolerances that originate from the alignment deviation between the element module and the reference and docking part of the setup. These tolerances can be found in appendix A.
2. After the module is inserted into the setup the element has to be positioned in its nominal X, Y, Rz orientation. This is done by the X, Y, Rz positioners. However, these could cause a small displacement in Z. Although they are designed to counter any deviation in Z, this could still add a certain tolerance and will therefore be tested in the next chapter.
3. After the element module is docked and the element is positioned in its nominal X, Y, Rz, the pillars can be measured. The pillars have a geometric tolerance discussed in section 4.3.3.
4. The measurement of the planefit also has a certain deviation to account for which is discussed in section4.3.1.
5. Furthermore, the tolerance due to the wobble (deviation in Z when moving in X and Y) of the stages.
6. Then there is a temperature tolerance to account for due to a possible change in temperature in-between measuring the pillars and the element (as discussed in section 2.2.1.5).
7. While measuring the element, just as with the element a deviation on the planefit occurs as a reaction on the as with the pillar measurement.
8. Once both the pillars and the element are measured, the element can be adjusted to the desired height. The tolerance of the actuator needs to be taken into account.
9. Once the element is adjusted to its desired orientation, the dynamic pins need to be locked again. Since the position of the dynamic pins could be altered by this process, the corresponding tolerance should be taken into account (as discussed in section 2.4.5).

The values of these tolerances can be seen in table 4.1. In the next chapter these values will be verified.

	Tolerance in Rx [mrad]	Tolerance in Ry [mrad]	Tolerance in Z [µm]
1.1 Dowel pin repro	See appendix A		
1.2 Dowel pin pin			
1.3 Dowel pin hole			
2. X, Y, Rz Positioners			0
3. Reference setup	0.27	0.33	40
4. Sensor Pillars	0.01	0.01	1
5. wobble stages	0.05	0.05	5
6. Temperature difference			1
7. Sensor element	0.011	0.011	0.067
8. Adjustment	0	0	0
9. Locking tolerance	0.23	0.27	8
Total tolerance (Half quadratic, half linear)	**0.73**	**0.56**	**80**

Table 4.1: Tolerance chain

Chapter 5 Verification

In this chapter, the setup will be verified through a series of tests. First, an overview of the different tests will be given. After that, the different tests will be elaborated and the results will be given.

5.1 Overview of different tests

To verify if the setup works as intended, the operation of the subsystems must be tested to see if all parts work as intended and to find the required calibration values. Furthermore, the different parts of the tolerance chain need to be tested to verify whether they deviate from the previously calculated values. In this way, it can be checked whether the setup works as expected and whether any unexpected deviations could be explained and improved in future versions of the tool. For the tests a a element module will be used with the setup, this module will from now on be referred to as "test module".

Three different kinds of tests can be identified:

- Functionality test: These are tests to verify whether the function of a particular component is working as expected with a possible “yes” or “no” answer. An example is, does the stage move to the right when prompted in the software?
- Performance test: These are tests to measure the performance of certain components of the setup. For a performance test, the expected value is given and will be compared to the result of the test. If the test value deviates from the expectation, a root cause for the deviation will be investigated and its impact discussed. An example of a performance test is measuring the repeatability of the sensor. This will then be compared with its calculated value from chapter 4.
- Calibration test: These are tests to find out the necessary variables for the system, shown in figure 4.17. Examples are the settling time or the coordinates of the pillars. A calibration test produces a certain value that will be implemented in the software.

Now that the different kinds of tests are identified, a table of the different tests will be given. The test landscape can be seen in table 5.1 on the next page. The results of each of the different tests will be implemented in this table at the end of this chapter. The extra information in the table refers to the part of the tolerance chain which is tested in case of a performance test or when a specific component needs to be calibrated in case of a calibration test.

Subsystem	Test	Type of test	Extra information	Expectation	Discussed in
Sensor	Surface measurement	Functionality test		element surface can be measured	5.3.1
	Sensor parameters	Calibration test	Required for new sensor		5.3.1
	Repeatability of the sensor	Performance test		±0.4µm	5.3.3
	Software sensor	Functionality test		Software works	5.3.4
Sensor on stages	Software stages	Functionality test		Software works	5.4.1
	Acceleration and settling time	Calibration test	Required for new stages	Allowed acceleration: 30mm/s^2 settling time: 1 sec	5.4.2
	Repeatability sensor on stages	Performance test		Almost equal (+=0.2µm) to the repeatability without stage	5.4.3
	Wobble stages	Performance test	Corresponds to tolerance 5	±5µm	5.4.4
	Repeatability stages	Performance test		±1µm	5.2.1
	Location Reference pillars	Calibration test	Required after each assembling	±1mm	5.4.5
Docking	Measurement locations	Calibration test		Locations are correctly selected	5.5.1
	Pillar plane fit and element plane fit	Performance test	Corresponds to tolerance 4 and 7	1% of total tolerance each, as calculated	
	Deviation in Z of X, Y, Rz positioners	Performance test	Corresponds to tolerance 2	±5µm	5.5.2
	Location element within given deviation	Performance test		Repeatability <±50µm	5.5.3
	Repeatability element module integration	Performance test	Corresponds to tolerance 1.1	See appendix A	5.5.4
	External vibrations	Functionality test		The change in sensor output ±10µm	5.5.5
Adjustment and Locking	Software actuators	Functionality test		Software works	5.6.1
	Begin position actuators	Calibration test	Required after each assembling	Start extension between ±0.2mm of 7.12mm	5.6.2
	Stick-slip test	Functionality test		No stick-slip	5.6.3
	Adjustment reproducibility	Performance test	Corresponds to tolerance 8	Around 1% of the stepsize	5.2.2
	Locking Repeatability	Performance test	Corresponds to tolerance 9	Ry<±0.27 mrad, Rx<±0.23 mrad, Z<±0.008mm, can partially be predicted	5.6.4
Total system	Convergence element adjustment	Performance test		System will converge in 2 iterations to required spec	5.7.2

Table 5.1: Test landscape

The different tests in table 5.1 will be elaborated and executed in the following sections.

5.2 Tests that will not be preformed

Most of the specifications of the electrical components are given from when they are used under optimal circumstances. Therefore, some specifications should be tested to verify if which repeatability they reach under the circumstances of this setup. However, if the given specifications of the electrical components satisfy the requirements for the setup with a factor bigger then 20 and there is no reason to believe that the circumstances in which they operate are far from ideal, the specifications do not have to be verified for this setup.

5.2.1 Performance test: What is the repeatability of the stages in X and Y

It is important to know the repeatability of the stages to be certain that the measurements are made in their desired location, within tight tolerances. However, while there are no big deviations from the ideal situation in which the stage is tested for its specification, the Expectation is that the repeatability of the stages is somewhere around $1\mu m$, as specified in 4.7 of the previous chapter. Since a repeatability around $50\mu m$, which is a factor 50 higher than the specifications, would be sufficient for this setup, it does not have to be tested thoroughly.

5.2.2 Performance test: What is the repeatability of the adjustment actuators?

The tolerance added due to the stepsize of the picomotor is more than 1000 times smaller than the tolerance budget, as can be seen in figure 3.15b. The repeatability on this stepsize does not have to be tested as it does not have to be taken into account as tolerance. Since the displacement of the element after each use of the actuators will be measured with a planefit, any deviations can be accounted for in another adjustment iteration. This will be elaborated in the final test in section 5.7.1.

5.3 Sensor verification

First, the sensor needs to be verified. This will be done individually without the rest of the setup. To verify the functionality of the sensor, first, a functionality test needs to be done to test if the sensor can measure the surface of the element. After that, a calibration test will be done to see which alterations of the sensor parameters improve the sensor output such that they can be implemented in the software. Then, a performance test will be done to assess the repeatability of the sensor. Lastly, for the sensor, a test needs to be done if the software can read the sensor output as expected.

5.3.1 Functionality test: Can the surface of the element be measured?

This can be tested by seeing if the sensor gives a signal when it measures the same type of surface as the element, being gold-coated silicon.

Expectation

The Expectation is that the sensor will give an adequate signal (a video signal above 15%) when measuring the gold-coated silicon. Although the sensor it is known that this type of sensor has difficulties with reflective surfaces, the gold-coated silicon is less reflective than a mirror and should therefore be measurable.

Implementation

Different samples of gold-coated silicon are measured with the sensor. The measurement is done by measuring different points on each sample while looking at the video signal of the sensor. When the sensor outputs a higher video signal than 5%, as can be seen in figure 5.1a, it gives a stable output signal. If this is the case it can be concluded that the surface is measurable.

Results

Not all samples of gold-coated silicon that were tested gave a good signal due to their reflectiveness. This could be a result of them having a slightly different coating and thus having a slightly different reflectiveness. However, the surface of the element in the element module available for the testing of the setup provided a valid video signal. Therefore, it can be concluded that the sensor can be used for the feasibility demonstrator that only has to measure the element of the element module available for testing. For the production-ready design, another sensor would be more suitable to eliminate the risk of a bad video signal, as will be discussed in the next chapter during the recommendations. In figure 5.1a a good video signal can be seen, the sample is thus measurable by the sensor. In figure 5.1b a bad signal can be seen, this sample gave a lot of errors in its sensor output.

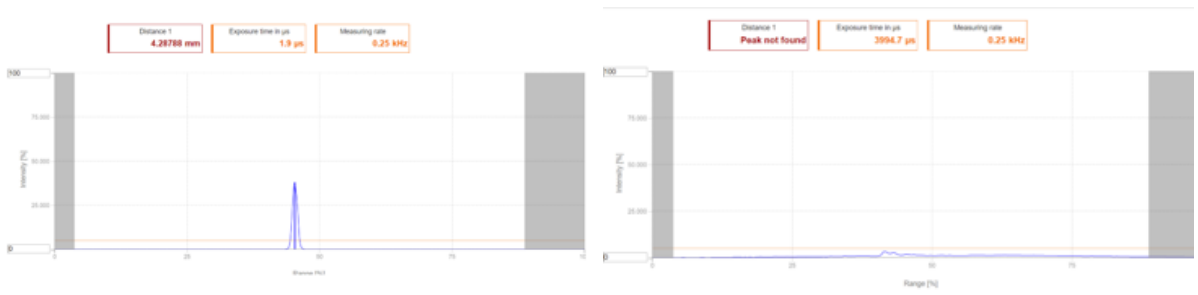

(a) Good video signal

(b) Bad video signal

Figure 5.1: Video signal of lasertriangulator

5.3.2 Calibration test: which sensor parameters should be used for the sensor?

The sensor has multiple parameters that can be adjusted, for example measuring rate, exposure time, and signal quality. Depending on the test it is important to have a high measuring rate and see as many sensor outputs as possible or to have a more accurate measurement and see an averaged value of multiple data points. For both of these modes, different settings apply. Next to these settings, an increase or decrease of the angle of the sensor with respect to the sample may improve the sensor output as well and should also be tested.

Expectation

It is expected a faster measuring rate would require a smaller exposure time and a lower signal quality and the opposite is expected for a more accurate measurement. Furthermore, it is expected that due to the reflectiveness of the surface, a small tilt of the sensor could help to reflect more of the laser into the light-receiving element of the sensor, which can be seen in figure 2.6a.

Implementation

This is a combination of reading the documentation of the sensor[32] and testing the output of the sensor with different settings. The optimal settings will be tested by looking at the video signal of the sensor.

Results

No improvement of video signal was seen by varying the angle between $-10°$ and $10°$. Therefore it is decided that the sensor will be mounted into the setup with its laser perpendicular to the element.

The settings of the sensor can be seen in figure 5.2. Not all settings where thoroughly tested but it was found a good repeatability of the sensor signal was achieved with these settings. To filter out some of the deviations of the sensor, the controller sends the median of 9 sensor values to the computer. There could be some more setting alterations to improve the repeatability of the sensor signal if even more tests would be done, but this is not needed for this project.

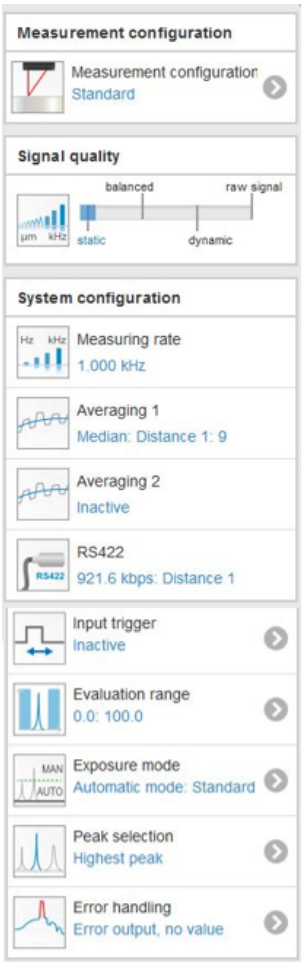

Figure 5.2: Sensorsettings

5.3.3 Performance test: What is the repeatability of the sensor?

Although a repeatability of 0.4 μm is specified by the manufacturer of the ILD 1900 lasertriangulator, as can be seen in figure 4.4, the repeatability of the sensor while measuring the gold-coated silicon could vary. It is important to know the repeatability of the sensor to determine how many instances are needed for each measurement to reach a certain precision.

Expectation

The circumstances for the measurement are not ideal, the gold-coated silicon has a relatively high reflectance and the lasertriangulator uses diffuse reflection as specified in section 2.3.1. Therefore, the repeatability value of the sensor is expected to be higher then specified. It is expected to be somewhere between 0.4 μm and 2 μm.

Implementation

To test the ILD1900 lasertriangulator it is mounted into the height map measuring device of AMSL, consisting of a high-end lasertriangulator, the LK-G10 model from Keyence[31] which has better specifications that the ILD1900, and a X, Y, Z stage configuration. The advantage of having another lasertriangulator is that the test can be done with both sensors and the results can be compared. The stages within the device can be used to measure multiple coordinates. A picture of the ILD1900 mounted into the height map measuring device can be in figure 5.3, and the specifications of the keyence sensor can be seen in figure 5.4.

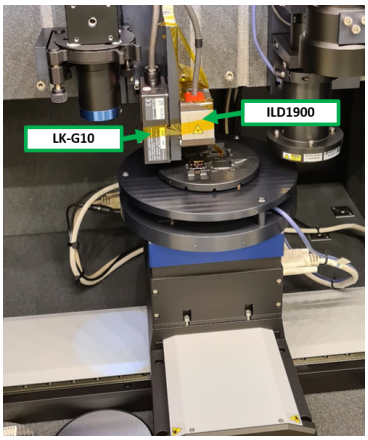

Figure 5.3: lasertriangulators inside height map measuring device

Model	LK-G10
Reference distance	10 mm 0.39"
Measuring range	±1 mm ±0.04"*1*2
Linearity	±0.03 % of F.S. (F.S.= ±1 mm ±0.04")*3
Repeatability	0.02 µm (0.01 µm)*4

Figure 5.4: LK-G10 Keyence sensor specifications (from[31])

A rectangle made of 24 points is three times measured with the ILD1900 and with the LK-G10. The repeatability tolerance of the ILD1900 is equal to the point that has the biggest deviation from the mean of the LK-G10 measurements.

Results

In figure 5.5 the results of one of the sides of this rectangle with the biggest deviation can be seen. The biggest deviation can be seen around the 0 point. This is equal to roughly 6 μm. Although this is a lot larger than what was initially expected, the sensor can still be used for the setup. Using the formula discussed in section 4.3.1, a certain amount of data points can be chosen to lower the sensor tolerance to an appropriate amount.

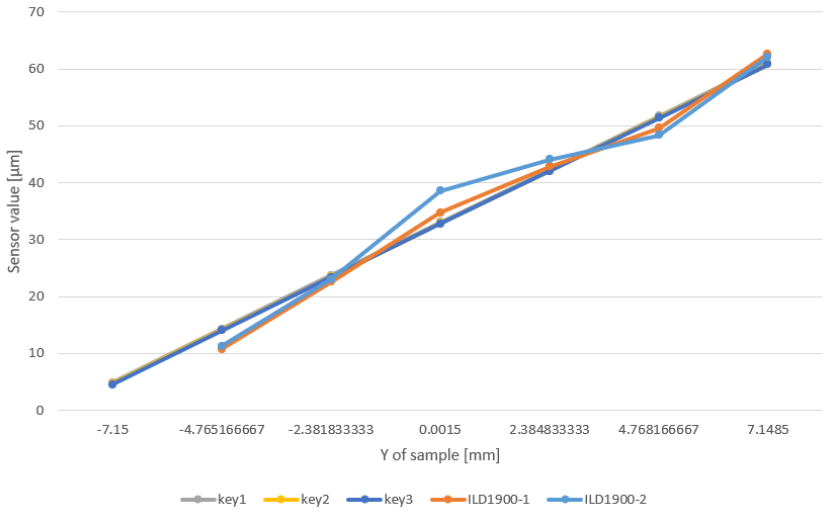

Figure 5.5: Biggest deviation result of repeatability test

The value of 6 μm cannot be used as the value for the tolerance of the sensor however. This is because other influences could have caused this deviation. For example, the values of both sensors where not received on precisely the same spot of the sample. Furthermore, there might be stage wobble that could account for a certain amount of deviation since the measurements where not taken at the same point of the stages . Better data for the repeatability could be received by measuring two points multiple times instead of measuring a lot of different points only a few times. This initial test for the repeatability of the sensor made sure that the sensor can be used for the setup but a more accurate test to test the repeatability of the sensor has been done after the setup has been built and gave different results.

To measure the repeatability of the sensor more accurately the sensor is made to measure one point alternately on two of the reference pillars. First point 1 is measured a hundred times with a 1 second interval, then point two is measured a hundred times with a 1 second interval, then point 1 again, until both are measured 300 times, so 600 measurements in total. In this way any repeatability tolerance coming from external factors can be filtered out and by looking at the deviation during each of the hundred measurements, the repeatability can be determined.

As can be seen in figure 5.6a and figure 5.6b the deviation during each of the hundred measurements is a lot smaller then previously thought and around the specified 0.4μm of the manufacturer. The difference between each of the hundred measurements is caused by a decrease of repeatability when using the sensor in combination with a stage. This will be more thoroughly tested during the sensor on the stage repeatability test in section 5.4.3.

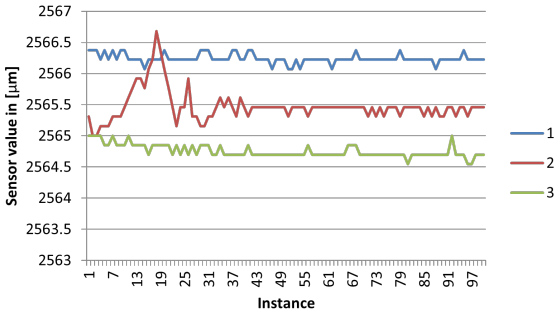

(a) Sensor repeatability point one

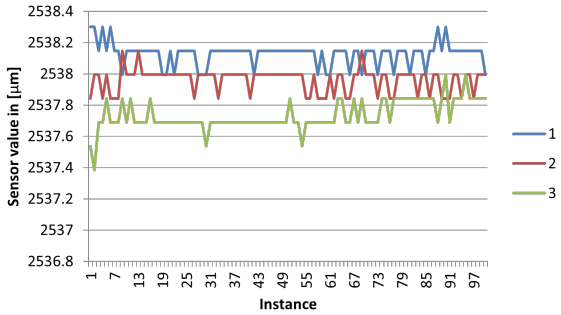

(b) Sensor repeatability point two

Figure 5.6: Sensor repeatability point two

The standard deviation (S) can then be calculated with:

$$S = \sqrt{\frac{\sum_{i=1}^{N}(x_i - \bar{x})^2}{N-1}} \tag{5.1}$$

With N is the amount of datapoints (600).
x_i is the sensor value of each datapoint.
$\bar{x}$ is the average of the hundred points of which that data point is part of.

This gives a standard deviation of $0.12\mu m$ for the sensor. Taking 2 times S so that 95.8% of the values are inside the range gives a repeatability of $\pm 0.24\mu m$ which corresponds to a repeatability of $0.48\mu m$ and is approximately equal to the value of $0.4\mu m$ which is specified by the manufacturer. Since multiple points are used for the measurement of the plane fit and since if one in 20 (due to 95.8% being inside the calculated $\pm 0.24\mu m$) of these points are larger then the calculated repeatability it would not influence the measurement too much, 2 times S suffices.

5.3.4 Functionality test: Does the software for the sensor work as intended?

Until now the integrated software of the sensor is used to read out the sensor output. However, to use the sensor with the other systems, the software is required that can print the value that the sensor outputs at a specific time.

Expectation

It is expected that the software can print the value that the sensor gives at that moment.

Implementation

The printed value by the created software is compared with the value of the integrated software of the sensor.

Results

The values that the designed software uses for the planefit are equivalent to the values that can be seen in the software of the manufacturer.

5.4 Sensor on stages verification

Now that the sensor is tested individually, the sensor will be mounted onto the stages. First, a functionality test will be done to test if the stages work as intended with the software. Then, a calibration test will be done to find a suitable acceleration for the stages and a suitable settling time such that they do not interfere with the measurement. Subsequently, a performance test will be done to test what the repeatability of the sensors is on the stages. Then, a performance test will be done to test the wobble (deviation in Z while moving in X and Y) of the stages. In the end, the reference pillars are assembled onto the setup such that the position of the reference pillars with respect to the stages can be tested with a calibration test.

5.4.1 Functionality test: Does the software for the stages work as intended?

For the incorporation of all the different electronic elements it is important that they work as intended with the designed software.

Expectation

The expectation is that the stages follows the instructions provided by the software.

Implementation

Multiple variables and functions of the stages will be tested. The homing function of the stages will be tested; the stages will be inspected to see if they go to their "0" point. The acceleration of the stages will be tested; the result of the implementation of different accelerations into the software on the stages will be reviewed. The implementation of different X and Y coordinates will be tested; the stages will be inspected to see if they reach their desired destination.

Results

The software of the stages work as intended. The stages reach their Home point (X=0 and Y=0 for the stage coordinates) and can be ordered to reach a set of coordinates specified in the software. Both the velocity and acceleration can be altered via variables in the designed software.

5.4.2 Calibration test: what acceleration and settling time should be used for the stages?

It is important to inspect the disturbances on the sensor due to the acceleration of the stages. These can be filtered out by increasing the settling time; the time to wait after the movement of the stages until doing the measurement.

Expectation

Due to the connection between the sensor and the stages being a stiff construction, there is little room for vibrations due to the acceleration of the stage. It is expected that using an acceleration around $30\frac{mm}{s^2}$ with a settling time of 1 second, should be sufficient to prevent any influence for the movement of the sensor output.

Implementation

This test is done by looking at the sensor output during a measurement while varying the acceleration of the stages. Since the stage vibrates during movement, by looking at the sensor output it can be seen how long it takes for these vibrations to subside after the movement.

Results

The results of a stage with its speed equal to $15\frac{mm}{s}$ and its acceleration equal to $30\frac{mm}{s^2}$ can be seen in figure 5.7. On the Y axis is the distance value of the sensor in mm and on the X axis is the time. The stage stops with movement around 0.24 seconds, indicated with blue line. It can be seen that the signal of the sensor is settled in around 0.16 seconds.

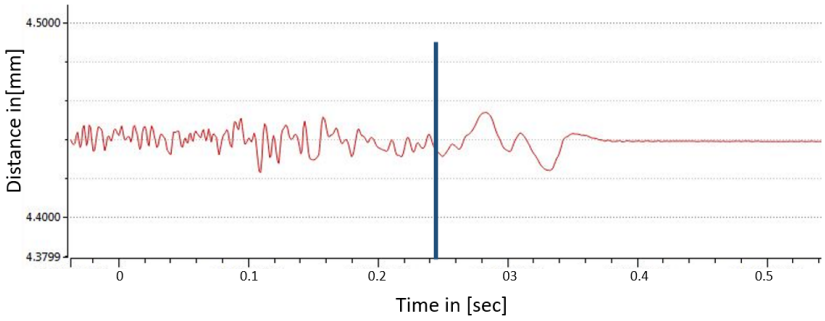

Figure 5.7: Settling time of the sensor after stage movement

It was found that errors could occur if the stage would be accelerated at its maximum acceleration. Therefore, since an acceleration of $30\frac{mm}{s^2}$ is not needed for the setup, an acceleration of $10\frac{mm}{s^2}$ is chosen for the setup. A time of 0.35 seconds in-between the movement of the stage and the measurement is chosen to be on the safe side and to be sure that there is no influence of the vibrations due to the movement of the stages.

5.4.3 Performance test: what is the repeatability of the sensor on the stages?

During the test in section 5.3.3, a rough approximation of the repeatability of the sensor is given. Although the repeatability of the sensor on the stages should be roughly the same, some external factors could influence the repeatability. It is important to understand which external factors influence the repeatability of the sensor on the stages to know how the setup can be improved and what tolerances could be achieved for the plane fits.

Expectation

The repeatability of the sensor is expected to be somewhat the same as the repeatability of the sensor without the stages, Since the stages should in theory not alter the distance between the sensor and the measurement surface in-between measurements. However, as can seen in figure 5.12 due to the space in-between each set of measurements, the repeatability of the sensor on the stages is most likely lower then the sensor. These deviations could be a result of the repeatability of the stages itself resulting in not measuring the same spot repeatedly and thus having a different out come each time. Another result could be a temperature influence that could change the distance between the sensor and the measurement surface in-between each measurement due to thermal expansion.

Implementation

The test will be done by measuring 3 locations on each measurement surface, so 3x3 for the pillars and 3 for the element resulting in 12 measurement locations, repeatedly over a long period of time. These locations can be seen in figure 5.8 with the colours referring to the coloured plots of the graphs in the results. Calculating the average of each point and subtracting it form all values measured for that point, the deviation can be calculated. If all deviations would be put into one graph, the tolerance and characteristics could be determined.

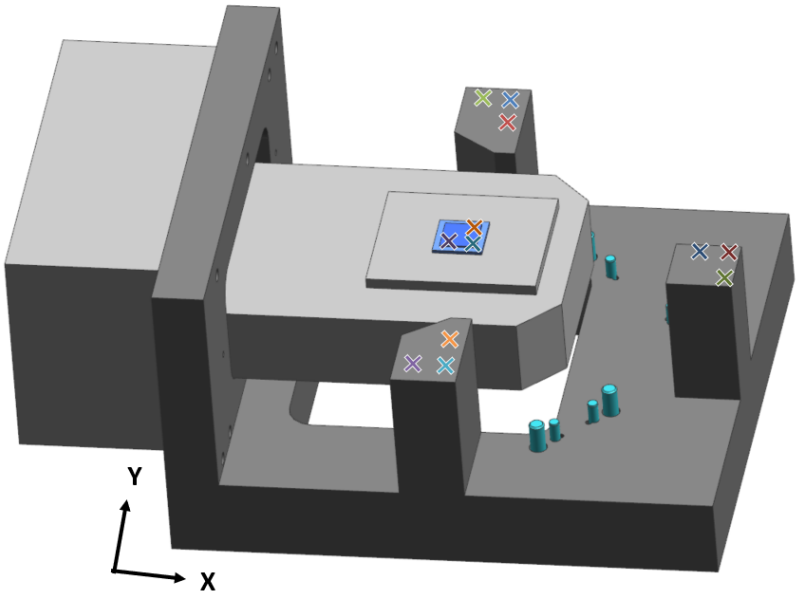

Figure 5.8: The measurement locations

Results

These 12 measurement locations are first measured, 500 times, resulting in a measurement over a time span of 12.5 hours. As can be seen in figure 5.9, the distance between the sensor and the measurement locations changes in the first couple of hours until it reaches a steady state. Then after 9 hours it changes again.

The characteristics of the graph seem to resemble a system that changes due to heat expansion caused by a change in temperature. It can be assumed from the graph that once the stages start, they increase the temperature of the setup until it reaches a steady state. The change after 9 hours could be caused by a change in temperature inside the cleanroom. Which, after looking at the cleanroom log files, indeed changed two degrees around that time.

It is interesting to see that the measurements of two measurement locations deviate from the other measurement locations, which all react to the same way to temperature deviation. These are the two points which have the highest X values (The two most right points in figure 5.8). This could be caused either by the pillars in which the pillar with the highest X value (the right pillar in figure 5.8) bends in Ry due to the thermal expansion, by the stages in which the bottom stage is tilted in Ry due to thermal expansion, or by the stage portal that could bend in Ry due to thermal expansion. This last could be likely since the vertical beams of the stage portal has holes in it.

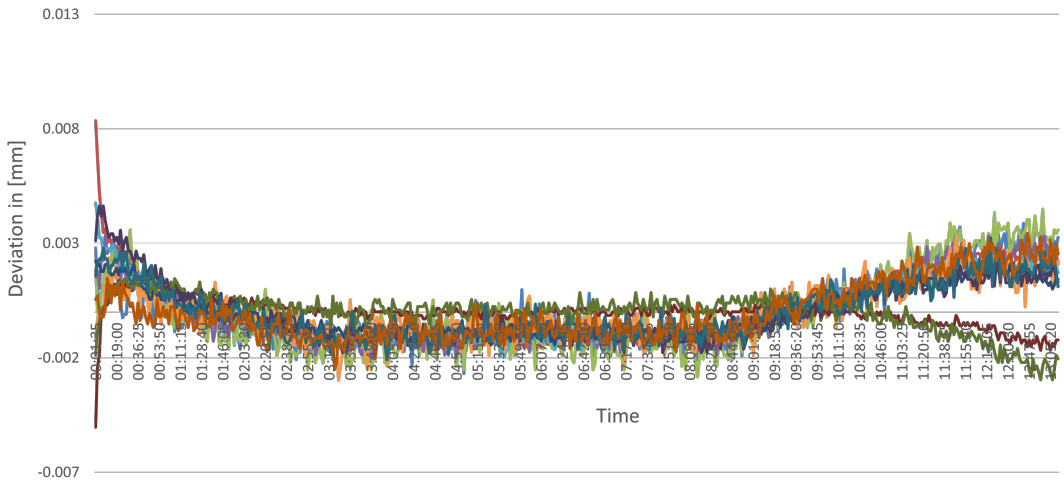

Figure 5.9: 12.5 hours long measurement

To confirm that the deviation could be caused by temperature deviation, the test is done several times. Figure 5.10 represents the test done for 18 hours. It starts with an even bigger deviation. This could be caused because the stages were not used for a longer time before starting the test and thus where colder to begin with. This will be used for the calculation of the temperature tolerance. After the heat up period of the first few hours, no deviations are seen. Since the temperature in the cleanroom stayed more constant during this test, this is as expected.

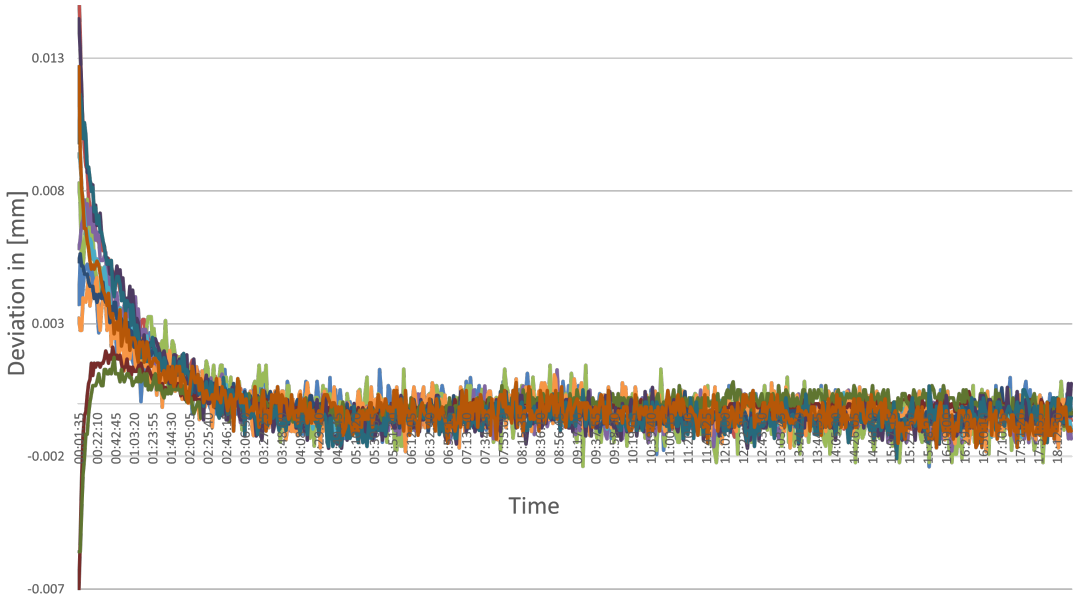

Figure 5.10: 18 hours measurement

When zooming in to the first 2.5 hours of the 18 hours measurement, as can be seen in figure 5.11, the decrease in deviations between points can seen be more clearly. After the 15 minute mark, the biggest deviation between the points has subsided. Since the other points almost have the same deviation value, only the deviation value of the bottom two lines, representing the locations with the highest X values, will be looked at. Since they are within 6 μm of the other lines and since the right pillar is approximately 100 mm away from the other measurement locations, the added Ry tolerance due to the temperature deviation inside the setup is calculated to be $\pm 0.06 mrad$. This also accounts for the temperature deviation in the cleanroom since the bottom lines in figure 5.9 are also within 6 μm of the other lines at the moment of the temperature change.

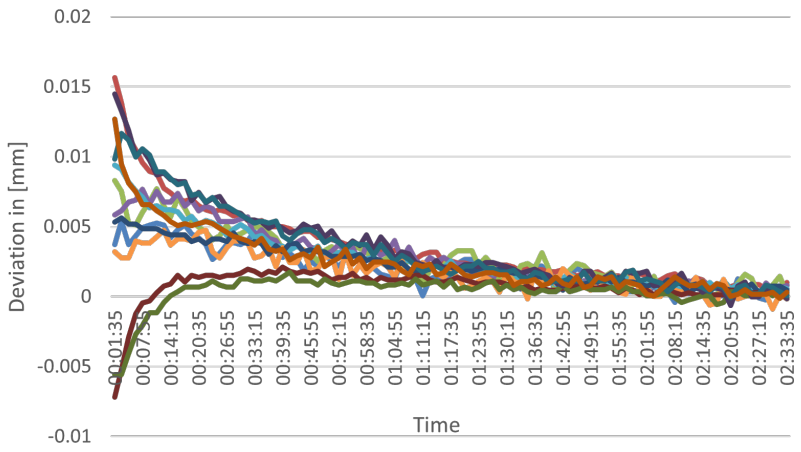

Figure 5.11: Zoom-in on first 2.5 hours of the 18 hours measurement

As can be seen in figure 5.11, the repeatability of the sensor on the stage is dependent on how long the measurement is done. This strongly implies that the deviation is coming from a change in temperature. Since this same phenomena of a big deviation at the start that slowly subsides occurs during repeated testing, it is assumed that this deviation comes from the stages that heat up after repeated movement. After approximately 15 minutes this deviation becomes within $\pm 4 \mu m$. since this is an acceptable time for warming up the stages before each measurement. This is taken as the tolerance for the repeatability of the sensor on the stages.

5.4.4 Performance test: what is the wobble of the stages?

As can be seen in the tolerance chain in table 4.1, the wobble of the stages (the deviation in Z while travelling in the X or Y direction) accounts for a part of the tolerance during each measurement. As explained in section 4.3.2, the wobble is not specified by the manufacturer and therefore should be tested.

Expectation

Since the wobble of the stage is not specified it is hard make a expectation for the wobble of the stage. It could be around $\pm 5 \mu m$, but lager is also possible.

Implementation

An optical flat with a diameter of 100 mm that will be placed in the middle of both stages will be measured repetitively. The measurement is done by measuring the surface of the optical flat in steps of 1 mm in X and Y. By measuring the optical flat, certain characteristics can be determined for the wobble of the stages by looking at the sensor values. The sensor values should be a straight line in X and Y while measuring the optical flat, any deviation to this straight line could be caused by the stage wobble.

Results

The optical flat with a diamter of 100 mm gave too big of a deviation inbetween measurement points to accurately determine a characteristic for the wobble of the stage. From the deviations that can be seen in figure 5.12a, it can only be said that there are no wobble characteristics that are greater than 20μm, since no clear wobble pattern emerges . The big deviations are most likely caused due to the optical flat that was damaged resulting in a rough measurement surface with the deviations being scratches in the surface. The damaged optical flat can be seen in figure 5.12b.

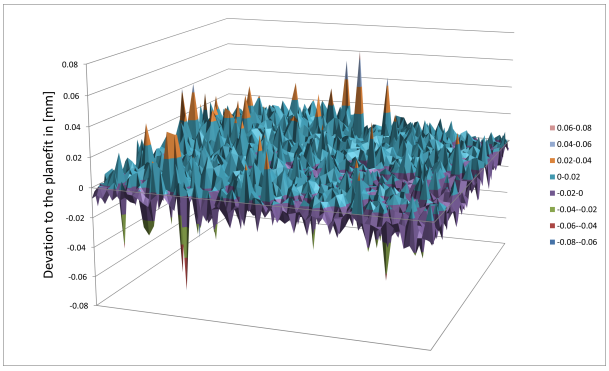

(a) Measured deviation to the planefit

(b) Damaged optical flat

Figure 5.12: Stage wobble test

To be able to determine the wobble more accurately, a new undamaged optical flat is measured. This can be seen in figure 5.13. However, as was found in section 5.3.1, the laser-triangulator can not measure all types of reflective surfaces. Unfortunately the surface of the new optical flat is too reflective for the sensor, resulting no signal output. The wobble of the stage is thus not measurable with the currently used sensor. If another sensor that preforms better on all types of reflective surfaces would be chosen, as will be discussed in the recommendations, the wobble of the stages test should be preformed again.

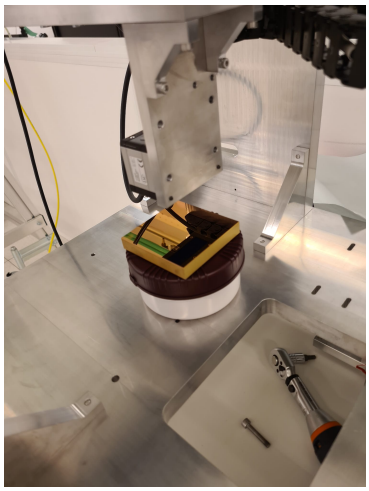

Figure 5.13: Measurement done with new optical flat

5.4.5 Calibration test: What are the calibration values for the location of the reference pillars

As discussed in section 4.4.3, the location of the setup in respect to the sensor needs to be calibrated. This value can then be implemented into the software such that the translation from the coordinate system of the stages to the coordinate system of the element works accurately.

Expectation

The possible deviation from the nominal location of the pillars differ is equal to the alignment and geometric tolerances of the part with the pillars, the underplate, all parts of the stage portal, the stages, and the connection between the stages and the sensor. It is expected that the calibration value would be somewhere around 1 mm.

Implementation

For the calibration, the pillar in the positive X direction is used, which can be seen in figure 5.14. The pillar is approached in steps of 20μm first from the X and then from the Y direction, in the positive direction of the stages, these are represented with the red lines in figure 5.14. The moment when the sensor gives a signal is the moment when the sensor has reached the side of the pillar. To factor out the width of the beam of the sensor, the other sides of the pillar will also be approached with the sensor to gain their location. The average of both the two X coordinates of the sides of the pillar and the Y coordinates of the sides of the pillar will be averaged to gain the coordinates of the middle of the pillar. The difference from the intended location of the pillar as it was designed, which is 27.5 mm for X and 62.25 mm for Y, will be taken as the calibration value.

Results

For X these values are 15.88 mm and 40.42 mm, averaging at 28.15 mm. For Y these values are 52.08 mm and 76.6 mm, averaging at 64.34 mm. The middle of the pillar is thus at X is 28.15 mm and Y is 64.34 mm with respect to the pillars. Since this should be 27.5 mm for X and 62.25 mm for Y, the stage would need to travel $28.15 - 27.5 = 0.65$ mm further in X and $64.34 - 62.25 = 2.09mm$ further in Y. These will be used as calibration values for the coordinate system, as discussed in section 4.4.3.

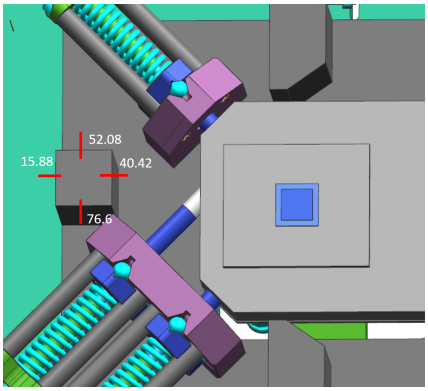

Figure 5.14: Calibration of the location of the reference pillars

5.5 Docking verification

Now that the sensor and the stages are tested, the docking will be validated. The docking represents the integration of the element module into the setup and using the X, Y, Rz positioners to bring the element to its nominal position. After the X, Y, Rz positioners and the integration tool have been assembled onto the setup, a calibration test will be done to see if the preselected measurement locations are correctly chosen. If these are correctly chosen a plane fit of the element can be made and its repeatability can be calculated. This will then also be done for the reference pillars. After that, a performance test of the X, Y, Rz positioners will be done to test the added tolerance in Rx, Ry, and Z due to the X, Y, Rz positioners. Next, a performance test will be done to test the repeatability of the positioners in X, Y Rz. Then the repeatability of the Rx, Ry and Z coordinates of the element will be tested from the integration of the module into the setup. Lastly, to test the influence of external vibrations on the sensor while its mounted onto the setup, the influence of large external vibrations on the sensor will be tested. In figure 5.15 a blurred version of the element module can be seen integrated into the setup.

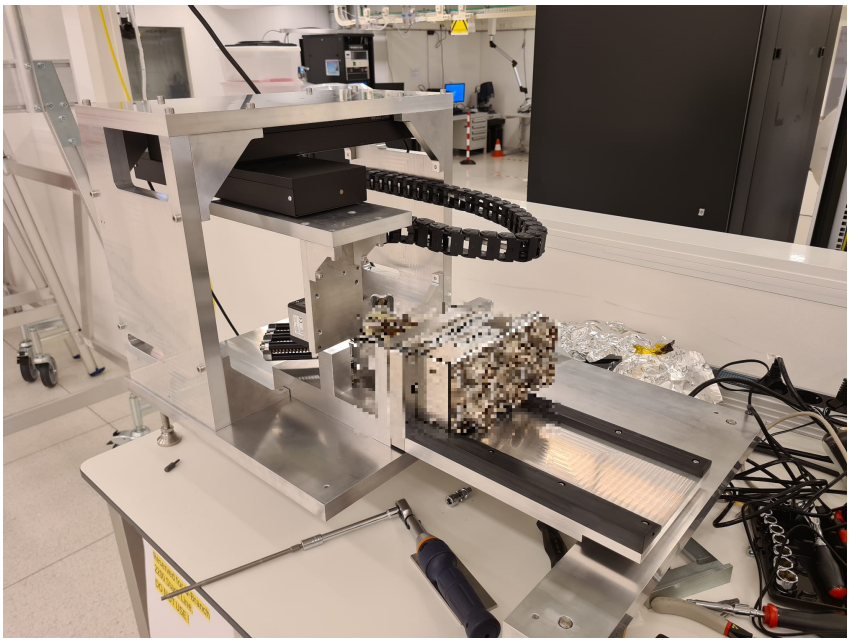

Figure 5.15: element module docked into the setup

5.5.1 Calibration test: Are the preselected measurement locations correctly chosen?

Before tests can test can be done that measure the surface of the element, it should first be tested if the preselected measurement locations are correctly chosen. The measurement positions are correctly chosen if all measurement positions are located on the element and can be measured by the sensor.

Expectation

It is expected that the coordinates, chosen in section 4.3.1, all give a valid sensor output while they are measured. A measurement would be valid if there is no strange deviation in the sensor value in contrast to the other points. This would be the case if the preselected measurement locations would not be within the borders of the element or hit a certain feature on the element, like a hole.

Implementation

To test this the selected coordinates are implemented in the software and are measured 5 times. While the measurement is done the measurement points will be inspected for irregularity by looking at their locations on the element. Also, The output will be examined for any deviations bigger than what is expected. If there would be deviations bigger than the calculated sensor repeatability, a different coordinate for the measurement will be chosen.

Results

A scan of the element with a 2 mm circumference on each side with 0.25 mm distance between each point has been done. This accounts for 72x72 points over a 18x18mm grid. This can be seen in the figure 5.16. The green square represent measurable locations on the stack, the red squares represent coordinates that gave errors when measured, and the white squares represent the measured coordinates around the 14x14mm part of the element.

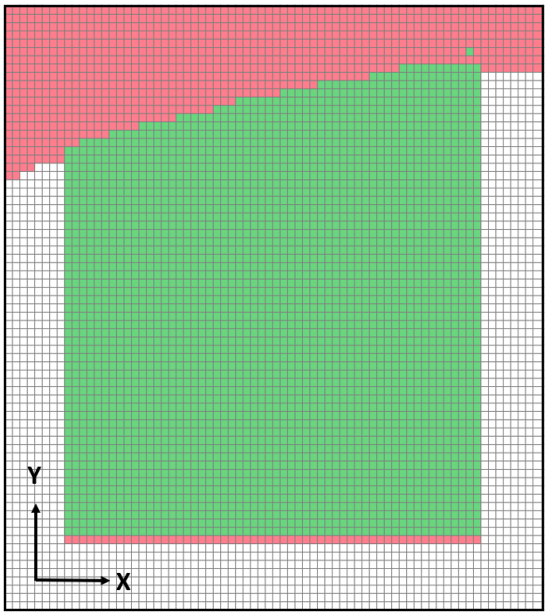

Figure 5.16: Measurable locations

As can be seen, not every point on the element is measurable. This is because, although the laser is perpendicular to the element surface, the light recieving element of the sensor makes a 45 degree angle, as can be seen in figure 2.6a. This path gets blocked on the coordinates of the red squares resulting in the sensor not being able to recieve the light and thus giving an error. This 45 degree angle deflection is in the positive Y direction of figure 5.16. This causes the signal to be blocked by the element when measuring next to bottom of the element resulting in the red beam at the bottom of the figure. The unmeasurable coordinates on the top of the figure are caused by cables of the element module located next to the element blocking the light receiving element of the sensor. Since some of these spots where originally planned to be measured, as can be seen in figure 4.6, a different set of preselected measurement locations for the plane fit of the element will be discussed during the next test. There could be a slight deviaton of measurable locations in between modules due to an deviation of the location of the cables. To account for this some extra distance to the unmeasurable locations will be taken when determining the preselected measurement locations. However, this calibration procedure should still be done when building a new instance of the setup to be sure that all points can be measured.

5.5.2 Performance test: what is the repeatability of the plane fit form the element and the pillars?

Now that the measurable locations on the element have been determined. A planefit can be made to measure the Rx, Ry and Z coordinates of the element. To determine tolerance contributor 7 of table 4.1 this is repeatably to calculate the repeatability of the plane fit. This is then also done for the pillars to determine tolerance contributor 4 of table 4.1. In the end both are compared.

Expectation

As calculated in section 4.3.1, the repeatability of the plane fit of the element is expected to be roughly 1% of the total tolerance. Since the distance in X and Y is between the measurement locations is bigger for the plane fit of the pillars, it should be able to have a better repeatability while measuring Rx and Ry. When looking at formula 4.1, since the average distance between the measurement points and the middle of the measured sample is roughly 8 times bigger, the repeatability for Rx and Ry of the plane fit of the pillars is expected to be 8 times smaller then that of the planefit of the element.

Implementation

Since not all locations on the element are measurable, as was concluded during the last test, the originally selected measurement locations of section 4.3.1 are altered. Since more locations can be measured in a shorter time as was found in section 5.4.2, 192 measurement locations will be used for the plane fit of the element. These 3 times 64 measurement locations are distributed as shown in figure 5.17. Since the repeatability in X and Y of the positioners is not yet known, a safe 1.4 mm border from the borders of the element are chosen so that there is no risk of preselected measurement locations that are not on the element. To gain the repeatability of this planefit, this scan will first be preformed 20 times. The repeatability of this planefit will then be calculated using the formula 5.1.

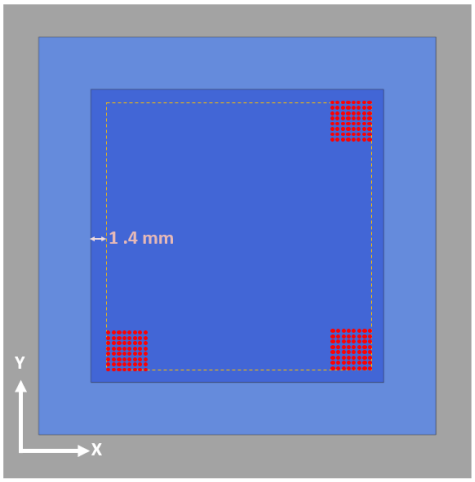

Figure 5.17: Preselected measurement locations used for the planefit

To calculate the repeatability of the plane fit on the pillars also 3 sets of 64 measurement locations are chosen, one set per pillar. Just like for the repeatability of the element plane fit, 20 plane fits will be made after which the repeatability will be calculated using formula 5.1.

Note that a boxplot will be used to represent the repeatability of the different tolerance contributors. To prevent confusion, the determination of the boxplot that can be seen in figure 5.18 will be used. The whiskers and the quartiles represent the spread of the values found from the measurements. Furthermore, the outliers will still be taken into account while determining the standard deviation of the repeatability.

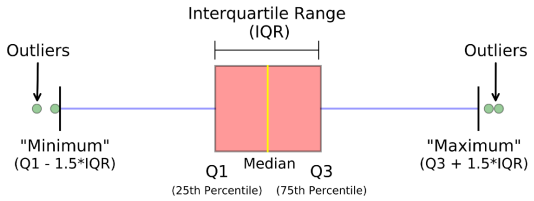

Figure 5.18: Determination boxplot

Results

First the repeatability of planefit of the element is measured. Using formula 5.1, the standard deviation (S) of Rx, Ry, and Z is 0.015 $mrad$, 0.011 $mrad$ and 0.44 μm respectively. This is suitable since it is only approximately 1.5% of the required ± 1 $mrad$ in Rx an Ry and ± 0.1 mm in Z. Since more tests will be done after which the repeatability needs to be measured, this means that any repeatability tolerance due to deviations of above 1.5% is observable which is appropriate since they are expected to be bigger then 1.5%, as calculated in the previous chapter. The spread of the results can be seen in the boxplot in figure 5.19a.

Next the repeatability of the plane fit is measured. Using the same process but excluding the first 4 measurements to exclude part of the added tolerance due to the thermal deviation found in section 5.4.3, the standard deviation (S) of Rx, Ry, and Z is 0.0014 $mrad$, 0.015 $mrad$ and 2.4 μm respectively. The spread of the results can be seen in figure 5.19b.

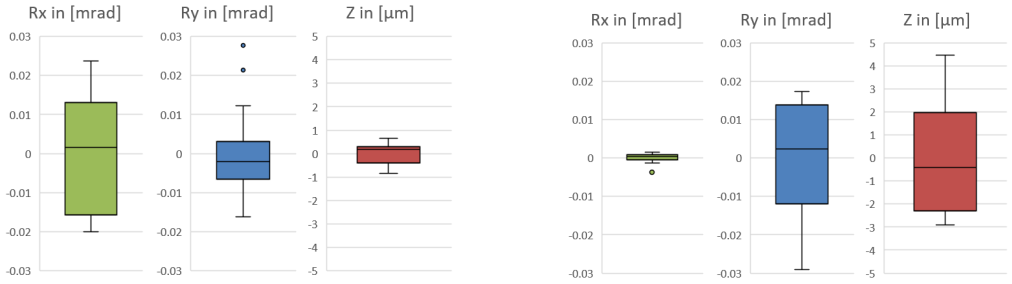

(a) Repeatability plane fit on element (b) Repeatability planefit on pillars

Figure 5.19: Repeatability planefits

It was expected that the repeatability of Rx and Ry of the planefit of the pillars was roughly 10 times more accurate then that of the element planefit. As can be seen in figure 5.19 this is the case for Rx. However, the Ry repeatability of the pillar plane fit is less accurate then that of the element plane fit. This could be a result of the thermal deviation that is not fully filtered out and plays a big role for the Ry of the pillars, as found in section 5.4.3. This is also what influences the difference in Z repeatability between the two planefits. However, since the planefit of the pillars is still only approximately 2% of the total tolerance budget, using the selected measurement locations should be appropriate for the plane fit of the pillars.

5.5.3 Performance test: What is the deviation in Rx, Ry, Z from using the X, Y, Rz positioners?

The X, Y, Rz positioners are designed to only alter these specific coordinates of the element. However, since there might be play in the internal mechanism of the element module it should be tested if using the X, Y, Rz positioners result in an Rx, Ry, Z movement of the element. This accounts for the second tolerance of the tolerance chain in table 4.1. The X, Y, Rz positioners can be seen in figure 5.20.

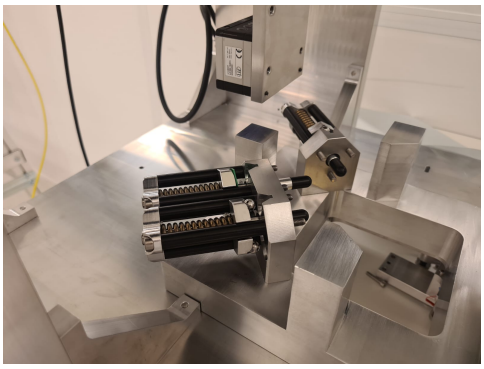

Figure 5.20: The Rx, Ry, Z positioners in the setup

Expectation

It is expected that using the X, Y, Rz positioners would not add a displacement of the element in Rx, Ry, or Z that is bigger than 1% of the tolerance budget (thus would be smaller than 0.01 $mrad$ in Rx, Ry and 1μm in Z). This is because the internal mechanism of the element module is designed with tight tolerance and is designed to have no play.

Implementation

To test the displacement in Rx, Ry, Z, the element will be brought to its nominal X, Y, Rz position the positioners will be tightened and loosened 10 times. After each time that the positioners are tightened, a planefit of the element, discribed during the previous test, will be made to calculate the Rx, Ry, Z position of the element. The results of repeatability of the tightened and loosened element will be compared with the reference plane fit to see if there are any deviations that are bigger then the repeatability of the plane fit.

Results

After the positioners are 10 times tightened and loosened with planefit measurements in-between, the repeatability of the X, Y, Rz positioners was higher then the repeatability of the plane fit. The average after each time the positioners where tightened was somewhat the same but the standard deviation was 0.086 $mrad$, 0.070 $mrad$ and 1.8 μm respectively. This is higher then expected and can be due to the fact that some simplifications where made from the original design of the X, Y, Rz positioners. However, since this is approximately 8% of the tolerance train it most likely not be the reason that the requirements will not be reached. If makes it one of the bigger tolerance distributors, improvements will be discussed in the discussion. The spread of the results can be seen in the boxplot in figure 5.21b.

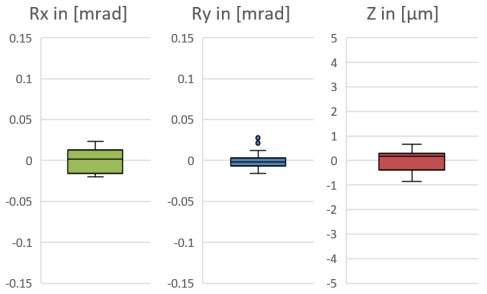

(a) Repeatability plane fit element

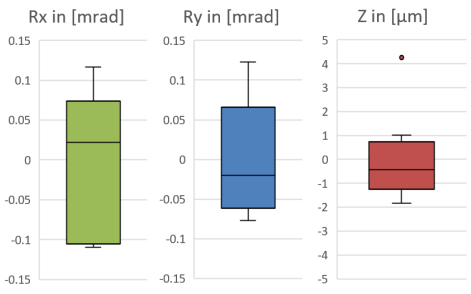

(b) Repeatability Rx, Ry, and, Z of positioners

Figure 5.21: Repeatability of the Rx, Ry and Z positioners with respect to the plane fit repeatability

5.5.4 Performance test: What is the deviation in X, Y, Rz from using the X, Y, Rz positioners?

The repeatability of the X, Y, and Rz coordinates of the element determine where the preselected measurement locations should be on the element. As discussed in section 4.3.1, the X, Y, Rz repeatability due to the positioners should be somewhere around $50\mu m$ for the total buffer to indeed be $500\mu m$. Since the X, Y, Rz positioners release the element mount from its endstops and bring them to a certain position independently how the module is inserted into the setup (in X, Y, Rz), the repeatability of the X, Y, and, Rz position of the element only depends on the repeatability of the X, Y, Rz positioners.

Expectation

It is expected that the tolerance would be approximately $50\mu m$.

Implementation

During the test to determine the repeatability of the element in Rx, Ry, and Z due to the X, Y, Rz positioners, each time when postioners are tightened, next to measuring the coordinates needed for the Rx, Ry, Z planefit, also 4 line scans were be made. For each linescan multiple points with $25\mu m$ inbetween each point over a length of 2 mm where made. These linescans can be seen in figure5.22. From the linescan the first point on the element can be determined for each line. From these coordinates the X, Y, and Rz coordinates of the element can be determined.

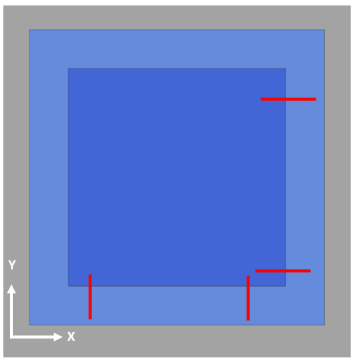

Figure 5.22: Linescans to deterimine X, Y, Rz of the element

Results

After 10 times that the positioners where locked and the linescans where mande, the standard deviation of X, Y, Rz is 25.8 μm, 26.5 μm and 1.22 $mrad$ respectively. The spread of the results can be seen in the boxplot in figure 5.23.

Since the measurement will fail if a row of the measurement points would not fall on the element, 95.4% (2 times S) is not enough. Furthermore, the sensor gave bigger deviations near the edge of the element due to its beam size, which already happened further from the border then expected in 4.3.1. To not risk any wrong measurements the, in section 4.3.1, previously calculated border of 0.5 mm will be expanded to 1 mm to avoid any risks.

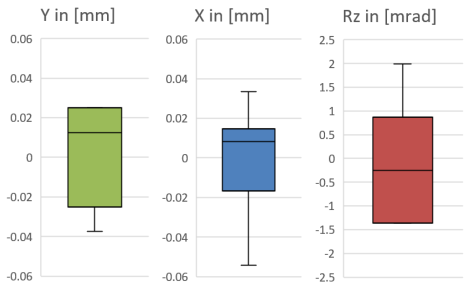

Figure 5.23: Repeatability X, Y, Rz of positioners

5.5.5 Performance test: What is the repeatability of the element module in Z due to the Docking?

Next to the tolerance of the X, Y, Rz positioners, integrating the module in and out of the setup also accounts for some tolerance, the dowel pin repro tolerance as specified in table 4.1.

Expectation

It is expected that the integration tolerance would be equal to the dowel pin repro tolerance calculated in appendix A.

Implementation

This can be tested in the same way as with the X, Y, Rz positioners tolerance: By integrating the module 10 times into the setup as discussed in 4.2 and tightening the positioners each time, a planefit can be made. After all 10 planefits are made and the tolerance of this planefit is calculated using formula 5.1.

Results

The standard deviation of Rx, Ry, Z of the module is calculated to be $\pm 0.16\ mrad$, $\pm 0.08\ mrad$, and $\pm 2.6\ \mu m$ respectively. Rx and Ry are higher then calculated in Appendix A. Expecially if you take 2 times S. This can be due to an accumulation of tolerances of other components, like the tolerance of the X, Y, Rz positioners, the repeatability from the sensor on the stage, and the thermal tolerances, which can not be separated from this measurement. The spread of the results can be seen in the boxplot in figure 5.24. Note that the 3 outliers are of three different measurements.

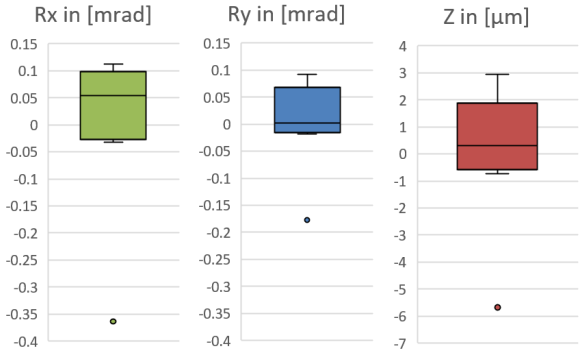

Figure 5.24: Repeatability of docking

5.5.6 Functionality test: to which degree do the external vibrations influence the sensor output?

As discussed in section 4.7.2, external frequencies also inflict a certain deviation to the measurement values. This can not be measured separately as it is included in the measured measurement repeatability. However, by increasing the external frequencies their influence can be seen in the change in the sensor output.

Expectation

Since the setup is fairly heavy and all connections are stiff, it is expected that the influence of external vibrations is small and that even large frequencies would only lead to small sensor deviations.

Implementation

Large external vibrations can be created by having a co-working jump up and down near the setup. By reading out the signal of a continuous sensor signal, while the sensor is measuring the element, the influence of external vibrations can be determined from the overshoot in sensor values caused by the jump. Depending on the magnitude of the overshoot, a conclusion can be made on the influence of external vibrations on the measurement values.

Results

As can be seen in figure 5.25, a big external vibration caused by a jump from a person next to the setup only caused a deviation of $2\mu m$. Since the normal external vibrations are expected to be a lot smaller then a jump, the influence of external vibrations on the setup can be neglected.

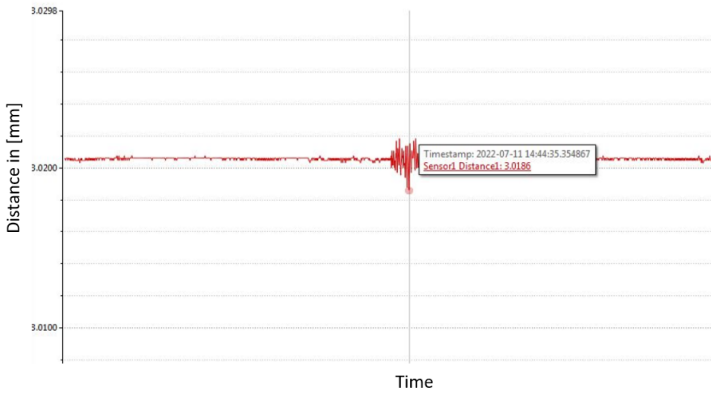

Figure 5.25: Deviation due to external vibrations

5.6 Adjustment and locking verification

Before the actuators are assembled onto the setup, a functionality test will be done to see if the adjustment actuators work as intended with the software. Next, the actuators will be assembled onto the setup. Then, a calibration test will be done to calibrate the start position of the actuators. Subsequently, a functionality test will be done to check if the dynamic pins can follow the motion of the actuators without stick-slip. After that, a performance test will be done by repeatedly locking and unlocking the dynamic pins to see what the influence is on the position of the element.

5.6.1 Functionality test: Does the software for the actuators work as intended?

Before the actuators will be assembled into the setup the software of the actuators will be tested to see if they work as expected. This is important to prevent the actuators from extending to unwanted positions and therefore may be damaging the element module.

Expectation

It is expected that the actuators can "home" to their start position, which would be their fully retracted state. Furthermore, it is expected that the actuators can extend to an implemented amount of extension.

Implementation

Because no custom software is written for the actuators, as discussed in section 4.6.2, the firmware will be used to test the actuators.

Results

The software of the actuators is a bit more limited then expected. There is no home function and the amount of intention of Z is not known. It is possible to adjust the acceleration and the velocity but for a change in position only an amount of steps can be given. During the slip-stick test in section 5.7.1, the average amount of displacement per step will be calculated. This is because the displacement per step varies with the amount of force that it needs to displace and is found to not be uniform.

5.6.2 Calibration test: what is the desired start position of the actuators?

Before the dynamic pins can be unlocked, the actuators, which can be seen in figure 5.26, would need to be extended so that they can prevent the dynamic pins from falling below their designed range. As described in 4.4.2, this starting position is not known, since the tolerance chain between the dynamic pins and the actuators is not designed with small enough tolerances. Therefore a calibration test is needed to find out what a suitable start position for the actuators would be. In this way, this start position could be used whenever the dynamic pins need to be unlocked. The tolerance on this position will be subtracted from both sides of the allowed range of the dynamic pins so that the actuator could not actuate the pins outside their range. To still remain with enough range, it is desired to do this test within $\pm 0.5mm$ tolerance.

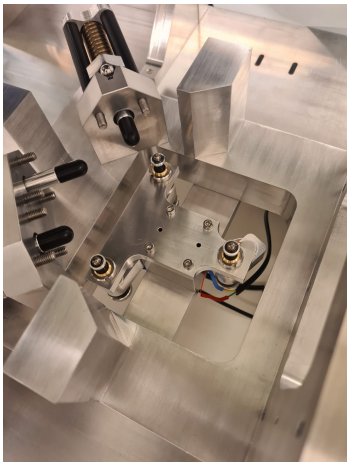

Figure 5.26: The actuators inside the setup

Since it is not desirable to calibrate the position of the actuators for each setup, during the recommendations an alternative will be discussed.

Expectation

It is expected that the desired position for the actuators would be around 7 mm of their extension, since this is the nominal distance between the tip of the actuator and the desired position of the dynamic pin if there would be no tolerances. With the tolerances, it is expected that the desired extensions would be between 6.8 and 7.2 mm.

Implementation

To calibrate the actuators the elevated ring that goes around the bottom of the element module can be used since it is known that the distance between the nominal position of the dynamic pins and this "ring" is equal to 0.8 mm. If a piece of stainless steel with a thickness of around 3 mm (with a tolerance smaller then ± 10 μm) would be placed against this ring at the location of the dynamic pins, as can be seen in the figure on the right, the actuator could be extended until it touches it. This could be felt by the operator due to the increased friction that the piece of stainless steel would undergo. If the actuator would touch the piece of stainless steel, it would be known that it would then be extended to 3.8 mm under the nominal position of the dynamic pin. The actuator would then have to extend 3 mm to be 0.8 mm under the nominal position of the dynamic pins and withhold the dynamic pins from falling below their range once they are unlocked.

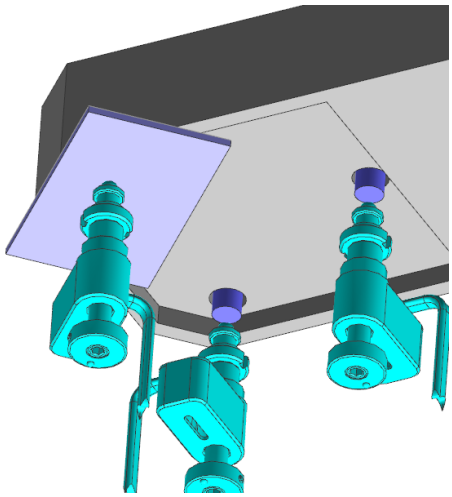

Figure 5.27: Actuator calibration

Note that if the dynamic pin would be positioned between 0.8 mm and 1.2 mm below its nominal range, it would be noticed while trying to hold the stainless steel plate against the ring. The dynamic pin would then first be unlocked while the operator pushes the stainless steel plate against the dynamic pin such that the dynamic pin would be retracted until it reaches its 0.8 mm location after which it will be locked again.

Results

Due to the limitations of the actuators, the test was not possible to carry out. This is due that the actuators did not reach the dynamic pins with the calculated amount of steps. Since the absolute extension of the actuators is not known, they could not be calibrated as intended. Instead eyesight was used to extend the actuators until they gently touched the bottom of the dynamic pins to calibrate the actuators to their begin position.

5.6.3 Functionality test: Do the dynamic pins follow the actuators without stick-slip?

Now that the start position of the actuator is known, the dynamic pins can be unlocked. In section 3.3.1, a test was done to see if there would be no large-scale stick-slip in the movement of the dynamic pins. However, this test should also be done with the sensor to see if there is stick-slip on a smaller scale since this would add to the tolerance of the adjustment.

Expectation

It is expected that there is no stick-slip as the dynamic pins are designed to move smoothly within the module.

Implementation

Each dynamic pin will be tested separately. This will be done by moving the sensor to reach a measurable location on the element as close to the tested dynamic pin as possible. In this way, the influence of the dynamic pin is the best visible. The dynamic pin will then be pushed up and down along its range. The sensor will measure the displacement continuously. From the sensor output, it could then be seen if there is stick-slip in the movement of the dynamic pin. A constant fluent change in the sensor output would refer to no stick-slip and a more stuttering signal would indicate the presence of stick-slip. This will be done for all three dynamic pins.

Results

After looking at the signal of the sensor during the movement of the actuator, the change in distance between the sensor and the element was continuous, as can be seen in figure 5.28. This indicates that there should not be any big stick slip movement of the dynamic pins. In the test of section 5.7.1, it will be indicated if small stick-slip might play a role in the movement of the dynamic pins.

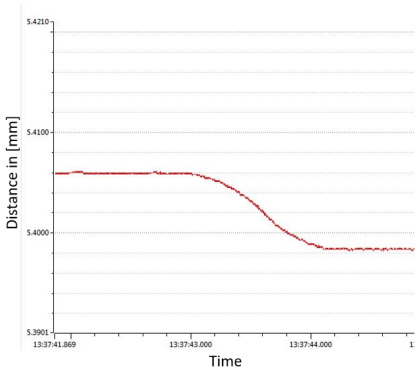

Figure 5.28: Sensor signal during the movement of the actuator

During this test also the height increase per step size was measured. By moving 1000 steps up and down with all three actuators an average change of 24 nm in the height of the element was found per step. This test was repeated for 10000 steps up and down. This gave an average of 25 nm up and 24 nm down. This difference could be due to a varying load on the actuators which could influence the distance per step. Since an inaccurate usage of distance per step would not cause any extra tolerance and could only cause some extra adjustment iterations, 24.3 nm is used for the displacement per step.

5.6.4 Performance test: What is the added tolerance due to the Locking mechanism?

As has been explained in appendix B, the locking mechanism presumably adds a certain tolerance. There are a couple of things that will be tested about the deviation of the element in Rx, Ry, and Z, due to the locking of the pins. The influence of the order of locking each pin on the tolerance will be tested, the total deviation caused by locking the dynamic pins, and if a part of the deviation is reoccurring. If a part of the deviation caused by the locking mechanism would be the same each time it is locked, then this could be compensated for and would not be added tolerance.

Expectation

Since the locking direction of each of the dynamic pins is different, as depicted with the blue arrows in figure 5.29, it is expected that the order in which the pins are locked matters for the deviation caused on the position of the element. Furthermore, it is expected that the measured deviation would be below the calculated deviation since the calculated tolerance, which can be seen in appendix B, is worst-case scenario. Lastly, it is expected that a big part of the deviation is repeatable for each time the pins are locked and can be accounted for and thus don't contribute to the tolerance chain.

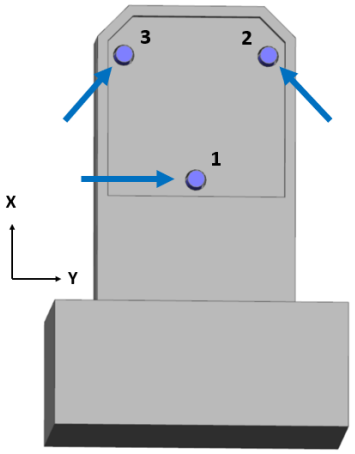

Figure 5.29: Locking directions pins

Implementation

To calculate the deviation caused by the locking mechanism, first, the actuators will go to their start position, after which the dynamic pins are unlocked. Then the coordinates, that were tested in section 5.5.1, will be measured and a plane fit will be made. After that, the pins will be locked and the coordinates will be measured again to make a new plane fit. This will be done 10 times for each of the 6 possible orders to lock the pins.

For each of the locking orders, the displacement will be calculated. This will be done by subtracting the plane fit after the locking from the plane fit before the locking for each instance after which the mean of these 10 instances will be calculated. Next to the mean, the sample standard deviation from the mean for each of the 6 locking orders will be calculated using formula 5.1. The locking order with the smallest sample standard deviation will be chosen to use during the measurement and adjustment process of the tool. A factor of 2S will be chosen for the added tolerance.

Results

In contrary with what was expected, the order of locking the dynamic pins did not change the result of the position of the element. The standard deviation of Rx, Ry, and Z due to locking are equal to 0.034 $mrad$, 0.025 $mrad$, and 0.26 μm respectively. Since the deviation due to the locking can be observed due to a measurement iteration after locking, only one times S would do for the added tolerance. The spread of the results can be seen in the boxplot in figure 5.30. However, next to the the repeatability tolerance an offset in Ry which of which the average is equal to 0.06 $mrad$ can be seen after each time the dynamic pins are locked. This will also need to be taken into account for the tolerance of the locking mechanism.

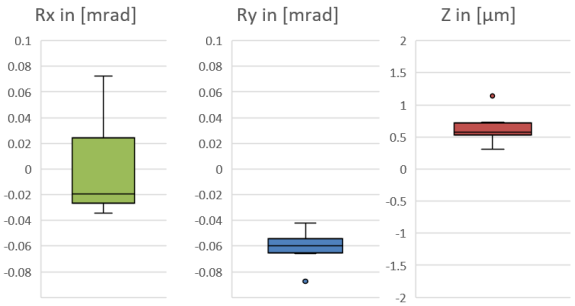

Figure 5.30: Repeatability of the locking mechanism

5.7 System verification

Now that all subsystems have been validated individually and all calibration values are found, the whole system can be tested as a whole. To test the system as a whole, a performance test will be done to check if the end position of the element converges to the desired position within tolerances.

5.7.1 Performance test: Does the element adjustment converge to a value within the desired tolerances after a certain amount of iterations?

For the setup to work as intended, the position of the element should converge to be within 10% of the total tolerance within a certain amount of measurement iterations.

Expectation

It is expected that only 3 measurement iterations are needed. One to measure the required adjustment, one to check if the element is adjusted to the right coordinates, and one to check if the element stays at this position after the dynamic pins are locked.

Implementation

The measurement and adjustment cycle will be done a couple of times times to test if the element can be adjusted within the required tolerance range and how many measurement iterations this takes.

Results

This test was carried out three different times from three different starting positions. In figure 5.31, the difference between the Rx, Ry, and Z coordinates of the pillar and the element can be seen after each adjustment iteration. The difference in coordinates can be seen on the vertical axis and on the horizontal axis the iteration step can be seen. In all three cases it took a total of 5 measurement and adjustment iterations and one final locking and measurement iteration to calibrate the position of the element. Although 5 measurement and adjustment iterations is more then expected, the fact that the position of the element converged in all three cases until its coordinates where within 5% of the requirements (± 1 *mrad* in Rx an Ry and ± 0.1 *mm* in Z) of the element means that the element can be successfully calibrated with the selected measurement and adjustment approach.

The stack could even be calibrated more accurately if more measurement and adjustment iterations would be used. The process could be optimised to require fewer measurement and adjustment iterations by altering the formula for the required actuator displacement chosen in section 4.4.3. A reason for the unexpected amount of required iterations could either be geometric deviations from the used geometrics to define the formula, the presence of stick-slip, or due to a difference in stepsize of the actuators due to different amounts of load.

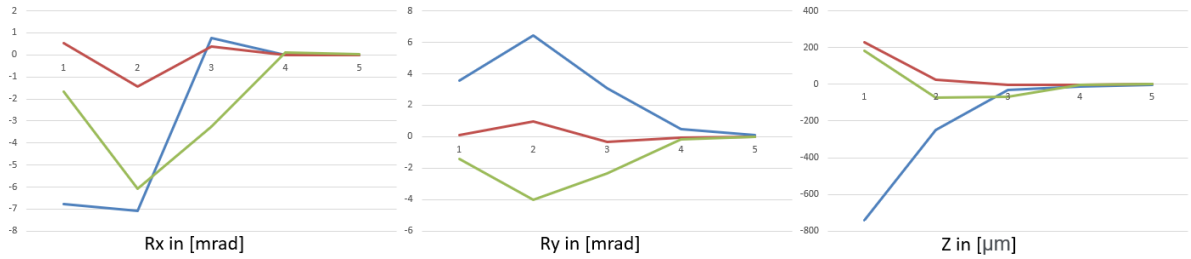

Figure 5.31: Adjustment iterations

This test is done one more time but then while adding the locking of the dynamic pins after which the element is measured one final time to see if it is still within the desired tolerances after the dynamic pins are locked. This is the complete process as described in the flowchart of section 4.6. As can be seen in figure 5.32, there is a slight deviation after the in Ry after the dynamic pins are locked, as was expected from the test in section 5.6.4. This could be accounted for by adding another adjustment step and giving it a negative Ry adjustment equal to the deviation found between step 5 and 6. This is however not necessary at the moment since the element is still within 13% of the total tolerance budget in Ry, which seems sufficient for now.

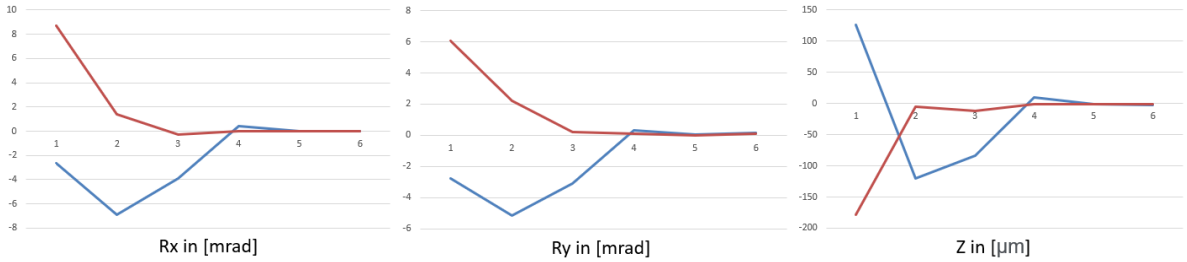

Figure 5.32: Adjustment iterations

Chapter 6 Discussion

In this chapter first the results form the tests will be discussed. After that the tolerance chain will be revisited to compare the expected tolerance chain from chapter 4, with the tolerance chain resulting from the tests in chapter 5. Then, the requirements stated in section 1.2.2 will be checked with the design to see if the requirements and boundary conditions are met. After this the recommendations for improvement will be discussed. Lastly, chapter 2 and 3 will be revisited to discuss some of the findings from these chapters.

6.1 Summary test results

Subsystem	Test	Type of test	Extra information	Expectation	Discussed in	Results
Sensor	Surface measurement	Functionality test		element surface can be measured	5.3.1	Partly doable
	Sensor parameters	Calibration test	Required for new sensor		5.3.1	
	Repeatability of the sensor	Performance test		±0.4µm	5.3.3	2S is equal to: ±0.24µm
	Software sensor	Functionality test		Software works	5.3.4	Software functions as expected
Sensor on stages	Software stages	Functionality test		Software works	5.4.1	Software functions as expected
	Acceleration and settling time	Calibration test	Required for new stages	Allowed acceleration: 30mm/s^2 settling time: 1 sec	5.4.2	Acceleration of 8mm^2/s is chosen with a settling time of 0.35 sec
	Repeatability sensor on stages	Performance test		Almost equal (+=0.2µm) to the repeatability without stage	5.4.3	±0.6mrad tolerance in Ry due to temperature tolerances after a heating period of 20 minutes
	Wobble stages	Performance test	Corresponds to tolerance 5	±5µm	5.4.4	Not wobble at around ±20µm, more accurate is not measurable
	Repeatability stages	Performance test		±1µm	5.2.1	Not done
	Location Reference pillars	Calibration test	Required after each assembling	±1mm	5.4.5	Calibration values are +0.65mm for X and +2.09mm for Y
Docking	Measurement locations	Calibration test		Locations are correctly selected	5.5.1	Not all parts are measurable, thus Measurement coordinates are altered
	Pillar plane fit and element plane fit	Performance test	Corresponds to tolerance 4 and 7	1% of total tolerance each, as calculated	5.5.2	S element plane fit: Rx is ±0.015 mrad, Ry is ±0.011 mrad and Z is ±0.44 µm S pillar plane fit: Rx is ±0.0014 mrad, Ry is ±0.015mrad and Z is ±2.4 µm
	Deviation in Z of X, Y, Rz positioners	Performance test	Corresponds to tolerance 2	±5µm	5.5.3	S is equal to: Rx is ±0.086 mrad, Ry is ±0.070 mrad and Z is ±1.8 µm
	Location element within given deviation	Performance test		Repeatability <±50µm	5.5.4	60 µm in X and Y
	Repeatability element module integration	Performance test	Corresponds to tolerance 1.1	See appendix A	5.5.5	S is equal to: ±0.16 mrad in Rx, ±0.08 mrad in Ry and ±2.6µm in Z
	External vibrations	Functionality test		The change in sensor output ±10µm	5.5.6	Negligible
Adjustment and Locking	Software actuators	Functionality test		Software works	5.6.1	Absolute location can not be obtained
	Begin position actuators	Calibration test	Required after each assembling	Start extension between ±0.2mm of 7.12mm	5.6.2	Calibration test not doable, calibrated by visual feedback
	Stick-slip test	Functionality test		No stick-slip	5.6.3	No visible stick slip
	Adjustment reproducibility	Performance test	Corresponds to tolerance 8	Around 1% of the stepsize	5.2.2	Not done
	Locking Repeatability	Performance test	Corresponds to tolerance 9	Ry<±0.27 mrad, Rx<±0.23 mrad, Z<±0.008mm, can partially be predicted	5.6.4	S is equal to ±0.034mrad in Rx, ±0.025mrad in Ry, ±0.26µm in Z, Rx has an offset of 0.06mrad
Total system	Convergence element adjustment	Performance test		System will converge in 2 iterations to required spec	5.7.2	element is within 5% of requirements of pillars after 5 adjustment iterations and 1 locking iteration

Table 6.1: Test landscape with results

In table 6.1, all the results of the different tests can be seen. Now, a summery of the test results will be given. The values will be discussed in the next section, section 6.2.

Although the sensor was not able to measure all types of samples of gold plated silicion, as has been found during testing in section 5.3.1, it was able to test measure the element of the element module available for testing. Since it was able to reach the same resolution as was prescribed by the manufacturer, as has been found during testing in section 5.3.3, the sensor made it possible to test the performance of the other subsystems. This is however with the exception of the stage wobble since the optical flat had a too reflective as discussed in section 5.4.4 and could only be measured within a lower accuracy than desired.

Although the stages added tolerance to the measurement due to thermal phenomena, as was found in section 5.4.3, with 3 sets of 8x8 measuring coordinate grids, it is found possible to make a planefit within 1.5% of the total tolerance budget, as has been found during the test in section 5.5.3. This made it possible to measure the tolerance due to integration of the module into the setup, the tolerance due to the X, Y, Rz positioners, and the tolerance due to the locking of the dynamic pins as long as they where bigger then 1.5% of the tolerance budget. These results will be discussed in the next section.

During the Acceleration and settling time, as discussed in section5.4.2, the required settling time was lower then expected. This makes it possible to measure more coordinates for the plane fit, within the desired 3 to 5 minutes measuring time, than expected. Not all points selected in section 4.3.1 were measurable due to the light receiving element being blocked by the cables on the element module due to its 45 degree angle, which was perceived in section 5.5.1.

The actuators where not able to make uniform stepsize, as was found in section 5.6.1, which made the calibration and the usage of the actuators a bit more difficult as was previously thought. However, it was possible to adjust the element within 5 adjustment iterations and one locking iteration to the same Rx, Ry, Z coordinates as the reference pillars, as was found in section5.7.1. This makes it so that the chosen concept design for this project is indeed successful. From the tests reconsiderations can be concluded to improve its performance. These will be discussed in section 6.4.

6.2 Tolerance chain comparison

Tolerance contributors	Calculated tolerances of chapter 4			Tested tolerances of chapter 5		
	Tolerance in Rx [mrad]	Tolerance in Ry [mrad]	Tolerance in Z [um]	Tolerance in Rx [mrad]	Tolerance in Ry [mrad]	Tolerance in Z [um]
1.1 Dowel pin repro	See appendix A			0.156	0.083	2.60
1.2 Dowel pin pin				See appendix A		
1.3 Dowel pin hole						
2. X, Y, Rz Positioners			0	0.087	0.070	1.82
3. Reference setup	0.27	0.33	40	0.27	0.33	40
4. Sensor Pillars	0.01	0.01	1	0.001	0.015	2.4
5. wobble stages	0.05	0.05	5	0.05	0.05	5
6. Temperature difference			1		0.06	
7. Sensor element	0.011	0.011	0.067	0.015	0.011	0.44
8. Adjustment	0	0	0	0.05	0.05	2
9. Locking tolerance	0.23	0.27	8	0.034	0.094	0.26
Total tolerance (Half quadratic, half linear)	**0.73**	**0.56**	**80**	**0. 69**	**0.57**	**67**

= maximum tolerance

= Standard deviation from the mean retrieved from tests

Table 6.2: Tolerance chain expected vs tested values

In table 6.2, the results of the tests can be compared with the in chapter 4 calculated values. Note that the values retrieved from the tests depict the standard deviation of the mean (S), which is the interval in which 68.2% of the measured values are within, and that the calculated values represent an absolute maximum tolerance for each component.

However, due to the standard deviation values, an approximation of the chance that the setup will not be within the requirements can be made. This can be done by looking at the standard deviation of the two biggest statistical tolerance contributors (in Rx, since Rx is most likely to go over the allowed tolerance budget), being the dowel pin repro, and the X,Y,Rz positioners (the reference setup tolerance is an absolute tolerance). The total tolerance would only be higher then the required required 1 $mrad$ in Rx and Ry and 100 μm if the dowel pin repro would be outside 3S and the X,Y,Rz positioners would be outside S. Since 3S covers 99.6% and S covers 64% of data points, The probability of an instance that would be outside both of these ranges would be approximately $\frac{1}{200} \cdot \frac{1}{3} = \frac{1}{600}$. The 1 in 600 modules that would be calibrated slightly outside the requirements would not pose a risk to the functioning of the microscope (only a slight deviation from the desired resolution) and 599 in 600 is most likely a sufficient score. However, this score could still be improved as will be discussed in the coming sections. Furthermore, The score is dependent on the wobble of the stages. For the calculation of the total tolerance, the expected values of the wobble where taken into account but the real values could lie between 5% and 20% of the total tolerance (as discussed in section 5.4.4).

Now that the total tolerance and its probability to be within the requirements has been explained, a closer the tolerance contributors will be discussed independently. Note that since all tested tolerances are measured with a plane fit. The tolerance of the planefit is included in all individual tolerances. This however can not be subtracted from each tolerance contributor to only leave the tolerance of that individual contributor, as is not possible with tolerance measurements. The tolerance of each component could therefore be lower then measured during the tests.

- Firstly, the Dowel pin repro scored worse then was expected in the calculation of appendix A. Next to tolerance of the plane fit being included in the measured tolerance, two other reasons could cause the deviation. The first reason could be the added tolerance the X, Y, Rz positioners. Next to the tolerance of the plane fit, the tolerance of the X, Y, Rz positioners is also included in the measurement since these are tightened each time the element module was docked into the setup. The second reason could be the added tolerance due to the temperature influences of the stages. Because the integration and disintegration of the element module takes time, almost 10 minutes where in-between each measurement, this could have cause extra added temperature deviations in the stages as explained in section 5.4.3. Since the docking itself is difficult to improve, as it follows a predefined procedure, the measurement for the tolerance can be improved by improving one of the causes discussed below.

- The Rx, Ry, Z positioners also scored worse then what was expected. This could be since a simplified verson of the Rx, Ry, Z positioners was used in this setup, as was explained in section 4.4.1. If this tolerance would need to be inproved, a redesign of the positioners could be made that would be closer to the original design. Another reason could be the fact that the stages cooled down inbetween each measurement. Although, since there was less time in-between each measurement then with the dowel pin repro tests (the time between each mesurement was approximately 5 minutes vs the 10 minutes during the docking tests), this should have less of an effect then with the docking.

- The used reference setup for feasibility demonstrator is not manufactured to be strictly within these given tolerances due to the time restrictions on the lead time. This can't be tested since the setup can not measure the absolute coordinates of the pillars but only measure the pillars in regard to the element. It can therefore not be guaranteed that the reference pillars are within the given tolerances which is required for the setup to be within the required tolerances. However, a production ready design would feature a reference within these tolerance which could be guaranteed by letting the manufacturer measure the reference after manufacturing. Therefore the original stated tolerances are used in the tolerance chain.

- As discussed in section 5.4.4 There could only be found that there was no wobble in the stages bigger than $20\mu m$. To determine the added tolerance due to the wobble of the stage more accurately the more reflective optical flat needs to be measured. This could be done if another sensor would be selected, as will be discussed in the recommendations.

- The tolerance due to temperature variation is unexpected. It was not expected that the stages would produce heat that would influence the tolerance of the setup. Furthermore, not all measurement points along the X axis seem to react the same way due to temperature change. This could be a result of a tilt of the stages in Ry due to unequal thermal expansion along the stage portal. It is found that the setup could only be within the desired tolerances if a 20 minutes warm up of the stages would be done before each measurement to reduce the tolerance to the 0.06 $mrad$ in Ry. This will be further elaborated in the recommendations.

- The tolerance due to the adjustment could possibly be even further reduced to be almost equal to the tolerance of the plane fit by adding more adjustment iterations. However, for now the tolerance left after 5 adjustment iterations, which is only 5% of the total tolerance budget, should be enough. This makes the required total required measurement iterations equal to 6, existing out of 5 adjustment iterations and one locking iteration during which another measuring scan needs to be done. This is a bit more then expected, since it should be possible to adjust the element to the desired coordinates within 1 adjustment iteration (instead of 5). This however was not the case, probably due to the actuators steps not influencing the dynamic pins as calculated due to their step size not being uniform or due to small stick-slip.
- The locking tolerance is lower then calculated in appendix B. It does however have an offset in Rx, which is not an statistical tolerance around a certain point but an offset in one direction. This is added to the tolerance in Rx in the table but can be accounted for as will be discussed in the recommendations.

6.3 Checking the requirements and boundary conditions

Now that the total tolerance of the setup is calculated and the different contributors are compared with the previously calculated values, the performance of the setup in regard to the initial requirements and boundary conditions will be discussed. These are the requirements and boundary conditions that were presented in section 1.2.2.

Is the tolerance requirement met?
As explained in the previous section, depending on what the missing tolerance value of the stage wobble would be, the setup has a 599 out of 600 probability to be within the requirement tolerance, which seems sufficient for now.

Does the setup damage the element?
The setup does not touch and therefore does not damage the element. This boundary condition is thus met.

Is the setup able to measure and adjust each element despite the small measurement surface and its high reflectivity?
Although the small measurement surface is not a problem for the setup, the sensor was not able to measure every type of gold coated silicon due to its high reflectivity. To fix this, an other sensor should be chosen, as will be discussed during the recommendations.

Does the setup generate particles?
The stages used are not tested to be cleanroom compatible and although multiple precautions have been taken to reduce the possibility of particles leaving the stage, it still is not fully prevented. Furthermore, the drag chain generates plastic particles while moving. This was not accounted for and will be discussed in the recommendations.

Does the setup fit on a table top?
It does fit on a table top, as was shown in section 4.5.2.

Is the setup intuitive to use for an operator?
The setup is intuitive to use for an operator, especially if the actuators would be integrated into the software (which was not the case for the feasibility demonstrator as was discussed in section 4.6.2). Then the operator would only need to integrate the element module into the setup, tighten the positioners, start the software, and unlock and eventually lock the positioners. This would not require special skills. Only the calibration of the actuators, which needs to be done when building the setup is in its current state prone to possible errors. This will therefore be discussed during the recommendations.

Can the setup actuator actuate the entire range of the actuators?
This is partly achieved. The range of the actuators is sufficient, but since their absolute position with respect to the element module is unknown, it is not known when the maximum or minimum of the range of the dynamic pins is reached. This could result in a risk of the actuator actuating the pins to a position outside their prescribed range. This will be discussed in the recommendations.

Are no changes required to the element or element module for the setup to function successfully?
This boundary condition is met. There are no changes to the element or element module required for the setup to function successfully.

6.4 Recommendations for improvement

In this section, the the proposed recommendations from the previous sections will be elaborated. Next to a possible implementation of each recommendation, its importance will also be discussed.

6.4.1 Changing the sensor to measure reflective surfaces

The most important recommendation would be to chose a different sensor for the setup. As was already explained in the first section of this chapter. The chosen sensor can not measure all gold plated silicon samples that were tested in section 5.3.1. Although the element of the element module could be measured, this means that it will most likely not be able to measure all elementes of different element modules. Which means the setup would not work entirely. There would be two alternatives for the sensor without having to change much of the setup. The first one being a lasertriangulator that is designed to measure reflective surfaces, as can be seen in figure6.1a. The second option would be to use a chromatic confocal sensor as these are these have no problem with reflective surfaces, as discussed in section 2.3.1, which can be seen in figure 6.1b. These were not chosen for the feasability demonstrator since they are a factor 2 or 3 more expensive and since the used lasertriangulator could measure the element of the testmodule, but are required for the production ready design to be able to measure the elementes of different element modules.

(a) Lasertriangulator which can measure reflective surfaces (from [16])

(b) Confocal sensor (from [18])

Figure 6.1: Alternative sensor options

6.4.2 Measuring the stage wobble and ways to reduce the wobble tolerance

With a sensor that could measure a reflective surface, the optical flat can be measured more accurately. This means that the stage wobble can be determined, as described in section 5.4.4, which is required to fully validate the setup. If the stage wobble would be too big for the tolerance budget to stay within the requirements there would be two options. Firstly, different stages could be chosen that are manufactured with tighter tolerances for stage wobble. Secondly, the stage wobble could be measured to get the offset as a function of the position of the stages. This could be used to calibrate the measured height values of the preselected measurement locations. This however is not desired as explained in 2.4.1 but could be implemented using calibration software that would measure an optical flat and implement the offset as a function of stage location for each setup to reduce the chance of errors during the calibration.

6.4.3 Fixing the unexpected temperature deviation

To fix the unexpected temperature tolerance found in section 5.4.3, an extra step should be added to the flowchart of section. The stages would need to warm up for 15 minutes by letting them move along their range during this time. This would decrease the temperature influence on tolerance to only a 0.6 *mrad* tolerance in Ry as calculated in section 5.4.3. A new flowchart with the added extra step can be seen in figure 6.2. This recommendation is necessary for the setup to stay within its required tolerance budget. The tolerance used in the total tolerance calculation in section 6.2 takes this extra step already into account.

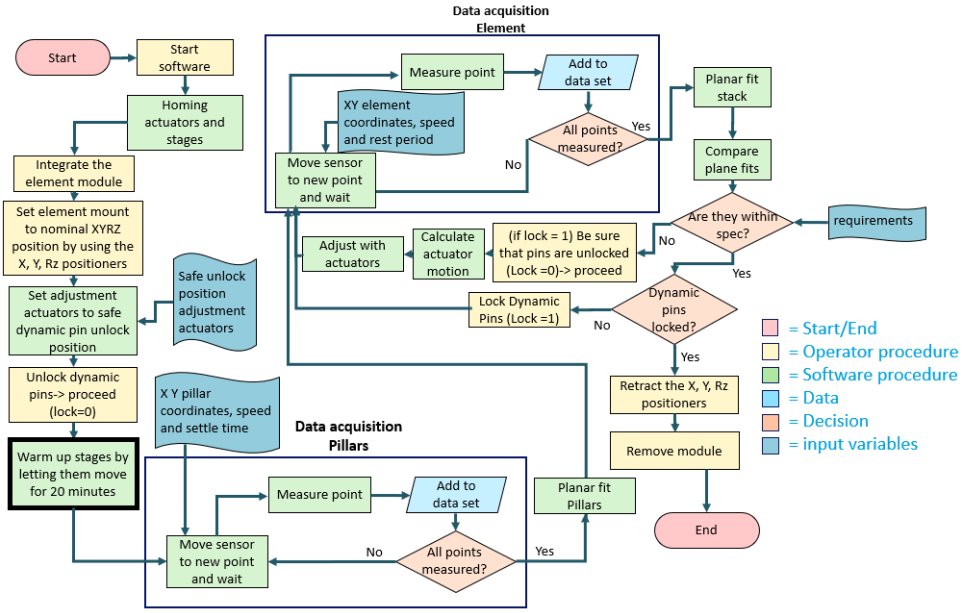

Figure 6.2: improved flowchart with stage warm up step

Another option to fix the temperature deviation would be to further investigate its origin. Maybe this could be fixed by using other stages that generate less heat. It could also be found that the temperature deviation could be reduced by using different materials that conduct the heat better.

6.4.4 Reducing the tolerance added due to the locking mechanism

Next to a reduction of the temperature tolerance, a reduction of the tolerance added by the locking mechanism can also be taken into account by altering the steps of the calibration process. The setup now takes 5 adjustment iterations and one locking iteration, as discussed in section 5.7.1. However, by adding another locking iteration this offset can be accounted for. By calculating the offset in the first locking iteration, the dynamic pins could then be unlocked again and the actuators could adjust the element to the coordinates of the pillars minus the calculated offset in Ry. When the pins would then be locked again and the element would be subjected to approximately the same Ry offset, the final position of the element would closer to the Rx, Ry and Z coordinates of the reference pillars. However, this is not necessary at the moment, since the tolerance added by the offset does not endanger the tolerance requirements enough.

6.4.5 Reducing the tolerance added due to the X, Y, Rz positioners

Although the added tolerance due to the tightening of the X,Y,Rz postioners does not add a too big part to the total tolerance at the moment, they still can be improved by keeping the design closer to the original design. For the feasibility demonstrator the decision was made to change the original ceramic parts for steel and aluminium parts, as described in 4.4.1. Since these have a lower stiffness than the ceramic parts, it could be the reason for extra play in the positioners. This is because the steel balls could create indentations in the aluminium due to the force of which they are pressed onto each other, making the positioners deviate from their position. This could result in a force which is applied with an angle onto the module, which could create the unexpected tolerances. To get rid of this extra play, the steel balls could be replaced with ceramic balls that press against ceramic plates again.

6.4.6 How to better calculate the different tolerance contributors

Now that the positioners add less tolerance and a better sensor might be able to make a more precise planefit and the tolerance due to the heat is reduced. All the tolerance components can be measured more accurately. This is especially interesting for the docking since this was calculated to be less than was tested. Eliminating the added tolerance due to the temperature, positioners and partially the tolerance of the plane fit, makes it possible to measure the docking more accurately. If the newly measured tolerance of the docking is still higher than what was calculated in appendix A, some unidentified tolerance contributors could be found. This could be interesting since the same dowel pin interface is used for the microscope itself. However, It does not have high priority since the tolerances of the setup are still within the required tolerance.

6.4.7 Fixing the particle generation

As discussed in section 6.3, there is a risk of particles being generated from the stages, the cables and the dragchain. A possibility to solve this would be to place the stages under the setup. The part where the module is "docked" with the pillars will then be placed on a X and Y stage and the sensor would then hang in a fixed place on a portal above the setup. In this way the only moving parts that could create particles would be the stages. Either this would satify the requirements since there would be no possibility that any particles would fall onto the element any more, or the stages would be swapped for cleanroom proof stages so that the whole setup would not create particles at all. A disadvantage would be that more weight would to be moved by the stages which could have negative effects on the tolerance and settling time of the stages. The other disadvantage would be that, since the docking requires a given torque (6Nm), this torque would ultimately act on the stages, which they may not be designed to handle.

Since the setup is at the moment not compatible to enter higher grade cleanrooms, due to the particle generation, and since the partners of ASML who would need the setup may want to install them into their higher grade cleanrooms, this problem would need to be solved. Depending on how strictly the requirements of particle generation are, the above mentioned solution could be further investigated. An easier option would be to change the dragchain for a more cleanroom proof type of dragchain, potentially fixing the problem of the particles generated from the cables of the sensor and the dragchain and thus solving the problem.

6.4.8 Choosing a different actuator

The current actuators have some flaws. Not only do they make a very loud noise when used, since the absolute extension is not known the calibration of the actuator is now done by looking

at when the actuator touches the bottom of the dynamic pins. This is not desirable since this process is prone to errors. The other problem due to the unknown absolute position of the actuators is that it is not known when the maximum or minimum of the range of the dynamic pins is reached, as discussed in section 6.3.

The first part of a solution would be to use an actuator with a build-in encoder. The second part would be to define the distance between the begin position of the actuator to the element module within ± 0.1 mm in Z. This tolerance is required since it would mean that the actuator could use the range of the dynamic pins minus 0.1 mm on the extremes of its range, as this would be uncertain territory, which is still enough to do the required adjustment. The tolerance train can be reduced to this ± 0.1 mm by using the calibration method proposed in section 5.6.2. Anothor option would be to reduce the tolerance train in from the actuators through the setup, through the dowelpins, to the element module, to the bottom of the dynamic pins to be within the ± 0.1 mm. If this last method could be done, the manual calibration method proposed in section 5.6.2 would not be needed. This would be more desirable since it does not require an extra step for the operator and is thus less prone to errors.

6.4.9 combining the Rx, Ry and Z measurement and adjustment setup with the X, Y, Rz measurement setup

Furthermore, a recommendation can be given how the Rx, Ry, Z setup with the X, Y, Rz measurement setup, discussed in section 1.1, could be combined into 1 setup. This has the advantage that it could be a much more compact setup and that the operator would have to perform fewer actions to measure the X,Y, Rz as well as to measure and adjust the Rx,Ry,Z. The X, Y, Rz could be measure in a way comparable as what was done in section 5.5.4. It is especially possible to achieve small tolerances on these coordinates if the confocal sensor is chosen to replace the lasertriangulator as it has a smaller beamwidth and can therefore measure the X, Y Rz position of the element with more precision. Perhaps the desired X, Y, Rz position can be determined with the use of an external golden reference, whereby the sensor on the stages can measure the deviation of the element relative to this desired position. The final setup would then use a combination of concept 4 to measure the X, Y, Rz and concept 5 to measure Rx Ry Z of the concepts mentioned in section 3.4.2 as can bee seen in figure 6.3. Next to a specially designed golden reference for the X, Y Rz coordinates, this would also require the X,Y,Rz positioners to be improved as indicated in a previous recommendation. The currently used positioners, which are less accurate then the original design, would otherwise otherwise add too much tolerance to the X, Y, Rz tolerance chain.

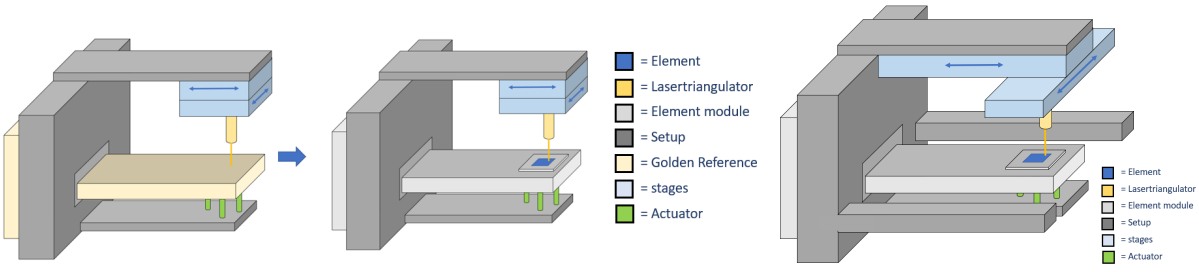

(a) Concept 4 for X, Y, Rz

(b) Concept 5 for Rx, Ry, Z

Figure 6.3: Measuring all 6 DOF of the element

6.5 Revisiting the theory and the concept generation

In this section the decisions made in the second and third chapter will be revisited to discuss in which circumstances other sensors and calibration approaches would be more favourable. Furthermore, now that the magnitude of the different tolerance contributors is known, it will be discussed which deviation source plays the biggest role when designing a measurement tool on the micro scale. Lastly, the concept selection will be revisited to discuss if the advantages of the chosen concept where actually true in practice.

6.5.1 In which circumstances were the other sensors more suitable?

Looking back at the different sensors found in section 2.3.1, next to the confocal chromatic sensor that was already discussed, a situation can be thought of in which slight alteration of circumstances the other sensors where more suitable. The probe, autocollimator and interferometer will be discussed, which can be seen in figure B

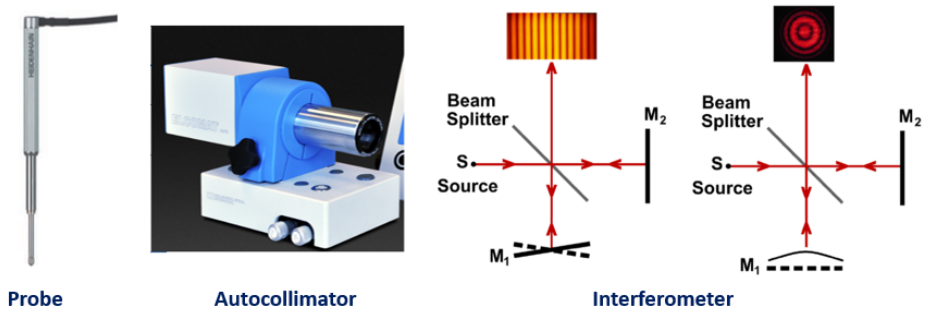

Figure 6.4: Alternative sensors

- The probe would most likely not be more advantageous compared to a lasertriangulator in under a slight alteration of circumstances because the mentioned risks of a particle at the measuring point and the possible generation of particles remain risky. Only if it could be verified that the probe would not generate any particles on contact with the element, and that the risk of measuring a particle would be low, the probe would have an advantage when needing to measure over a long range.
- If the element were larger so that both the diameter of the autocollimator and the laser triangulator could have fit above the surface of the element, this combination could have measured z, Rx and Ry quite accurately. Since the autocollimator has a 40 mm diameter and the laser triangulator would need 10 mm extra for it to measure on the element, a 50x50 mm element would be necessary to fit both sensors.
- An interferometer would not work for the setup in any case because an absolute displacement has to be measured, where as interferometers only measure relative displacements. A interferometer would make it impossible to calculate a required displacement for the actuators.

6.5.2 In which cases were the other calibration approaches more suitable?

Looking back at the different calibration approaches, discussed in section 3.1, a situation could be thought of in which other calibration approaches would be more suitable if there would be other boundary conditions.

- If the direction in which the element is integrated into the setup did not collide with the mounting surfaces of the mould, passive mould calibration would have some advantages. The main advantage would be its simplicity. It would lack the need of a sensor and any complications that a sensor could bring. A disadvantage of the usage of passive calibration would be that it would be difficult to test whether the final tolerance would be met. Furthermore, the force of which the element is pressed into the mould by the actuators could cause damage to the element which would be detrimental. The reason why it cant be used with the current boundary conditions is that, since the integration direction is horizontal, there would be a risk that the element would scrape against the mould during the integration.
- Only for a measurement in which the required tolerance budget would be far greater than the geometric tolerances, an absolute measurement would be possible. This would have the advantage that it is a simple design that does not need any testing or calibration. In this case it is not possible since this would require all precise dimensions to be known and as explained before this is not desired.
- If the element would not have a risk to be damaged, probes could be used. Due to their increased measuring range, the usage of a reference underneath the element module could be possible. This would have the advantage that no stages would be needed, thus eliminating thermal deviations and wobble tolerance from the stages.
- If the element would be bigger, three laser triangulators could be used to measure the Rx, Ry, and Z coordinates in reference to a golden reference. Since this eliminates the need for stages, the same advantages as mentioned above could be achieved.

6.5.3 What source of deviation was ultimately the biggest contributor to the tolerance budget on the micrometer scale?

In section 2.2.1, the different sources of deviation were discussed. Looking at the results from the tests and at table 6.2, the biggest contributor to the tolerance budget can be concluded.

The biggest sources of deviation for this setup would be the deviation caused by temperature influences and the deviation caused by geometric uncertainties. Temperature, in particular, was taken into account less than it ultimately appeared to be important because of the moving and thus heat-generating parts. The deviation due to the temperature influence would have been one of the biggest tolerance contributors if no alterations would have been made to let the setup heat up first.

Furthermore, when looking at table 6.2, it could be concluded that the geometric tolerance also accounts for a big part of the total tolerance. There would be two option in how to reduce the geometric tolerance. The first one would be to measure the reference after manufacturing. Since absolute dimensions would be known and could be implemented in the software of the calibration tool, the geometric tolerance would be eliminated. However, this has the disadvantage mentioned in section 2.4.1 and was chosen undesirable for this setup. Although, it would be possible if it would be required for the setup. The second option would be to apply stricter requirements for the manufacturing of the parts. However, some more research would need to be done how much stricter tolerances could be achieved for the manufacturing of the reference pillars.

6.5.4 In the end, what was the advantage of this measurement setup compared to the other concepts?

Looking back at the different concepts discussed in section 3.4.2, after building and testing the setup, it can be discussed what the advantages ultimately were of using the selected concept.

The advantage of using the selected concept was that multiple points can be measured, this turned out to be very useful with testing. Due to the wide range in X and Y, some adjustments were possible in the selected preselected measurement locations to achieve the planefit within the desired tolerances. A disadvantage of using this concept was the heat that was generated by the stages and the tolerance due to the wobble of the stages which where not measurable. If a concept would be chosen without stages, the wobble and the added tolerance due to the heat of the stages would not be a problem.

Under the current boundary conditions, this is still the most suitable measurement setup. However, if the element was a bit bigger and could fit 3 height sensors that could all measure on the element surface, this would eliminate the disadvantages of the stage (the wobble and the temperature deviation) and could measure and adjust the element faster, if that would be desired.

Chapter 7 Conclusion

Because the subsystems that could be measured are in line with expectations and the position of the element converges to that of the pillars after a number of measurement and adjustment iterations, the chosen concept for the calibration in Rx, Ry and Z is so far suitable. However, it does require some important adjustments to make it an production ready design. Firstly, the sensor must be adapted to be able to measure more reflective surfaces. Secondly, one of the proposed solutions must be implemented for the unexpected, too large, thermal expansion tolerance. When these changes were made, the stage wobble, which is the last partially unknown tolerance contributor, could be measured more accurately after which it can be fully concluded whether the setup reaches the requirements. In addition to these most needed changes, some optional recommendations have been given to further improve the setup.

In general, it can be concluded that especially the geometrical tolerance and the tolerance due to temperature play a major role in this design. Furthermore, it has been found that, with a small change in the boundary conditions, an arrangement without moving parts, and therefore without variable heat sources and stage wobble, would also meat the requirements. However, with the current specifications and boundary conditions, it can be concluded that the current design, provided that the necessary changes are made, is certainly suitable for the measurement and adjustment of the element in Rx, Ry and Z, within the required tolerance budget.

Bibliography

[1] Henzold, G. (2006). *Geometrical Dimentioning and Tolerancing for Design, manufacturing and inspection.* Butterworth-Heinemann. an imprint of Elsevier. 2nd edition.

[2] Edmund optics. (2014, Apr 11). *Understanding Error Sources in Precision Positioning.* Retrieved from *https* : $//www.edmundoptics.com.sg/knowledge-center/application-notes/optomechanics/understanding-error-sources-in-precision-positioning/$

[3] Paul, R ; Edwin, D. (2018). *Sensor for Mechatroncis.* Elsevier. 2nd edition.

[4] Danny, C. (2021, May 5). *Precision VS Accuracy, What is the difference.* Retrieved from *https* : $//www.mfg-space.com/precision-vs-accuracy-what-is-the-difference/$

[5] Rick, H. (2019 Apr 8). *How to Calculate linearity Uncertainty* retrieved from *https* : $//www.isobudgets.com/how-to-calculate-linearity-uncertainty/$

[6] Aalco. (2019). *Aluminium Alloy - Commercial Alloy - 6082 - T6 T651 Plate.* Retrieved from *https* : $//www.aalco.co.uk/datasheets/Aluminium-Alloy_{6}082-T6\ T651_{1}48.ashx$

[7] Bracewell, R. (2003). *Two-Dimensional Convolution.* In: Fourier Analysis and Imaging. Springer, Boston, MA. *https* : $//doi.org/10.1007/978-1-4419-8963-5_{5}$

[8] Sahani, A[jai] K[umar]; Jain, P[ramod] K[umar], Sharma S[atish], C. (2013). *Geometrical Tolerance Stack Up Techniques.* Chapter 52 in DAAAM International Scientific Book 2013. pp. 857-872. B. Katalinic . Z. Tekic (Eds.). Published by DAAAM International. ISBN 978-3-901509-94-0, ISSN 1726-9687. Vienna. Austria DOI: 10.2507/daaam.scibook.2013.52

[9] Chase, K. W. (1988). *Design Issues in Mechanical Tolerance Analysis.* Manufacturing Review 1(1): 10.

[10] Chase, K. W. and A. R. Parkinson (1991). *A survey of research in the application of tolerance analysis to the design of mechanical assemblies.* Research in Engineering Design 3(1): 23-37.

[11] Heidenhain (may 2021), *Length gauges*, Retrieved from *https* : $//www.heidenhain.nl/fileadmin/pdb/media/img/208945-2K_{L}ength_{G}auges_{e}n_{w}eb.pdf$

[12] Bunch, Bryan H; Hellemans, Alexander (April 2004). *The History of Science and Technology.* Houghton Mifflin Harcourt. p. 695. ISBN 978-0-618-22123-3.

[13] Hariharan, P. (2006 October 9). *Basics of Interferometry.* Elsevier Inc. ISBN 978-0-12-373589-8. Chapter 2.

[14] Strokes, A. (May 2013). *Advances in optical techniques for moisture and hydrocarbon detection*, Research gate, Retrieved from *https* : $//www.researchgate.net/figure/An-illustration-of-a-Michelson-interferometer-Top-left-The-measurement-mirror-M1-is_fig3_289374760$

[15] Keyence,(visited on February 2022), *1D Laser Displacement Sensors*, Measurement library, Retrieved from *https* : $//www.keyence.eu/ss/products/measure/measurement_library/type/laser_1d/$

[16] Micro-Epsilon (visited on February 2022), *Laser displacement sensors (triangulation)*, Retrieved from *https* : $//www.micro-epsilon.com/download/products/cat--optoNCDT--en.pdf$

[17] Aiko K. Ruprecht, Christof Pruss, Hans J. Tiziani, Wolfgang Osten, Peter Lucke, Arndt Last, Jurgen Mohr, and Peter Lehmann "Confocal micro-optical distance sensor: principle and design", Proc. SPIE 5856, Optical Measurement Systems for Industrial Inspection IV, (13 June 2005); *https* : $//doi.org/10.1117/12.612008$

[18] Micro-Epsilon. (visited on February 2022), *Confocal hybrid sensors for displacement, distance & position)*, Retrieved from *https* : $//www.micro-epsilon.com/displacement-position-sensors/confocal-sensor/confocal-chromatic-sensors/confocalDT_2403/?sr=1\&sc=2\&st=IFS2402+4$

[19] Zhaoxiang Ge, Xiangning Li, and Xiaoyang Wu "Two-dimensional real-time photoelectric autocollimator with double high sensitivity", Proc. SPIE 3898, Photonic Systems and Applications in Defense and Manufacturing, (4 November 1999); *https* : $//doi.org/10.1117/12.368507$

[20] Rajkumar Gupta. (visited on February 2022). *Principle of Autocollimator*, Mechanical jungle. Retrieved from *https* : $//mechanicaljungle.com/autocollimator-working/$

[21] Haag-streit. (visited on February 2022). *Elcomat product line*. Retrieved from *https* : $//www.haag-streit.com/moeller-wedel-optical/products/electronic-autocollimators/elcomat-product-line/elcomat-vario/$

[22] Kunzmann, H.; Trapet, E.; Waldele, F. (1990 Jan 25). *A Uniform Concept for Calibration, Acceptance Test, and Periodic Inspection of Coordinate Measuring Machines Using Reference Objects*. An imprint of elsevier volume 39 issue 1.

[23] Puerto, P.; Estala, B.; Mendikute, A. *A Study on the Uncertainty of a Laser Triangulator Considering System Covariances*. Sensors 2020, 20, 1630. *https* : $//doi.org/10.3390/s20061630$

[24] Mafalda, T. (2019 Jan 11). *What Is CNC Milling?*. craftcloud. Retrieved from *https* : $//all3dp.com/2/what-is-cnc-milling-simply-explained/$

[25] Leon, H. (2020 dec 16). *Everything You Need to Know About CNC Machining Tolerances*. Rapiddicrect. Retrieved from *https* : $//www.rapiddirect.com/blog/cnc-machining-services-tolerances/$

[26] Munnig Schmidt, R.; Schitter, G.;Rankers, A.; van Eijk, J.; (2020). *The Design of High performance Mechatronics*. Delft University Press.

[27] Mytri. (Visited on March 2022). *precision granite*. Retrieved from *http* : *//www.mytri.nl/indexnederland.html*

[28] Newport. (Visited on March 2022). *Picomotor^{tm} Piezo Linear Actuators*. Retrieved from *https* : *//www.newport.com/f/picomotor − piezo − linear − actuators*

[29] Thorlabs. (visited on April 2022)/ *150 mm linear translation stage, stepper motor*. retrieved from *https* : *//www.thorlabs.com/newgrouppage9.cfm?objectgroup$_i$d* = 2132&*pn* = *NRT*150/*M*

[30] Overes, F. (2020). *D000948364: Critcal Design Review XYrZ Alignment tool*. Retrieved from Teamcenter ASML.

[31] Keyence. (viewed on June 2022). *Sensor Head: Super Precision, Small spot, LK-G10*. retrieved from *https* : *//www.keyence.com/products/measure/laser − 1d/lk − g3000/models/lk − g10/*

[32] Micro-Epsilon. (viewed on June 2022). *operation instructions optoNCDT 1900*. retrieved from *https* : *//www.micro − epsilon.com/download/manuals/man − −optoNCDT − 1900 − −en.pdf*

[33] Viba. (visited on June 2022). *Helicoil*. Retrieved from *https* : *//www.viba.nl/nl/pageid/helicoil*.

Appendix A Dowel pin tolerances

Appendix B Locking tolerance

Appendix C Measurable locations

Appendix D Tolerance chains concepts

Appendix E Design calculations